The nature of the compact mass at the center of the Milky Way

Particle and Astroparticle Physics Colloquium
DESY, 25 November 2020

Andreas Eckart

I.Physikalisches Institut der Universität zu Köln
Max-Planck-Institut für Radioastronomie, Bonn

STRONGGRAVITY
EU FP7-SPACE research project 312789 2013 - 2017

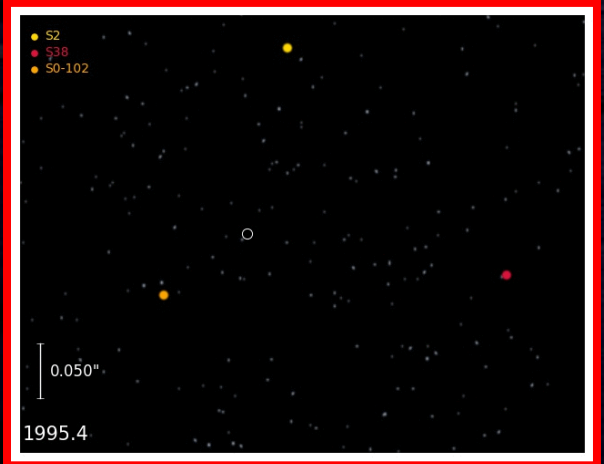

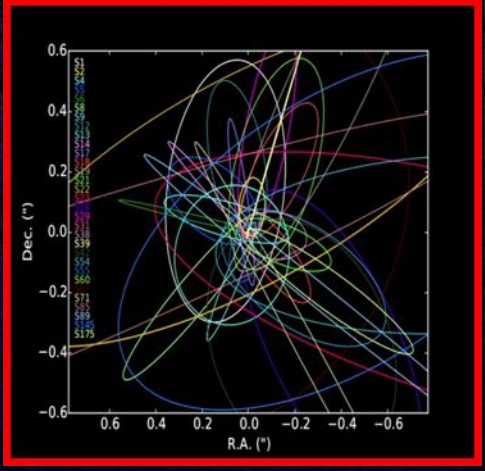

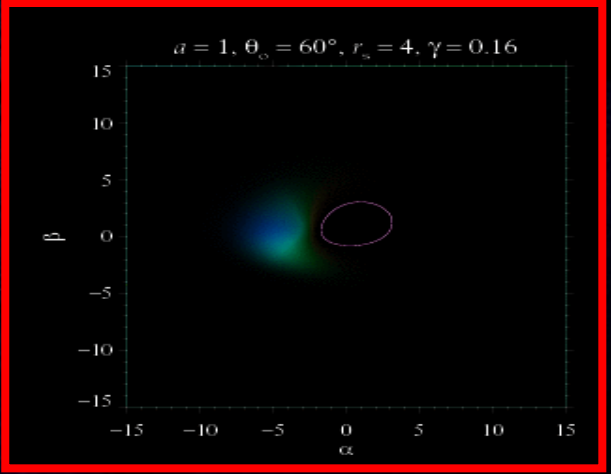

Nobel Prize in Physics 2020

Andrea Ghez
UCLA, USA

Reinhard Genzel
MPE, Germany

Roger Penrose
University of Oxford, UK

Why does one study super-compact masses?

Physics of extreme states of matter

No laboratory experiment possible (for massive black holes)

Test of the laws of physics in the high mass regime


The best place to
detect a super massive black
hole is the Galactic Center
It is the center of a galaxy closest to us and can
be studied with high precision

The Center of the Milky Way

Closest galactic nucleus
8 kpc distance
26.4000 lyrs
Extinction Av=30 Ak=3
Observations only in radio, infrared, X-ray

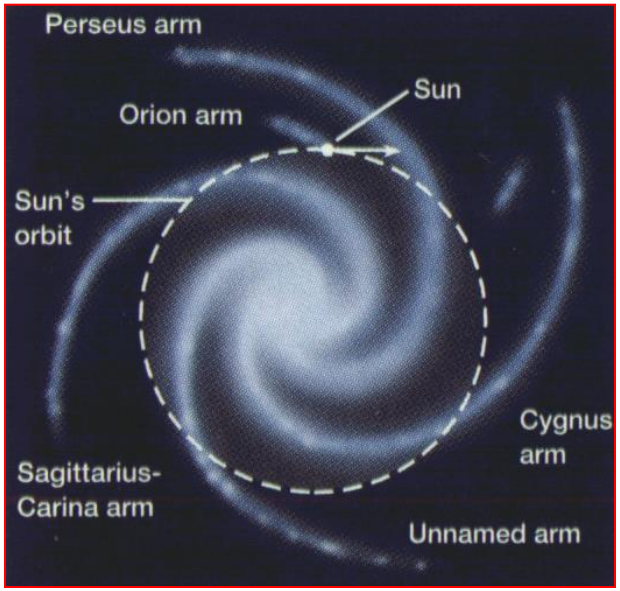

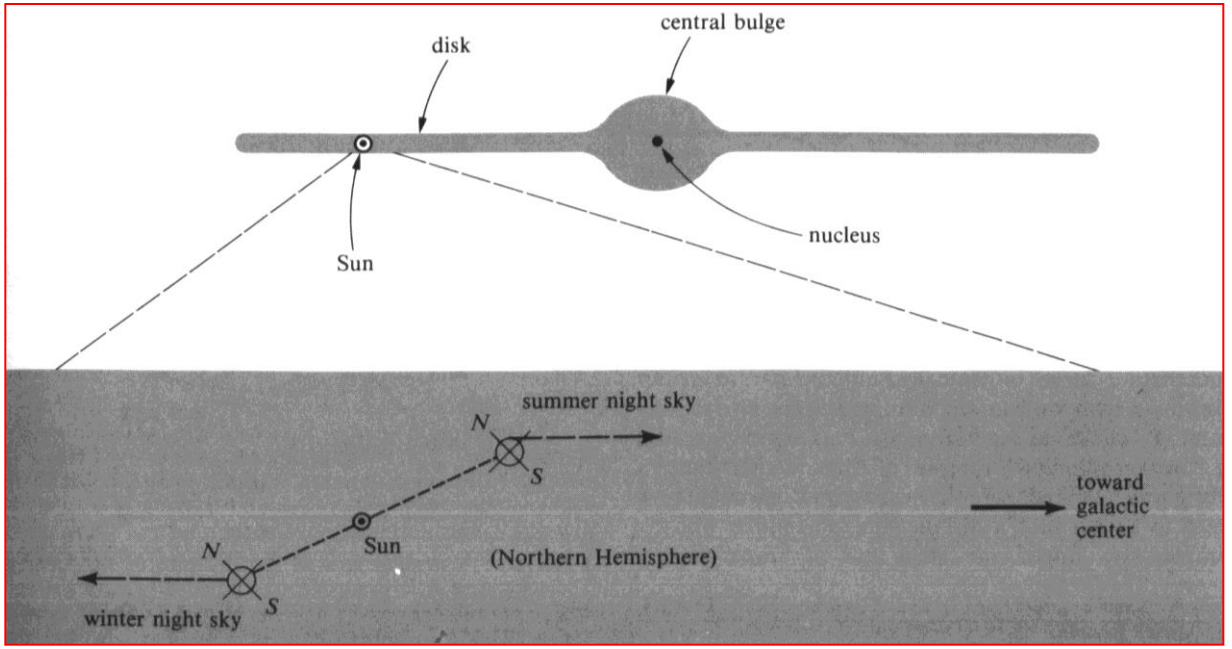

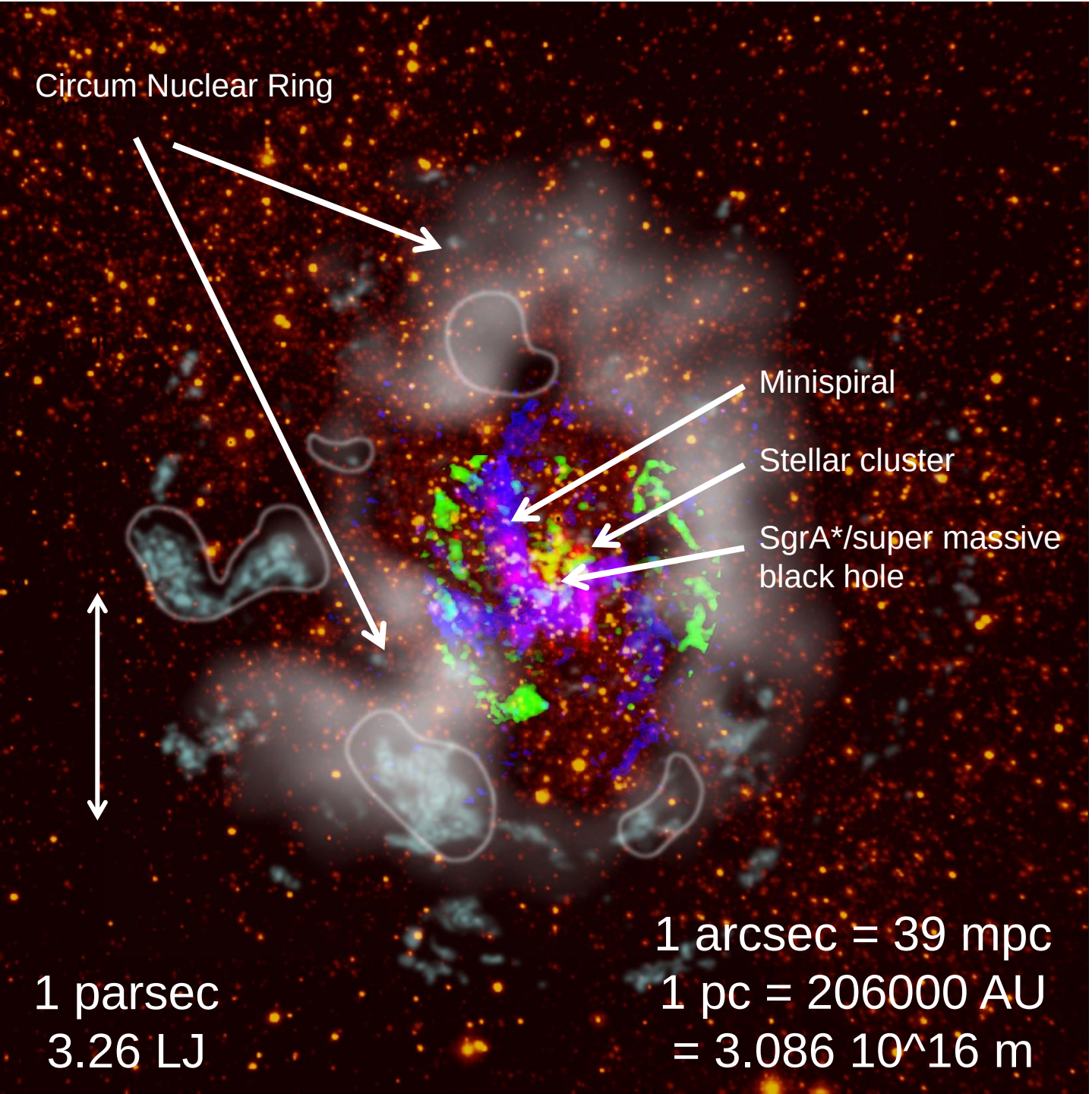

VLT infrared

ALMA submillimeter

Chandra X-ray

view of the Galactic Center

~1.5 arcmin across (11 light years)

Eckart et al. 2019 (UAE Sharjah - FISICPAC Proceeedings)

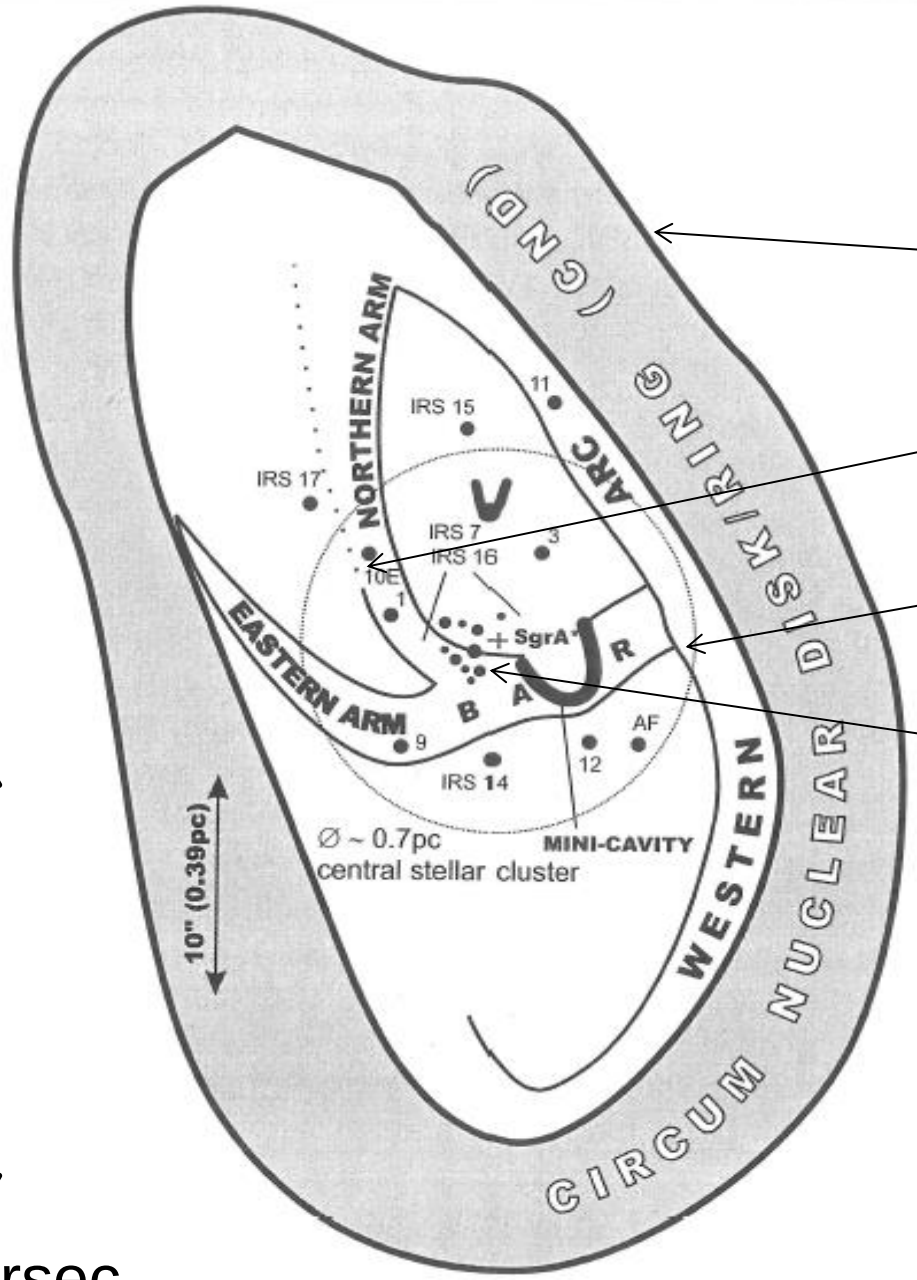

Circum Nuclear Ring

minispiral

stellar cluster

SgrA*/super massive black hole

1 arcsec = 39 mpc
1 pc = 206000 AU
= 3.086 10^16 m

1 parsec

The Galactic Center

SgrA*:
The situation
in the early 90s

400 km/s

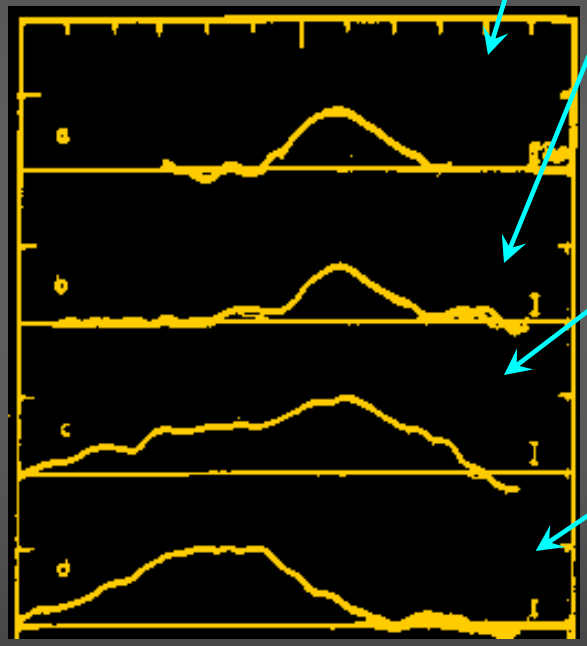

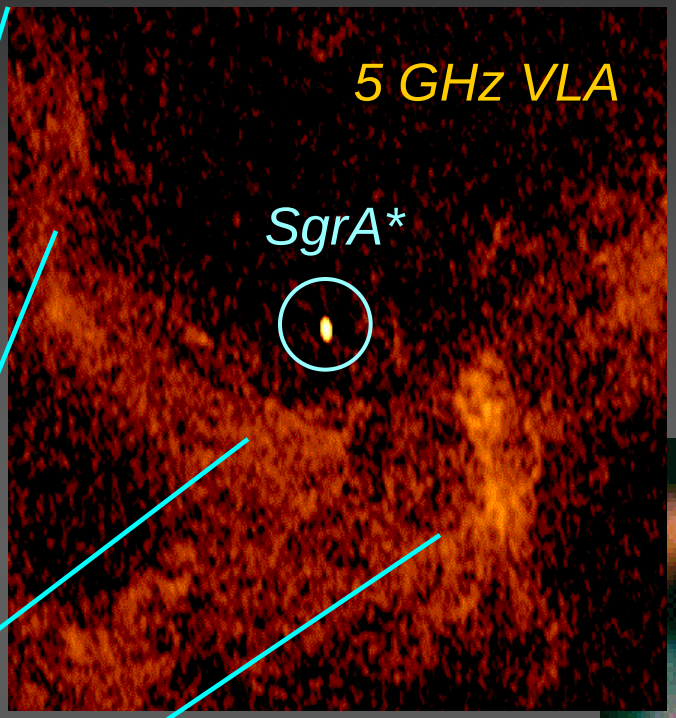

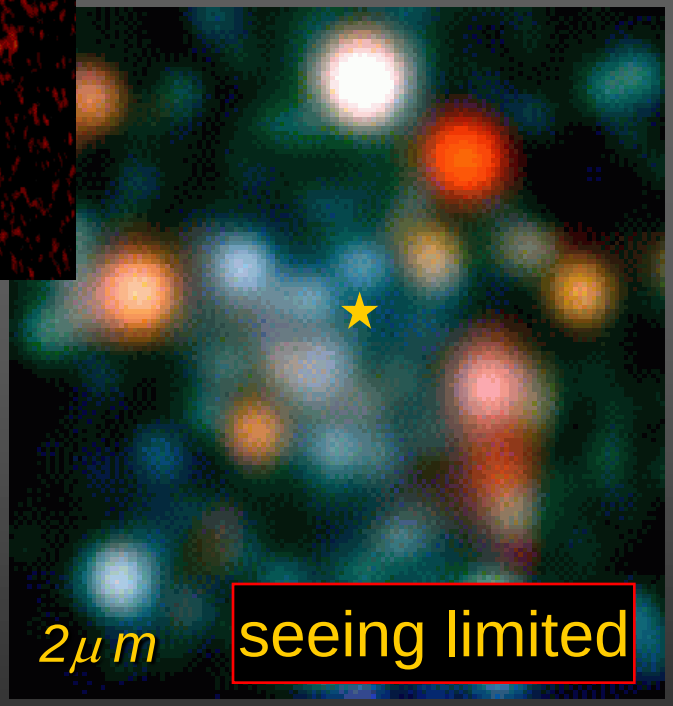

Wollman et al. 1977, Lacy et al. 1979, 1980,
Lo et al. 1983, DePoy and Sharp 1991

Followed in the 1980s-90s by several sub-mm observations of the ionized and atomic gas were carried out.


Chile.
Atacama Desert.


Chile.
It is a dry and isolated place

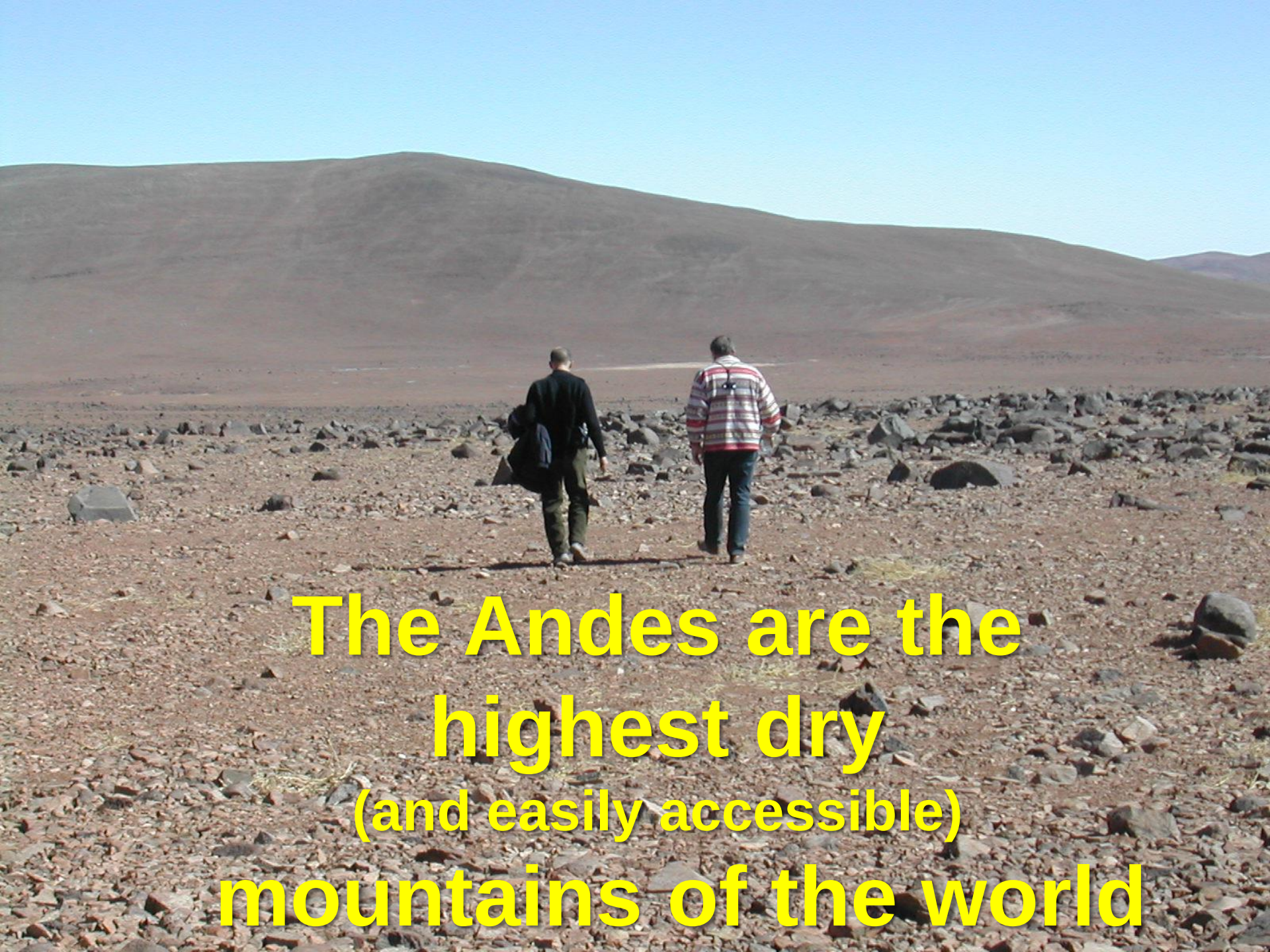
The Andes are the highest dry
(and easily accessible)
mountains of the world

Very Large Telescope (VLT) – Chile - Paranal

The MPE SHARP-Camera at the ESO New Technology Telescope (NTT) 1991-2002

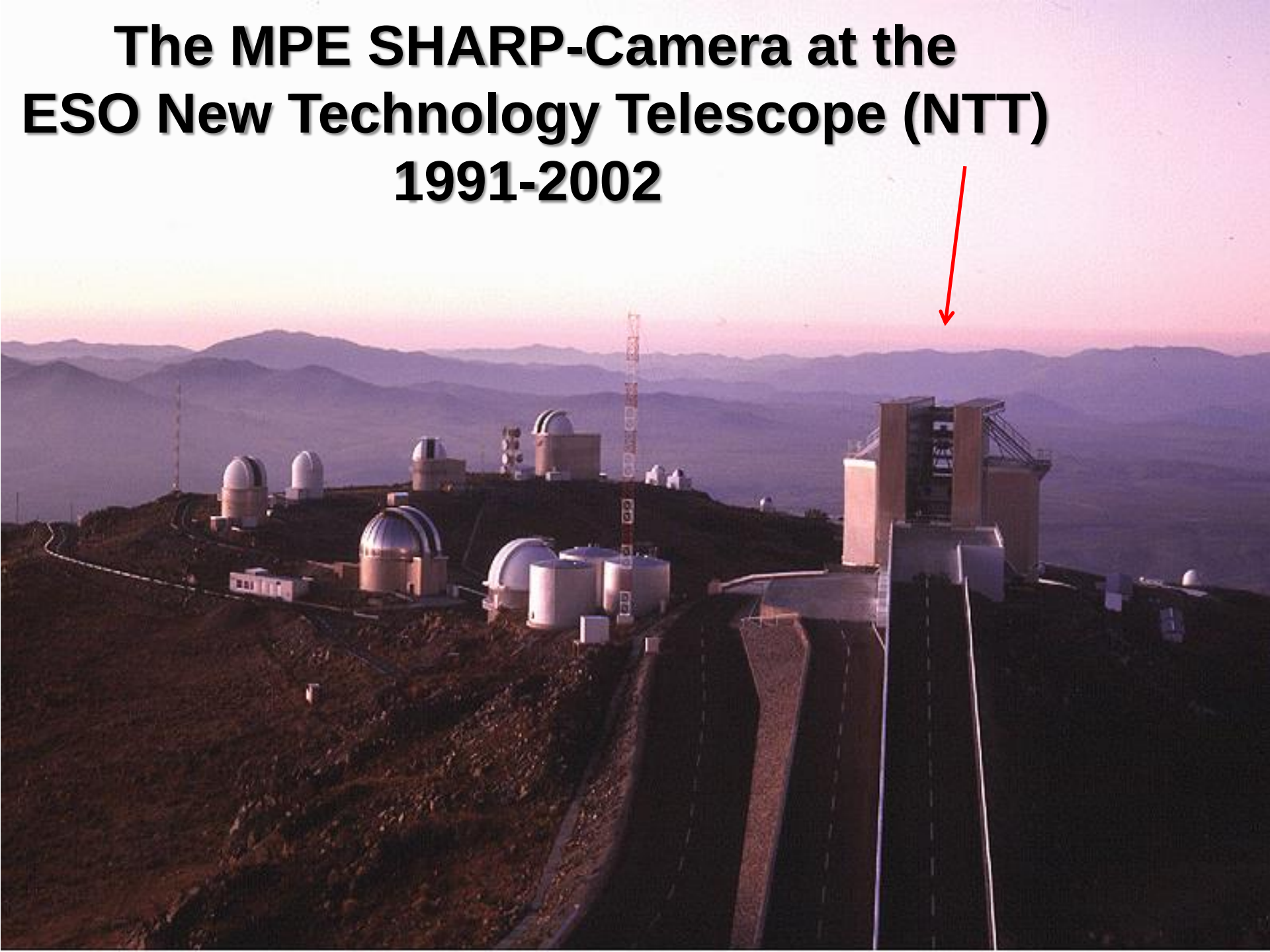

NTT Speckle Interferometry and

Proper motions:

SHARP I

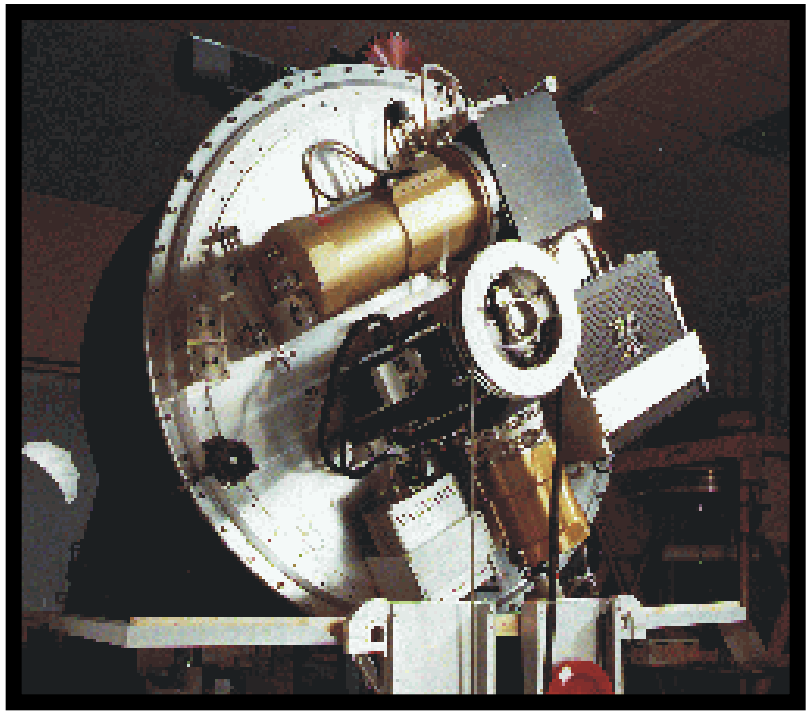

Speckle interferometry:
via short term recordings (a few 100 ms) the disturbing influence of the atmosphere are frozen in and recorded.

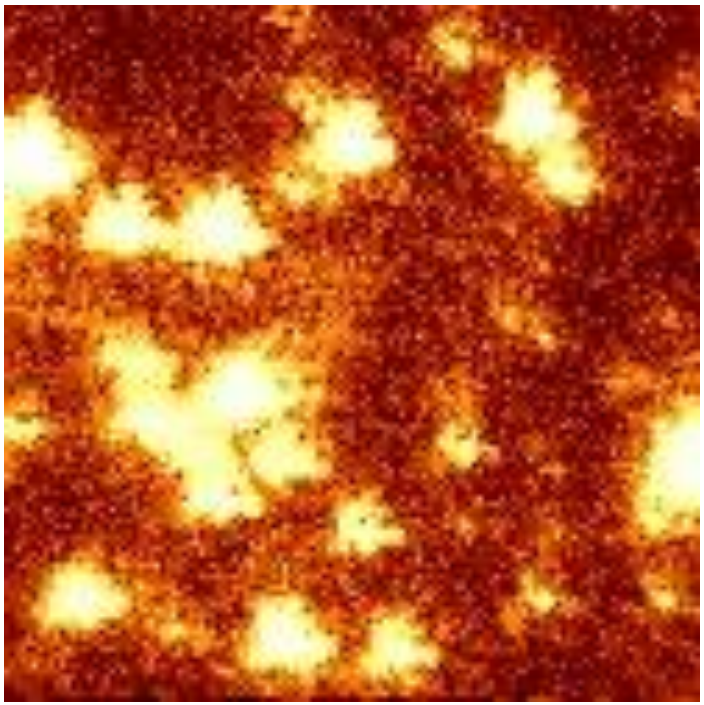

Short-term recordings from the SHARP Camera; Readout time 0.5 seconds

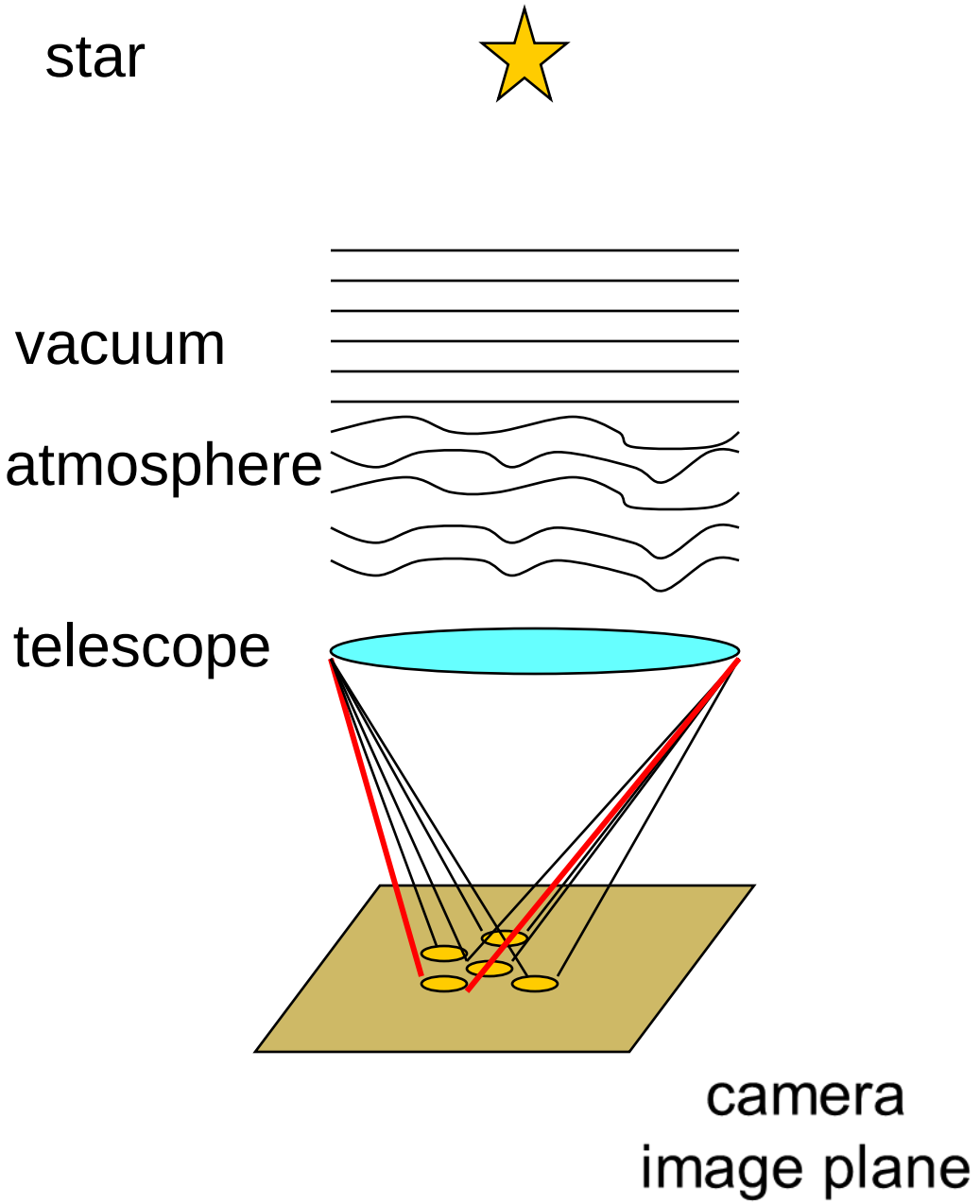

Proper motions

Stellar proper motions in the central 0.1 PC of the Galaxy
Eckart, A.; Genzel, R. 1996, Natue 383, 415

First Conclusive Evidence for a Massive Black Hole in the Center of the Milky Way
Eckart, Andreas; Genzel, Reinhard, 1997, MNRAS 284, 576

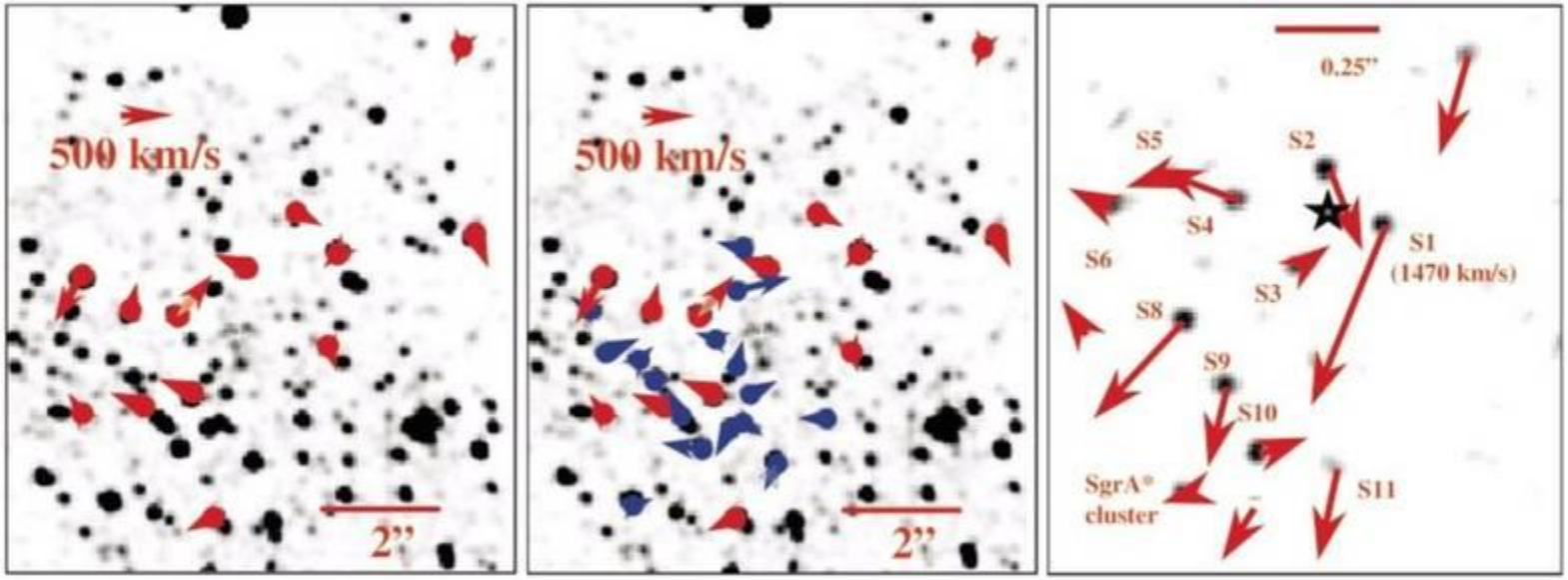

Proper motions

in the central SgrA* cluster 1992-2000

Eckart & Genzel, 1996, Nature 383, 415; 1997, MNRAS 284, 576.

Ghez et al. 1998, ApJ 509, 678.

0.5 “
6x10^{16} cm
4000 AU

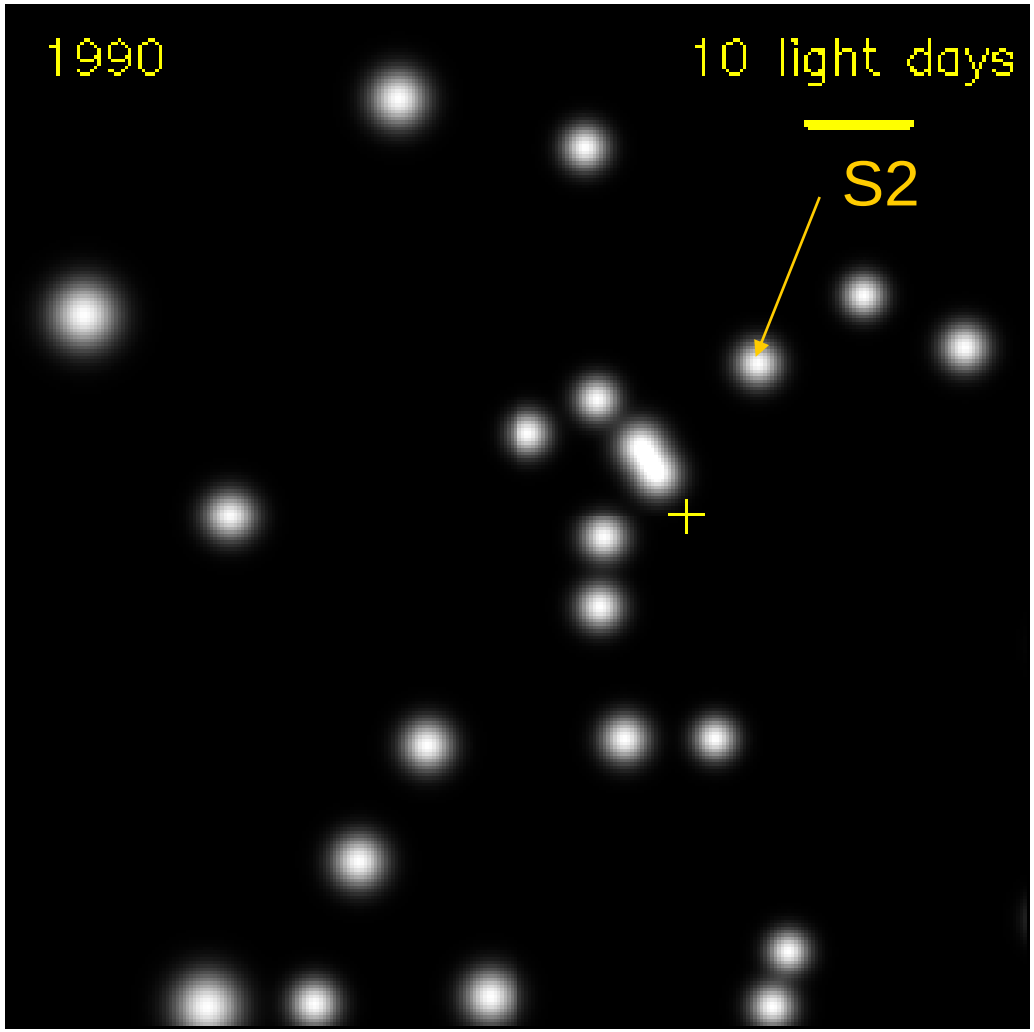

Stellar Populations

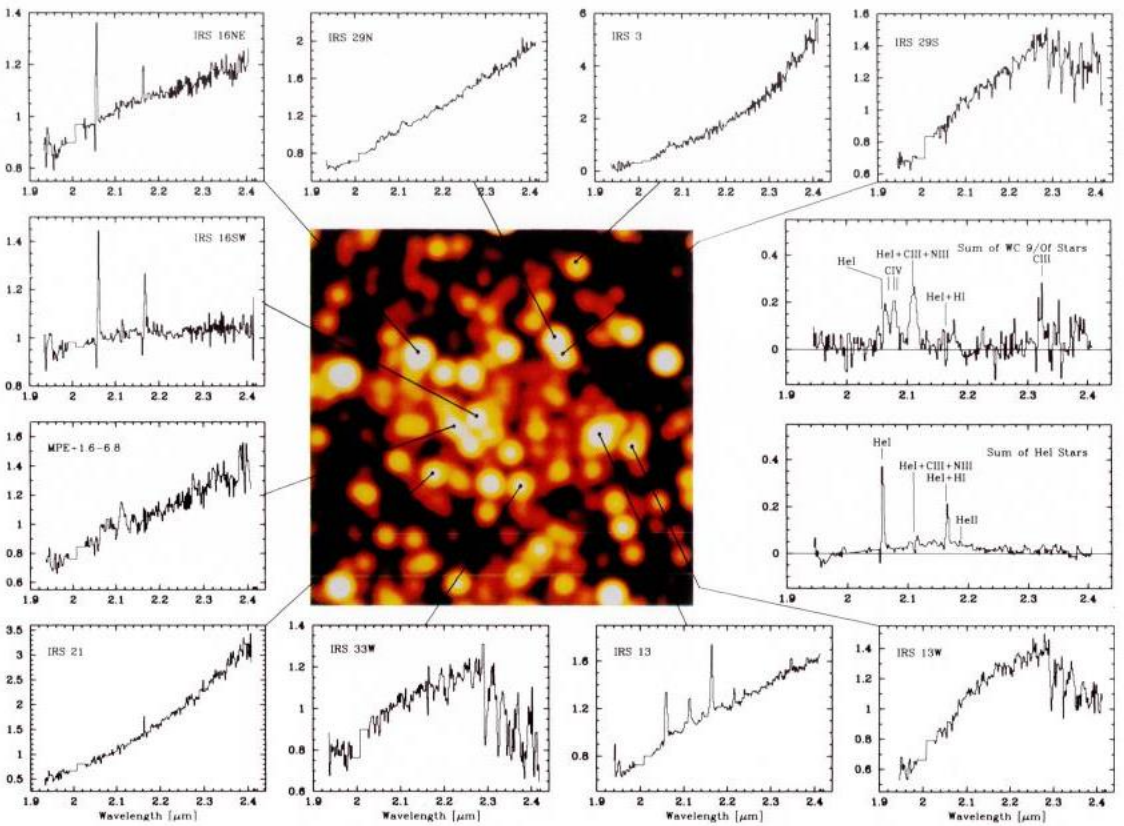

FIG. 1.—3D *K*-band spectra (resolving power 800–1000, spatial resolution 1") of 10 selected stars in the central 8", along with a smoothed (0".4) version of the *K*-band map of Eckart et al. (1995) showing the locations of the respective stars. The excellent resolution and sampling of the 3D data set allows us to characterize the individual stellar spectra in the crowded central few arcseconds in spite of contamination by diffuse nebular emission from the Sgr A West ionized gas streamers. The lower spectrum on the right-hand side is the sum of the appropriately shifted spectra of IRS 16C, IRS 16SW, IRS 16NE, IRS 16NW, IRS 34W, and IRS 33E. The upper right-hand spectrum is the sum of IRS 29N, IRS 6, MPE −1.0–3.5, and MPE +1.6–2.8, which we identify as WC9 (or Of).

KRABBE et al. (see 447, L95)

The Nuclear Cluster of the Milky Way: Star Formation and Velocity Dispersion in the Central 0.5 Parsec

Krabbe, A.; Genzel, R.; Eckart, A. *and 11 more* , 1995ApJ, 447, L95

Enclosed Mass Plots

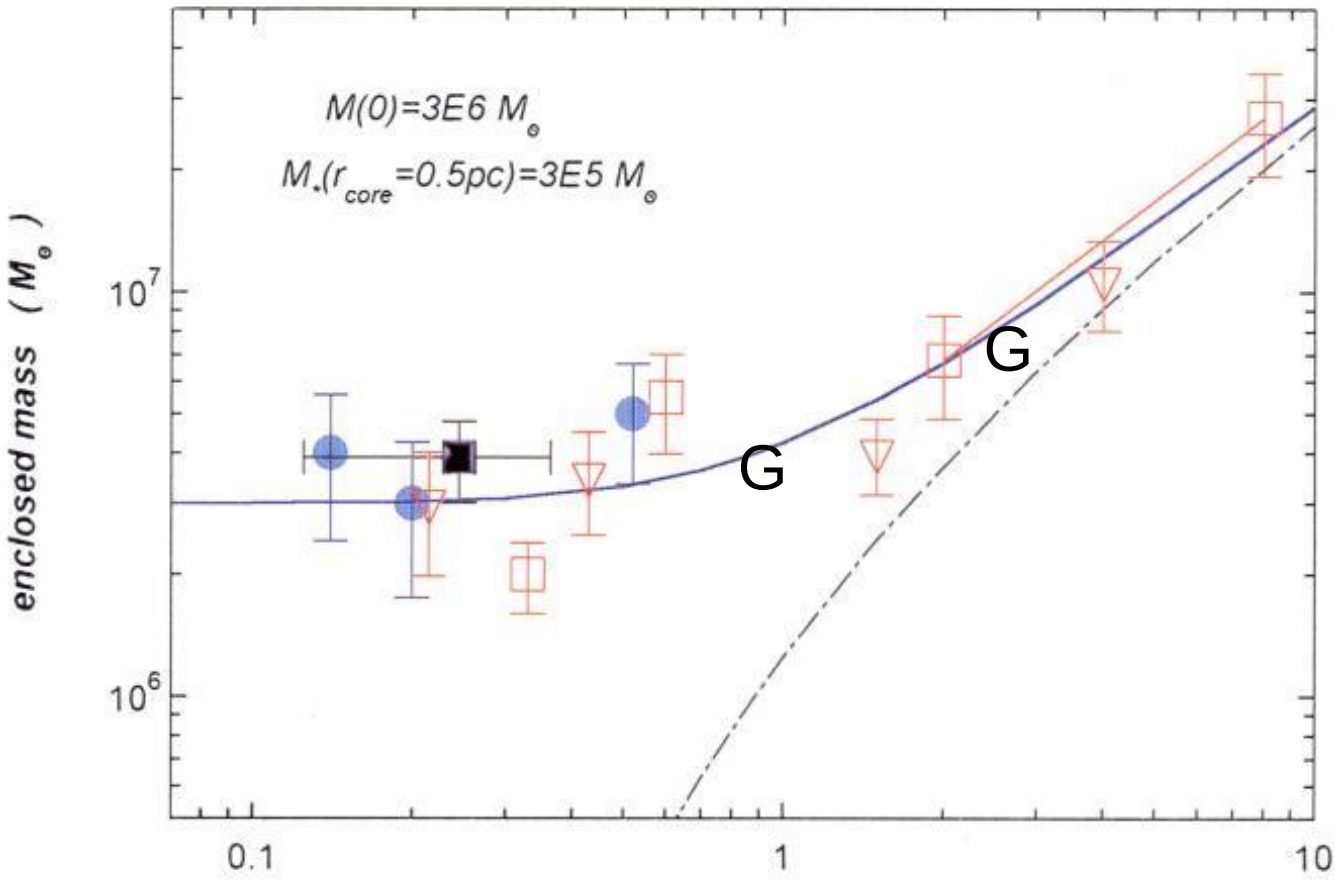

The Nuclear Cluster of the Milky Way: Star Formation and Velocity Dispersion in the Central 0.5 Parsec

Krabbe, A.; Genzel, R.; Eckart, A. *and 11 more* , 1995ApJ, 447, L95

NACO Astrometry

Masers in CONICA FOV

Positions and Proper motions **7 SiO**

measured with VLA/VLBA by

Reid et al. (2002, ApJ, submitted)

Accurate stellar positions

to ~10 mas

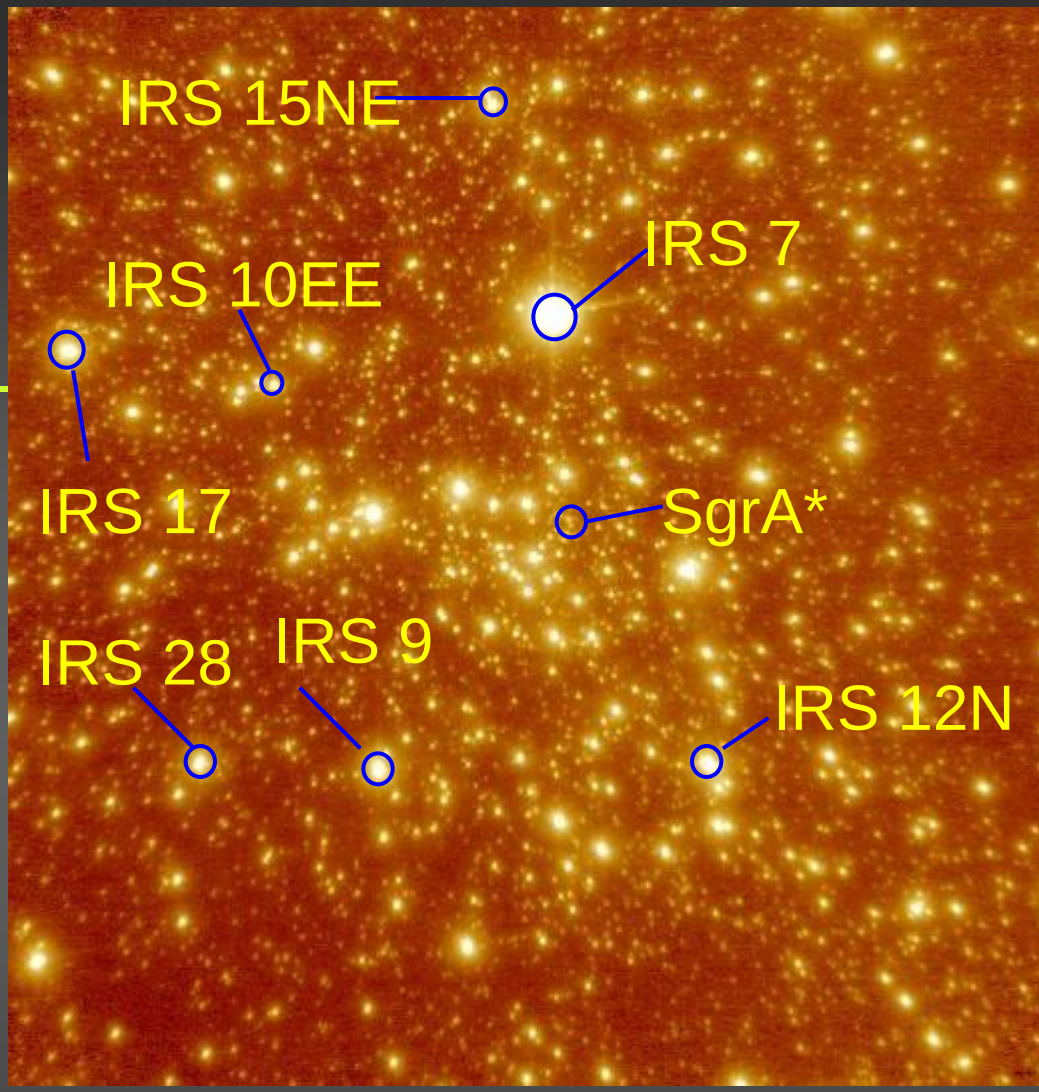

The Position of Sagittarius A*: Accurate Alignment of the Radio and Infrared Reference Frames at the Galactic Center

Menten, K. M.; Reid, M. J.; Eckart, A.; Genzel, R., 1997, ApJ 475, L111

Accelerations

2000, Nature 407, 349
The accelerations of stars orbiting the Milky Way's central black hole
Ghez, A. M.;Morris, M.;Becklin, E. E.

2003, ApJ 586, L127
The First Measurement of Spectral Lines in a Short-Period Star Bound to the Galaxy's Central Black Hole: A Paradox of Youth
Ghez, A. M.;Duchêne, G.;Matthews, K., et al.

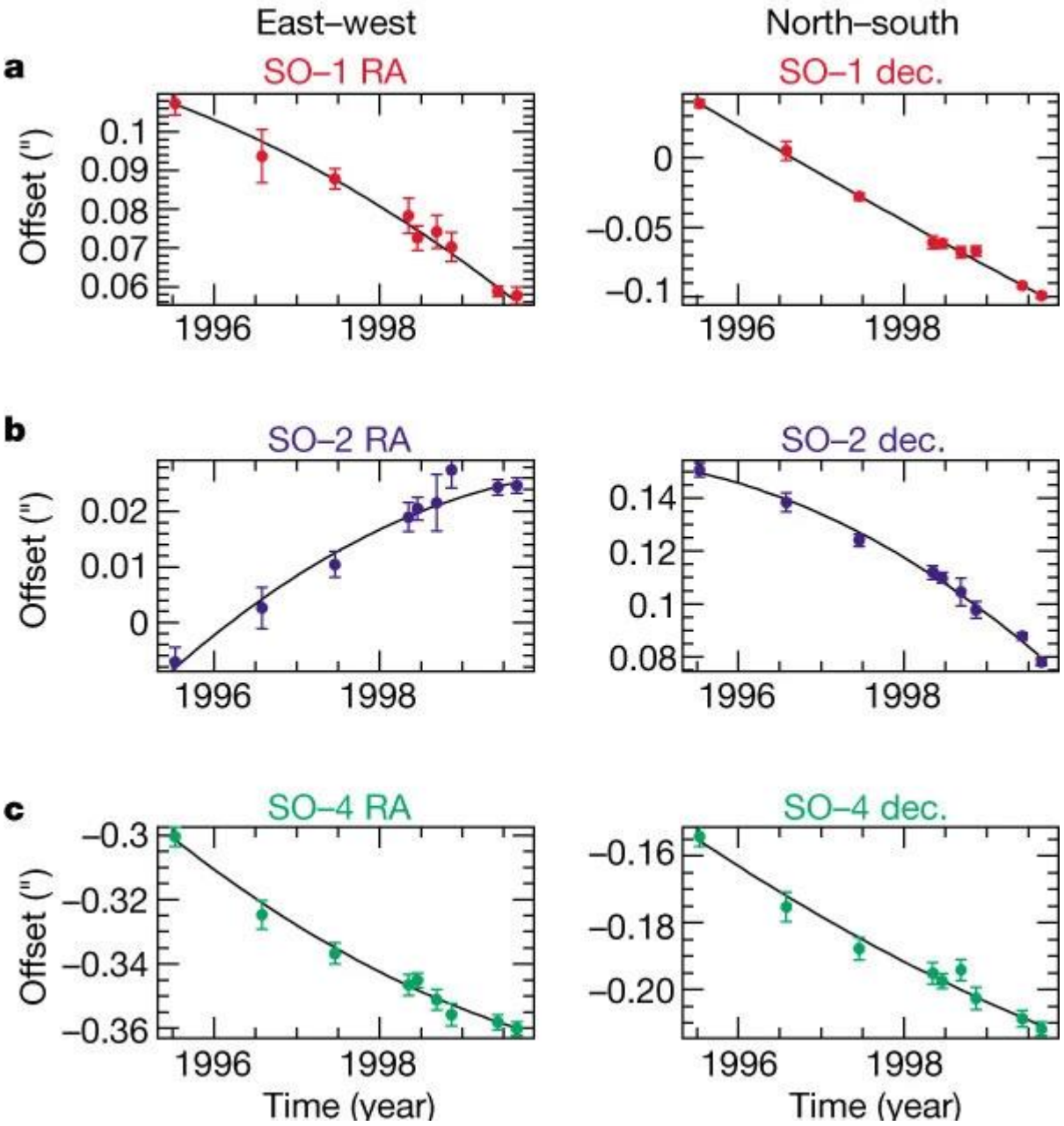

*Confirmation that S2 is in orbit around SgrA *.*

Determination of the SgrA * mass and position from the orbital accelerations of S2 measured with the SHARP camera on the NTT.

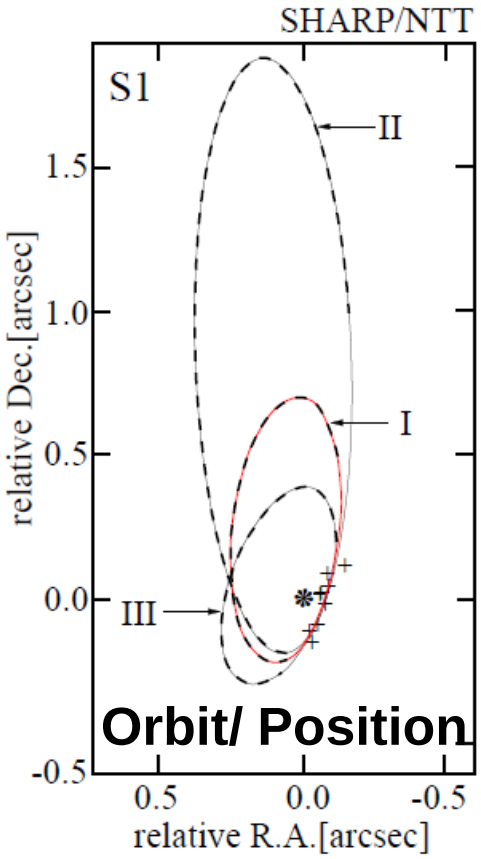

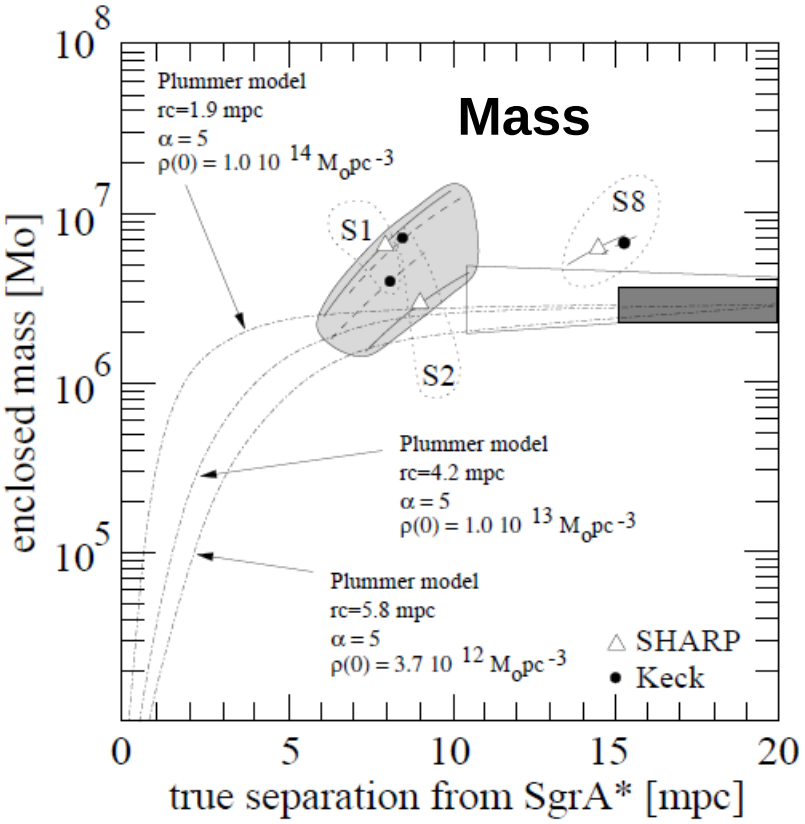

source	S2
i [°]	70^{+6}_{-17}
ω [°]	190^{+10}_{-10}
Ω [°]	23^{+27}_{-11}
e	$0.8^{+0.15}_{-0.40}$
a [mpc]	$5.6^{+0.7}_{-1.1}$
T [yr]	$2002.6^{+6.8}_{-2.2}$
P [yr]	$19.4^{+7.4}_{-3.0}$
s_α [mpc]	-0.38 ± 0.19
s_δ [mpc]	$+5.38 \pm 0.19$
s_z [mpc]	$+6 \pm 1$
v_α [km s^{-1}]	-290 ± 60
v_δ [km s^{-1}]	-694 ± 60
v_z [km s^{-1}]	0 ± 500

Stellar orbits near Sagittarius A*

Eckart, A.; Genzel, R.; Ott, T.; Schödel, R.

2002, MNRAS 331, 917

Very Large Telescope (VLT) - Chile - Paranal

NAOS/CONICA Adaptive Optics
observations in the infrared
at 2 micrometers wavelength


telescopes
Garden with a fire pond that provides moisture.
Hier wohnen die Astronomen

The 4 Very Large Telescopes (VLT) of the European Southern Observatory (ESO)

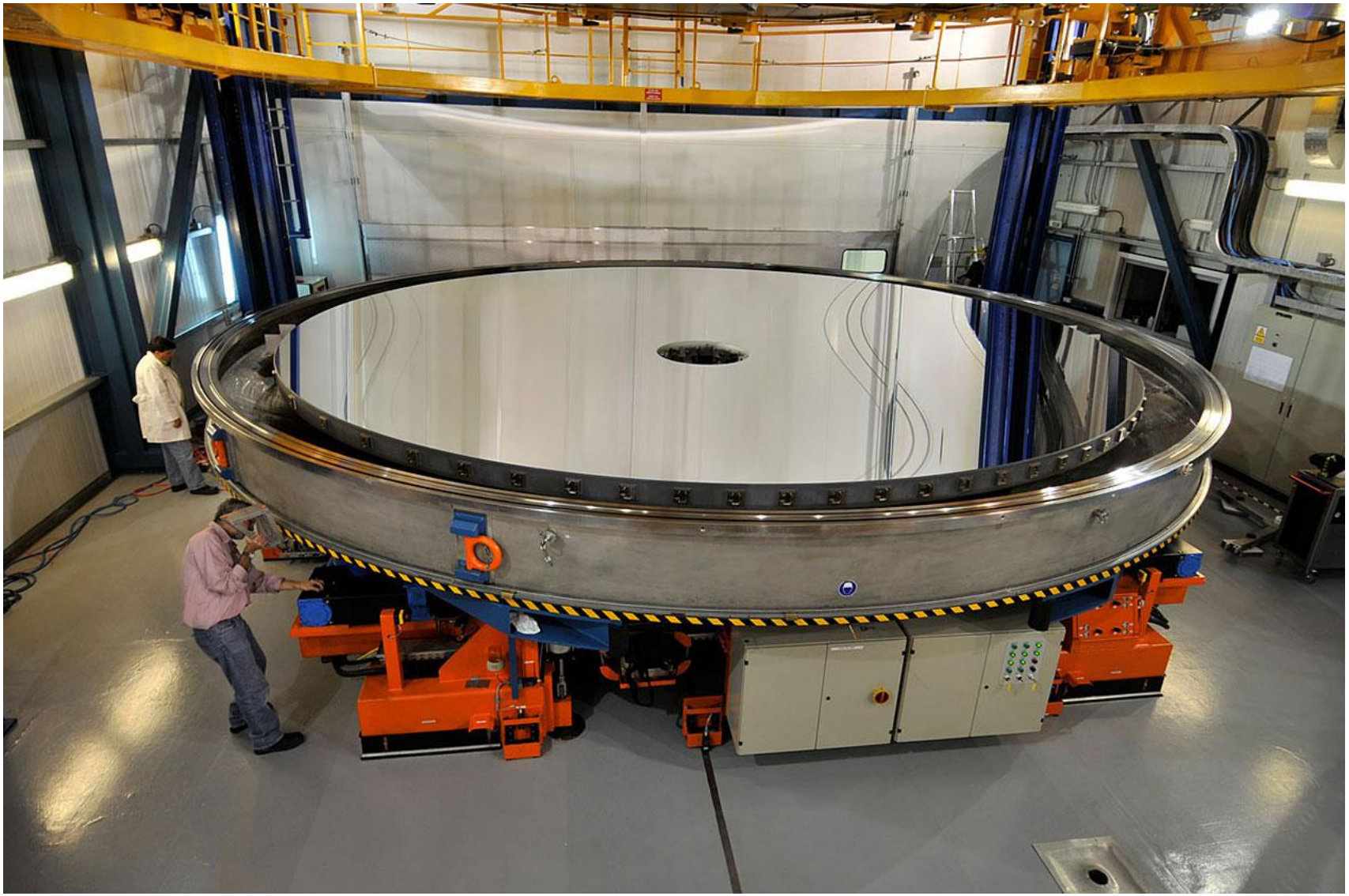

Telescopic structure:
Look at
the mirror cell
of one of the 8
Unit Telescopes (UT)

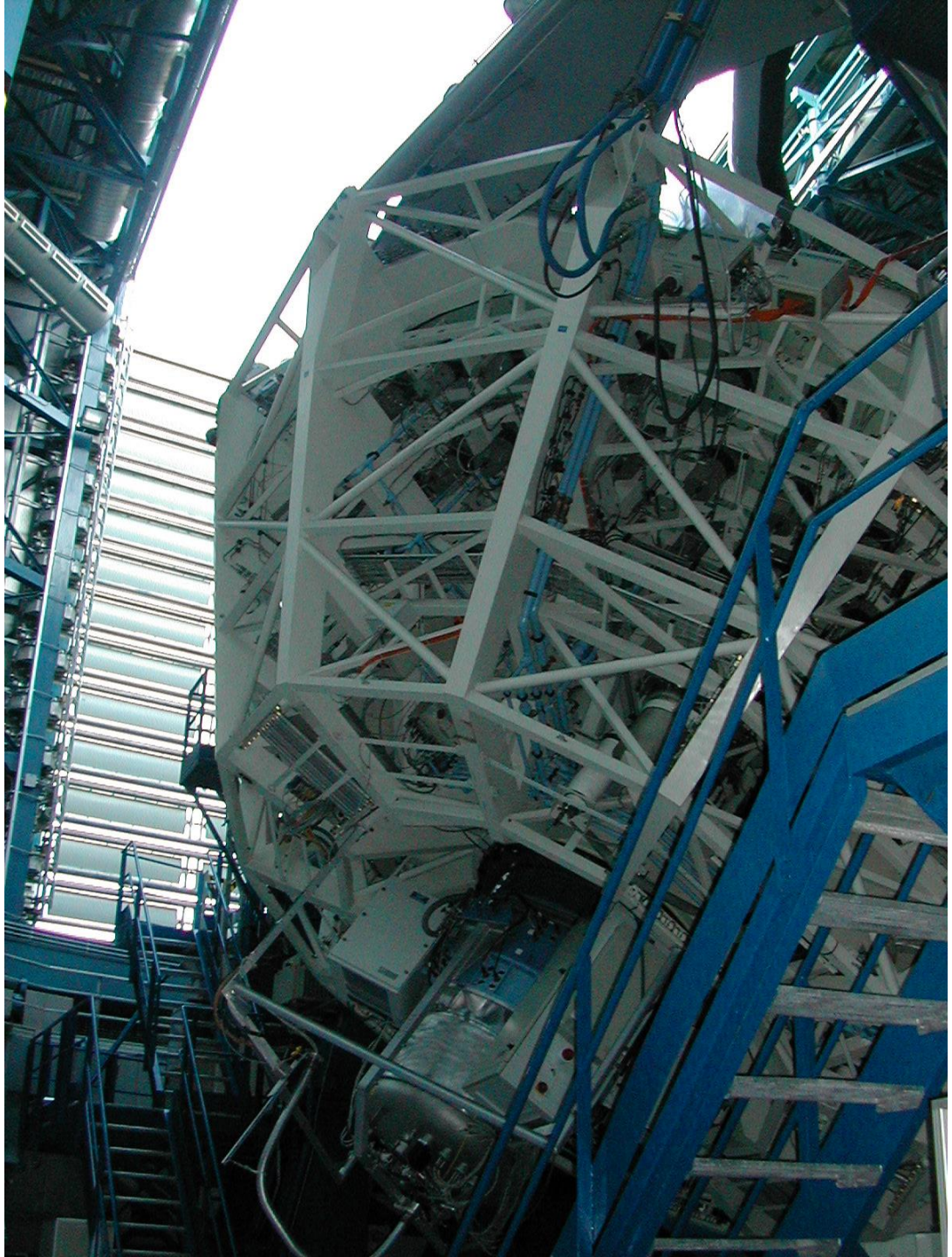

Adaptive Optics
Using a deformable tertiary mirror to straighten the wavefront

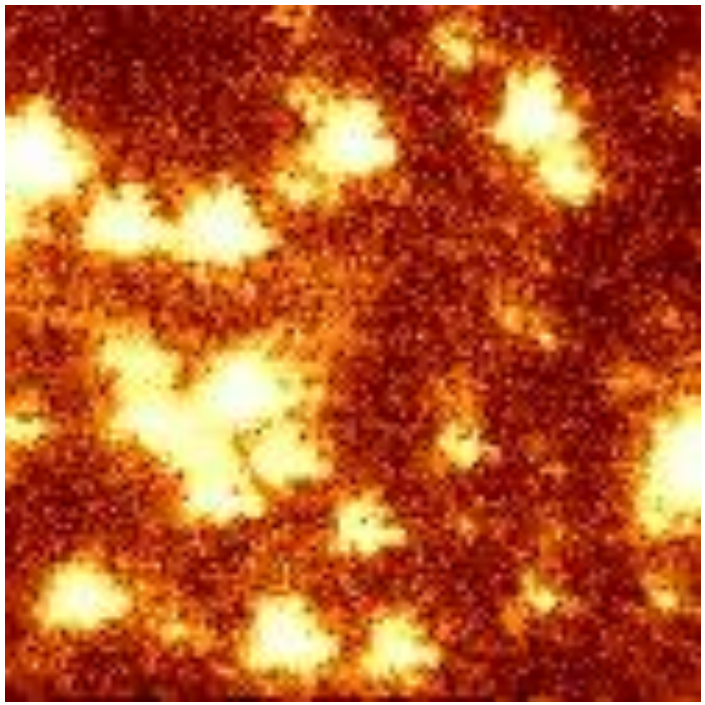

Short-term recordings from the SHARP Camera; Readout time 0.5 seconds

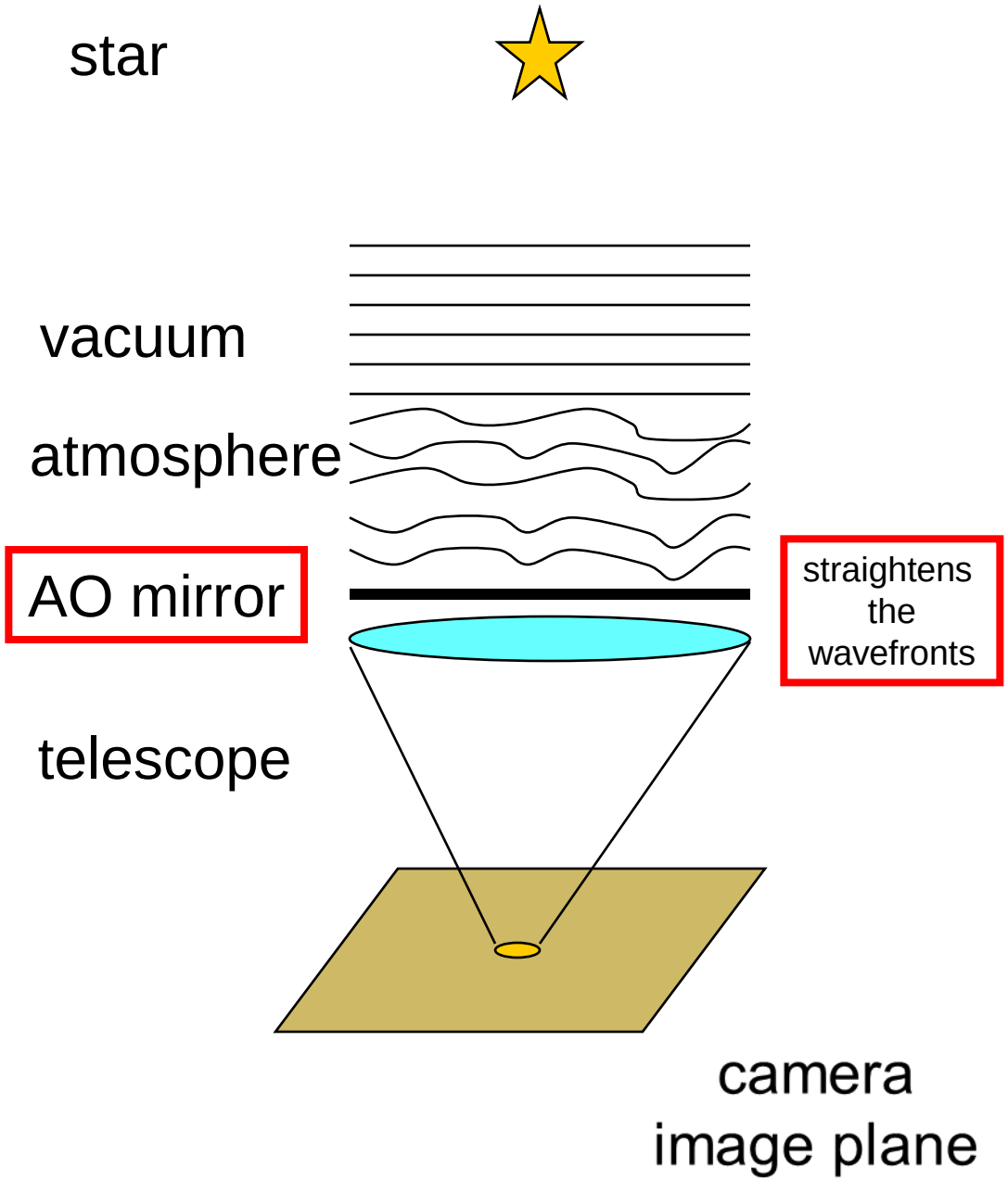

Adaptive Optics

The disturbed wavefront is measured online and straightened using a deformable mirror

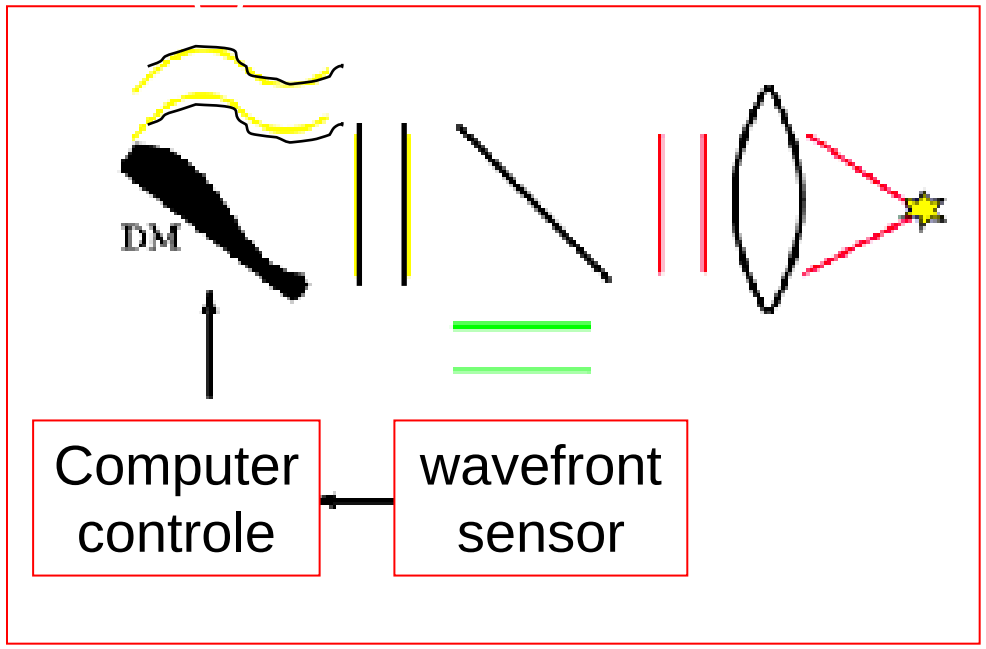

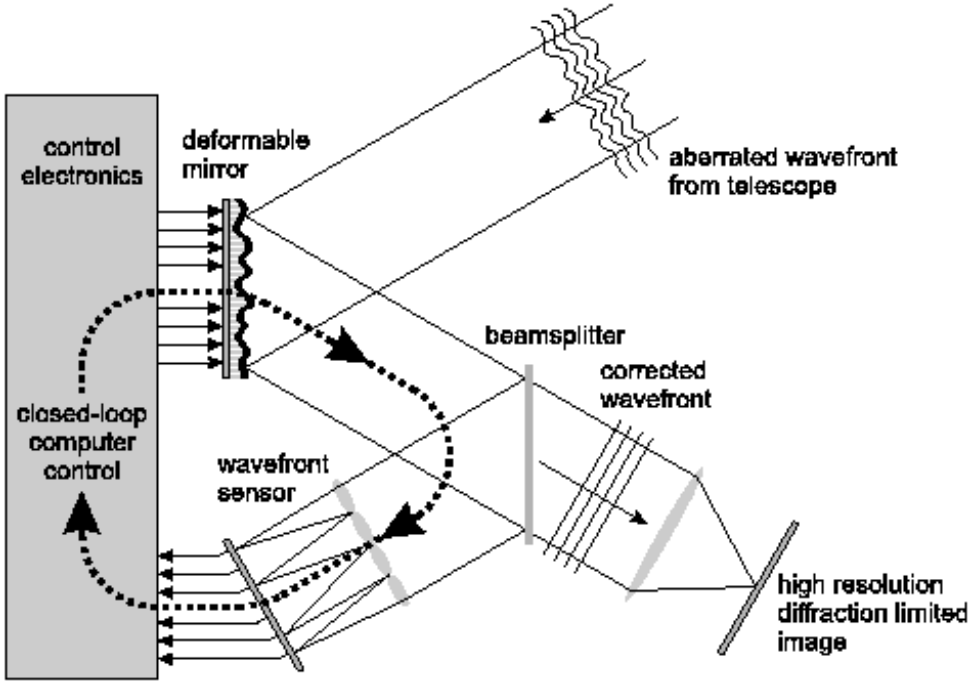

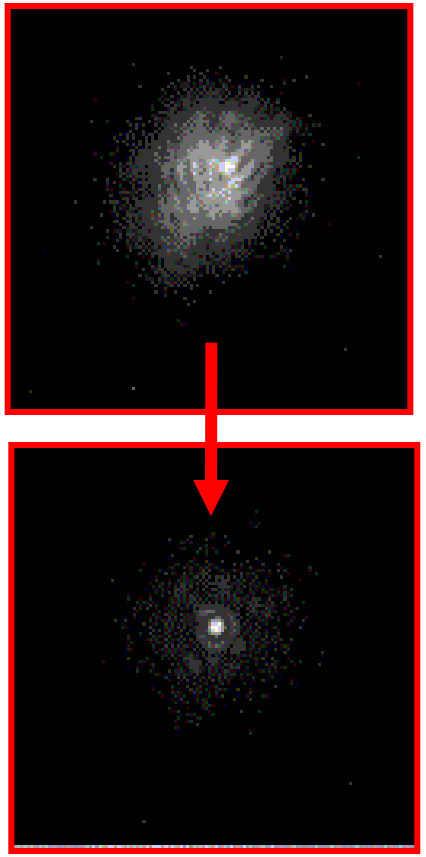

Adaptive Optics at the VLT in Chile

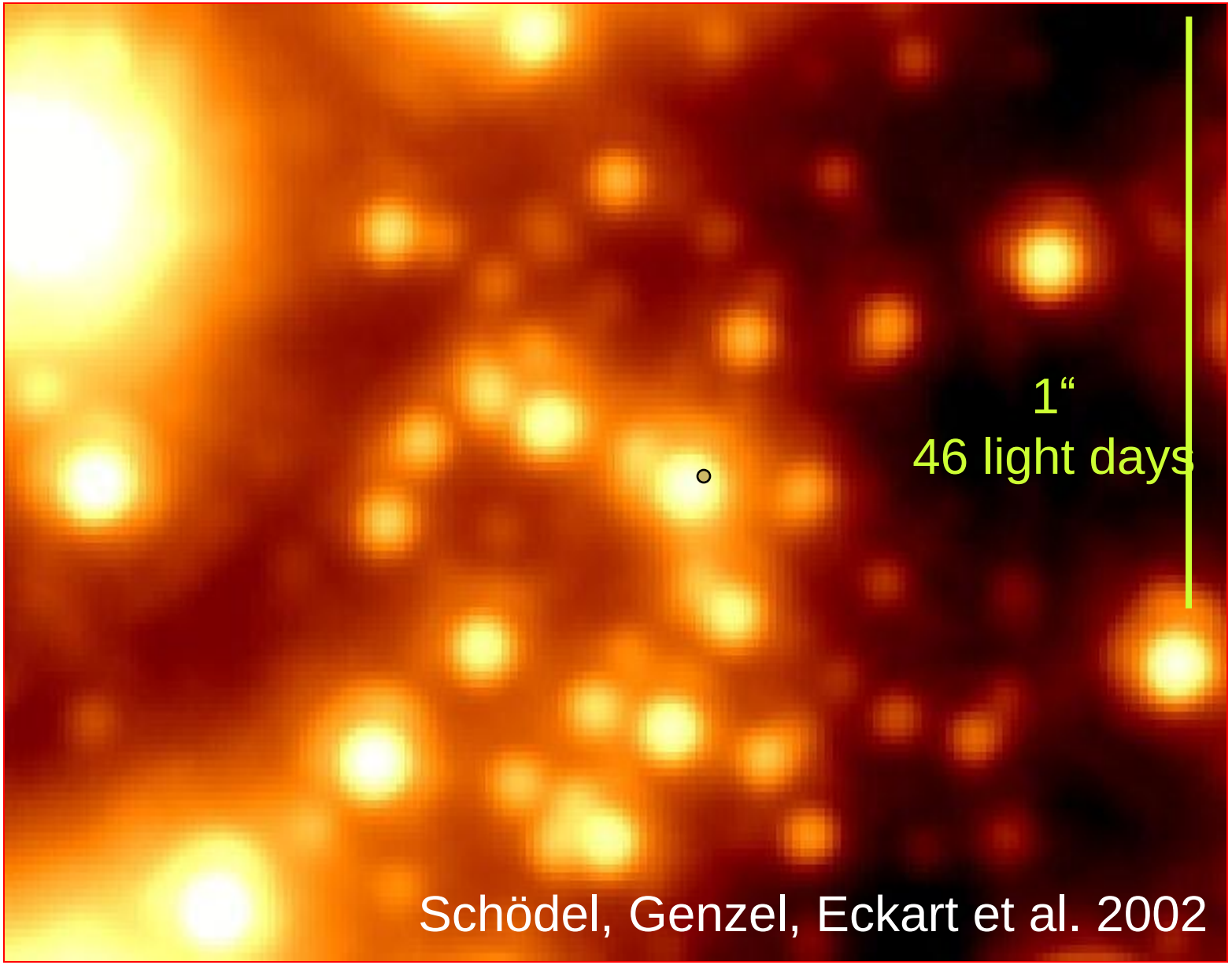

Determinaton of an exact orbit around SgrA * via VLT adaptive optics observations

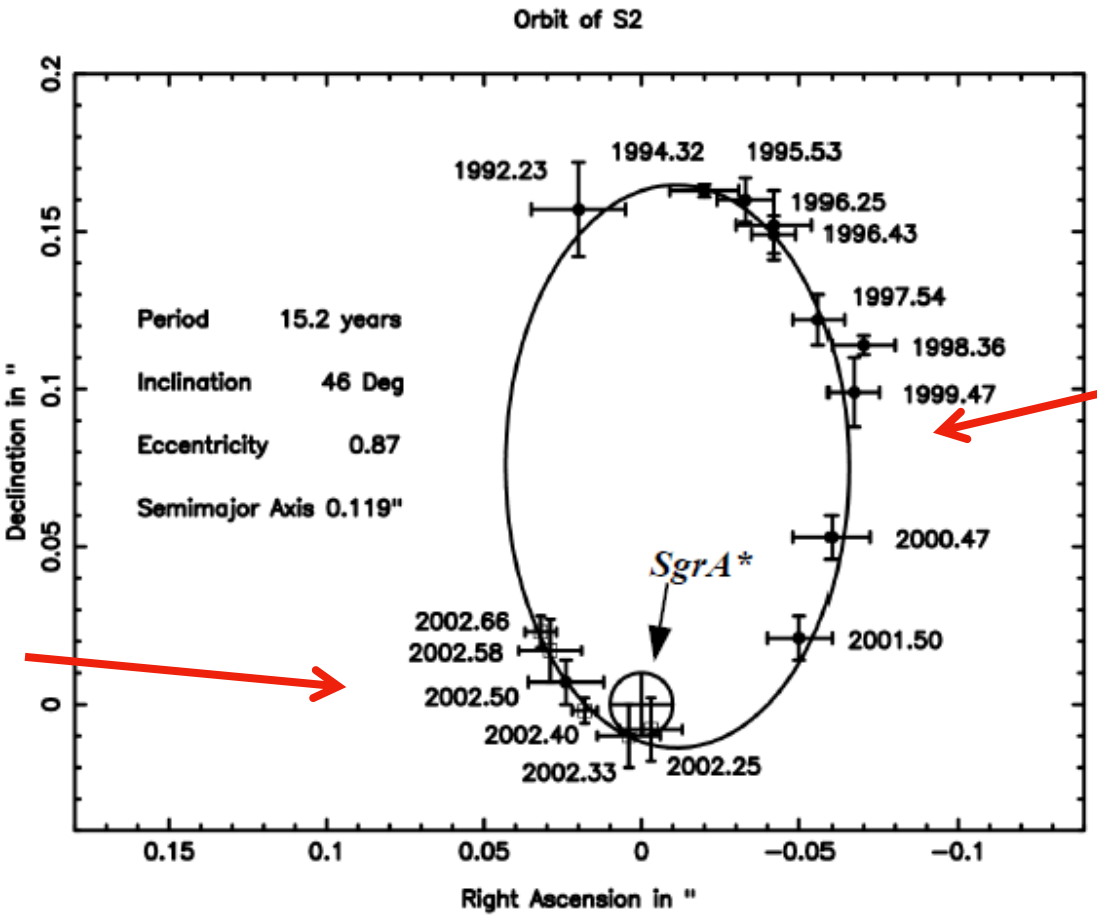

NTT SHARP data

VLT NACO data

A star in a 15.2-year orbit around the supermassive black hole at the center of the Milky Way
Schödel et al., 2002, Nature 419, 694

Bestimmung der Schwarz-Loch-Masse über S2

For S2 the 15.2 year orbit is closed.
Kepler's laws result in:

$$M_{S2} = \frac{4\pi^2}{G}\frac{a^3}{T^2}$$

With the orbital time scale **T** and the semimajor axes **a**.

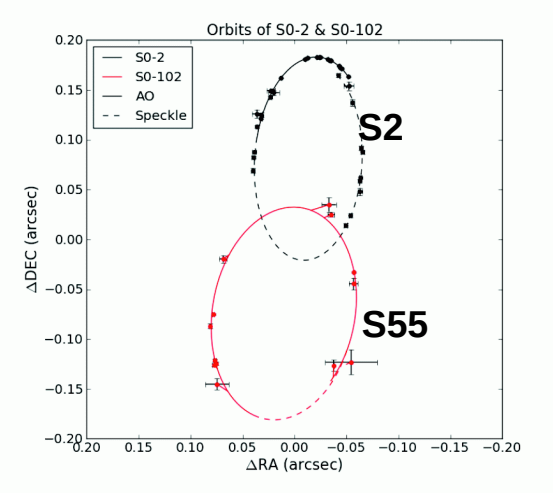

Meyer+ 2012

For S2 this results in:

$$M_{SgrA*} \approx (4 \pm 0.3) \times 10^6 M_o$$

One can solve for the distance at the same time and you get: 8 kpc

Eisenhauer et al. 2005

Data Analysis

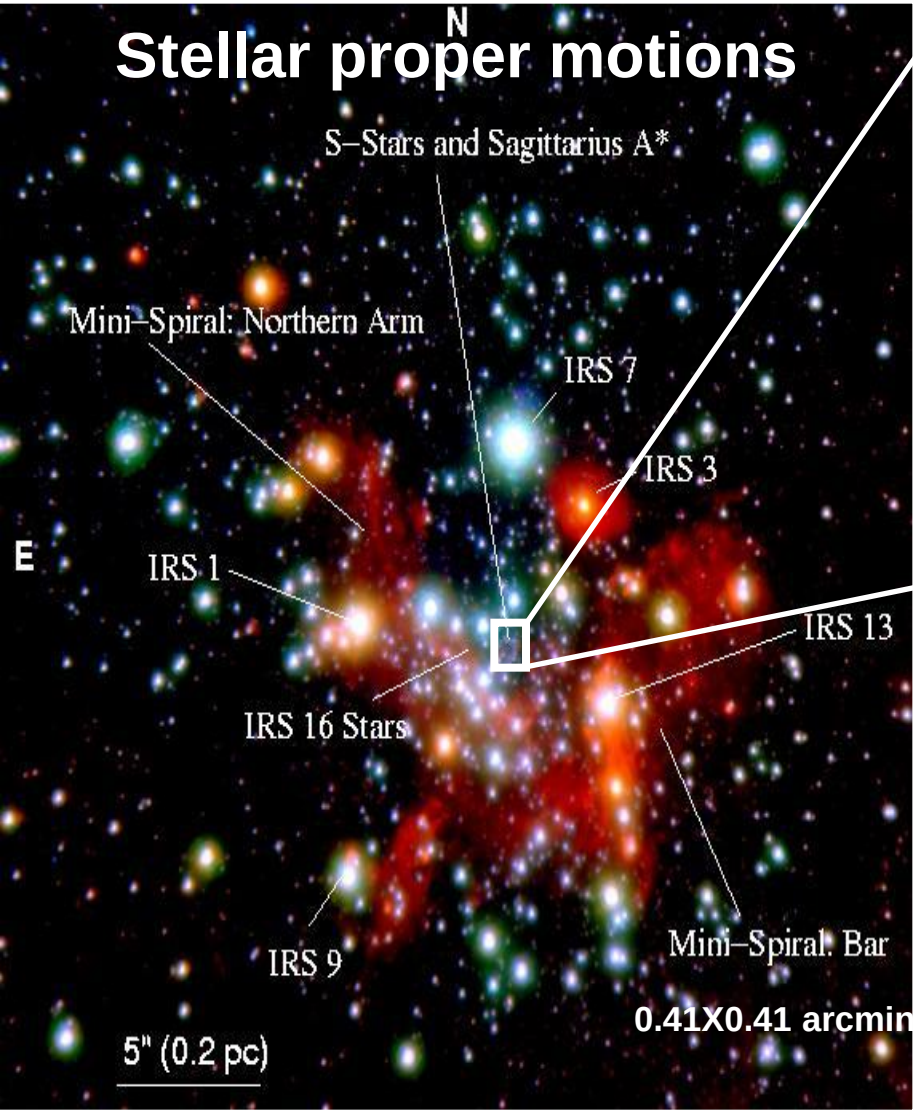

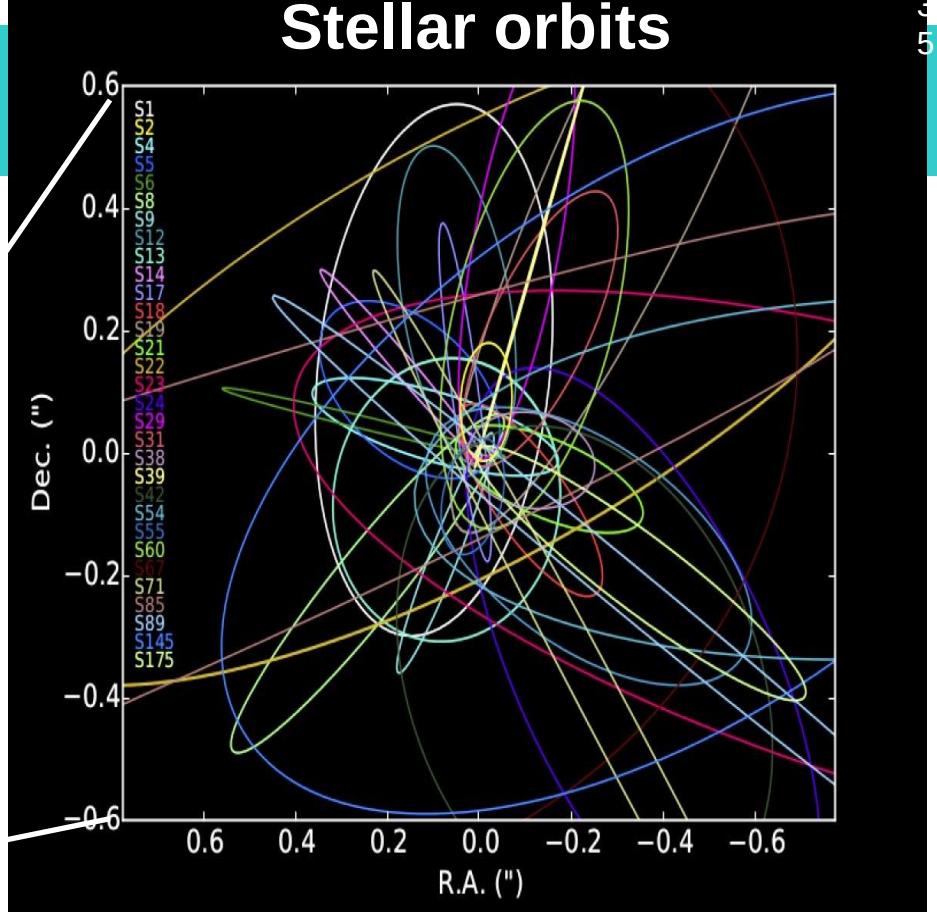

Orbits of almost 60 stars:

- **Ali et al. (2020)**
- **Parsa et al. (2018)**
- **Gillessen et al. (2017)**

First proper motions

- **Eckart & Genzel (1996/1997)**

Central Mass: 4 Million solar masses
Distance: 8 kpc ~ 27.000 light years

Schwarzschild Precession

Light:

Using the inner most stars as a probe for relativity

Probing for the Schwarzschild relativistic periastron shift for S2

M. Parsa, A. Eckart, B. Shahzamanian, V. Karas, M. Zajaček, J. A. Zensus, and C. Straubmeier, 2017 ApJ 845, 22

Relativistic and non-relativistic fits to the data

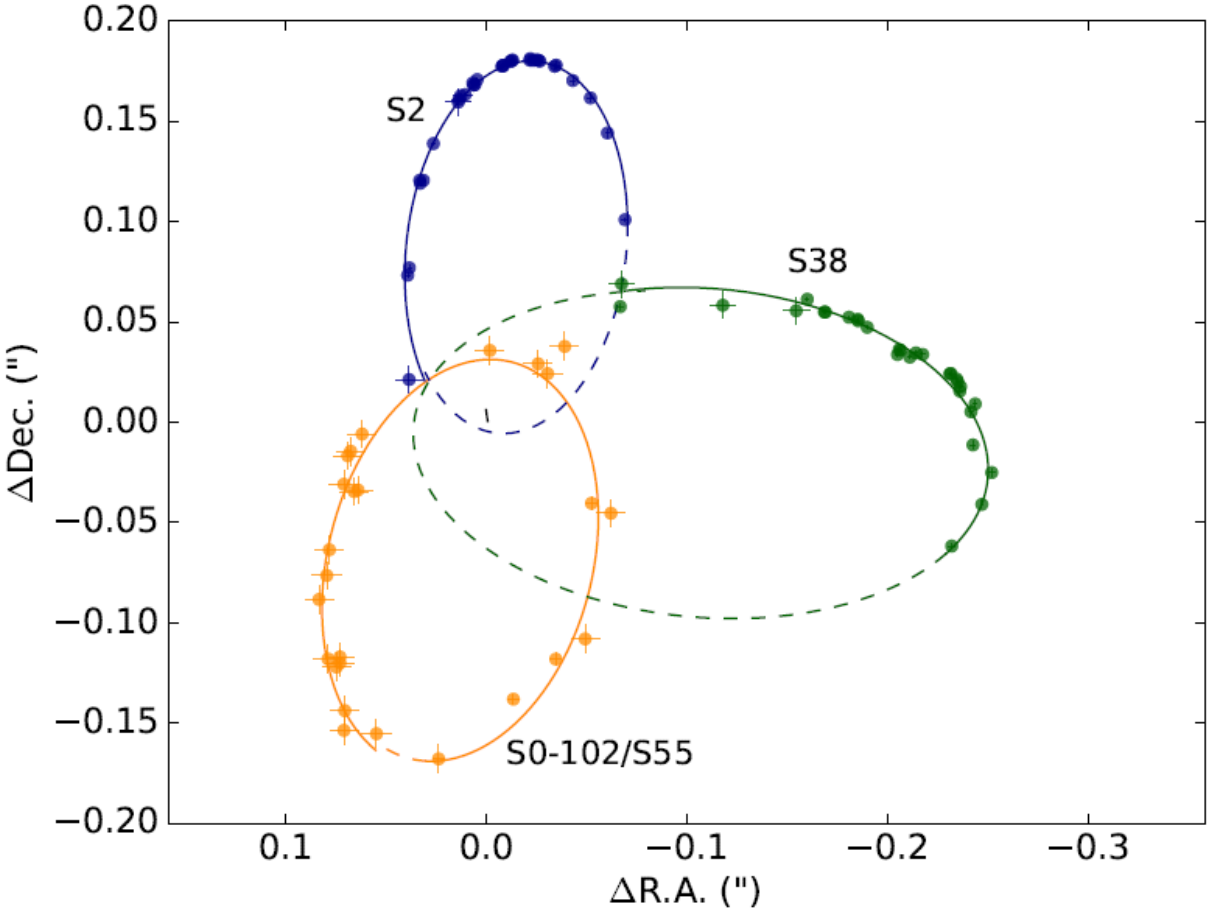

We modeled the stellar orbits in by integrating the equations using the ***4th* order Runge-Kutta method** with up to twelve initial parameters, respectively (i.e. the positions and velocities in 3 dimensions).

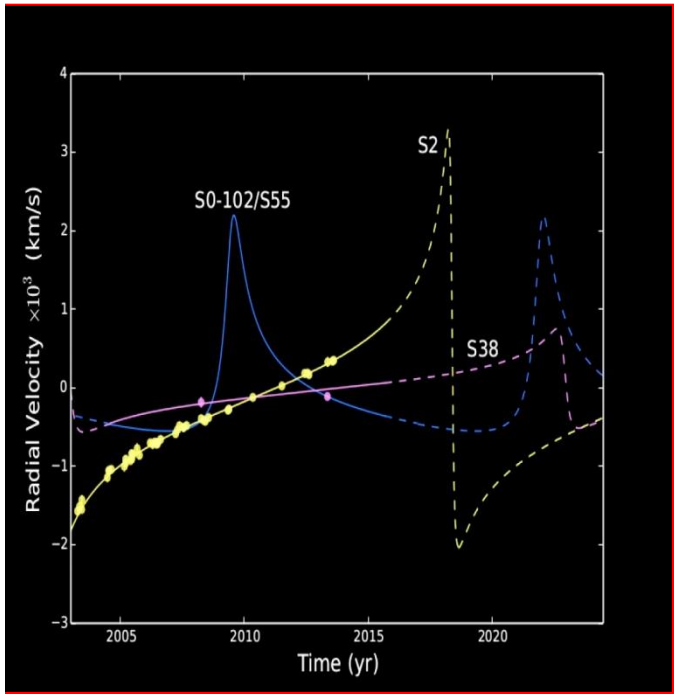

addition to the VLT data, we used published (not shown here) Keck positions by Boehle et al. (2016) in years 1995-2010 and radial velocities by Gillessen et al. (2009) Boehle et al. (2016)

Models

- Newtonian (Keplerian) Model: 6 orbital elements
- Post-Newtonian (PN) Model:
  - Approximate solution to Einstein's equations
  - Expansions of a small parameter: v/c
- Einstein-Infeld-Hoffmann (Einstein et al. 1938) equation of motion:

$$\frac{d\boldsymbol{v}_\star}{dt} = -\frac{GM_{BH}}{c^2 r_\star^3}\left\{\boldsymbol{r}_\star\left[c^2 + v_\star^2 + 2v_{BH}^2 - 4\left(\boldsymbol{v}_\star.\boldsymbol{v}_{BH}\right)\right.\right.$$
$$\left.\left. -\frac{3}{2r_\star^2}\left(\boldsymbol{r}_\star.\boldsymbol{v}_{BH}\right)^2 - 4\frac{GM_{BH}}{r_\star}\right] - \left[\boldsymbol{r}_\star.\left(4\boldsymbol{v}_\star - 3\boldsymbol{v}_{BH}\right)\right]\left(\boldsymbol{v}_\star - \boldsymbol{v}_{BH}\right)\right\}$$

- or for negligible proper motion of the SMBH (Rubilar & Eckart 2001):

$$\frac{d\boldsymbol{v}_\star}{dt} = -\frac{GM_{BH}}{c^2 r_\star^3}\left[\boldsymbol{r}_\star\left(c^2 - 4\frac{GM_{BH}}{r_\star} + v_\star^2\right) - 4\boldsymbol{v}_\star\left(\boldsymbol{v}_\star.\boldsymbol{r}_\star\right)\right]$$

Periaps shift has at least 3 major contributions:

1. **Prograde relativistic periastron shift**
2. **Retrograde Newtonian periastron shift**
3. **Plus a possible granularity of an extended mass**

(**Sabha et al. 2012**)

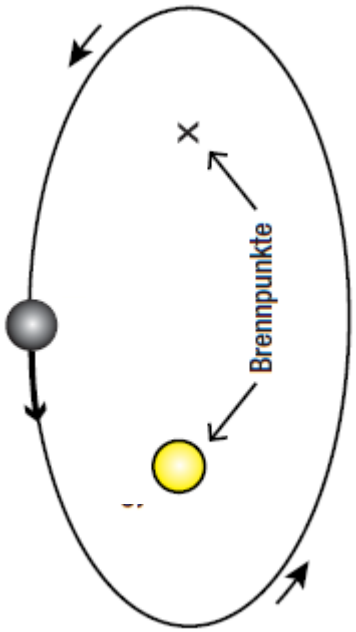

Kepler Mewton

The argument of the Periapse angle changes

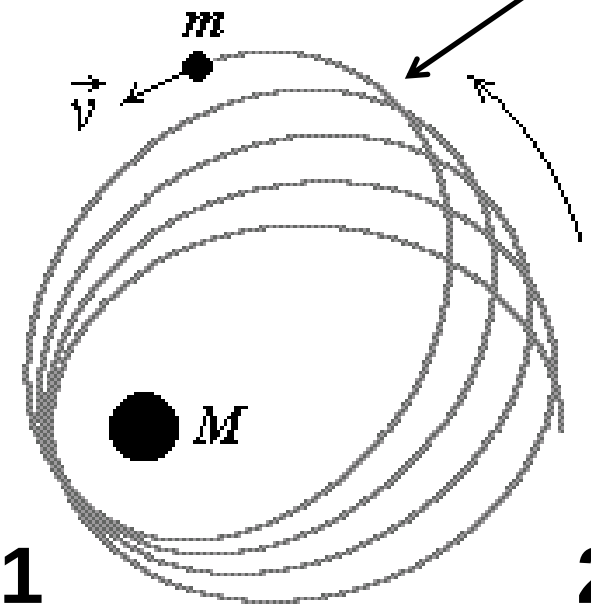

1

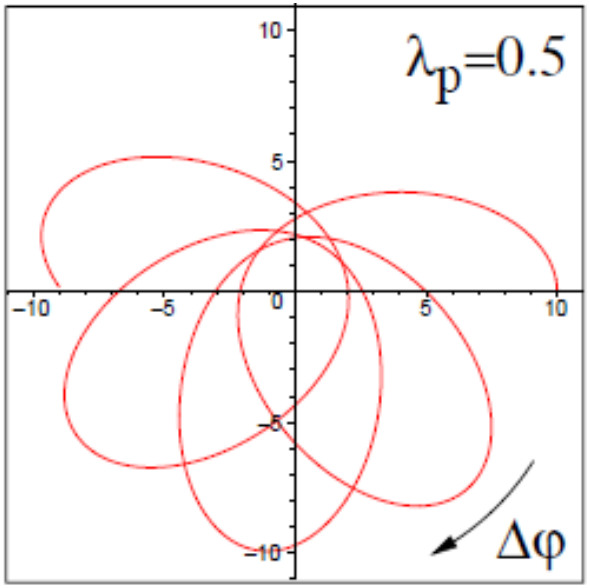

2

These effects become noticeable through a deviation from the elliptical orbit shape

Rubilar & Eckart 2001

Method

One can derive measures for non ellipticity.

All of these quantities measure the deviation from ellipticity and can be correlated with the degree of relativity:

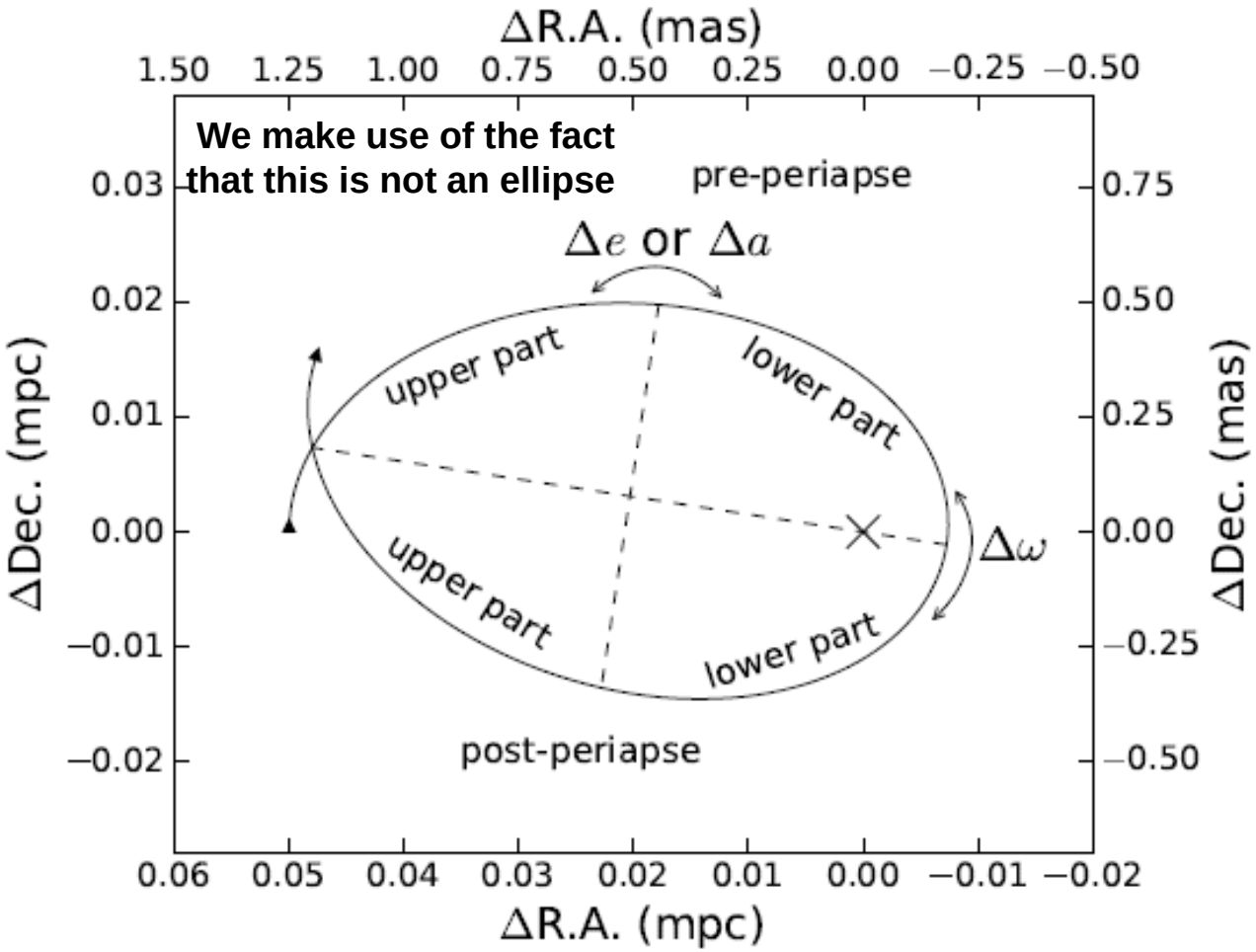

$$\chi^2_u \,/\, \chi^2_{u,\chi^2_l \to 1}$$

$$a_l \,/\, a_u$$

$$e_l \,/\, e_u$$

$$\Delta\omega$$

Visualization of Results

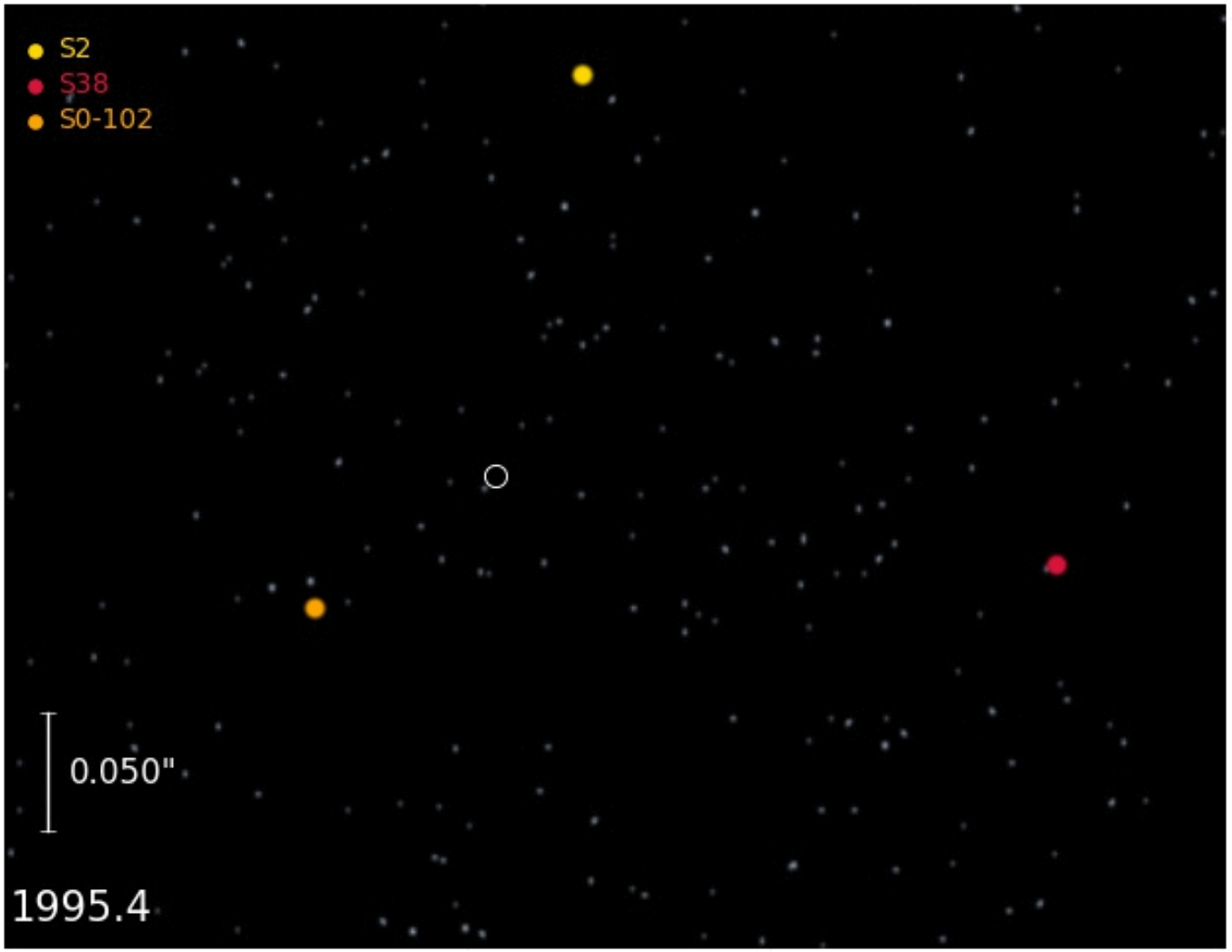

ESO press annoncement 9 August 2017: ann17051:
Hint of Relativity Effects in Stars Orbiting the Supermassive Black Hole at Centre of Galaxy

Parsa et al. 2017

Results

- The best estimates for the mass and the distance to Sgr A* are:

$$M_{BH} = (4.15 \pm 0.13 \pm 0.57) \times 10^6 M_{sun}$$

$$R_0 = 8.19 \pm 0.11 \pm 0.34 \ \ kpc$$

- The change in the argument of periapse of S2 is

$$\Delta\omega_{obs} = 14\ ' \pm 3$$

$$\Delta\omega_{expected} = 11\ '$$

- The changes in the orbital elements of S2 imply relativistic parameter of:

$$Y_{obs} = 0.00088 \ \pm 000065$$

Eckart et al. 2018

Parsa et al. 2017

$$Y_{expected} = 0.00065$$

Relativistic Parameter Y:
Zucker et al. 2006

$$Y = \frac{r_s}{r_p}$$

Relativistic Redshift

Light:

Using the inner most stars as a probe for relativity

Measuring the relativistic redshift of S2

GRAVITY Collaboration, 2018, A&A 615, L15

VLTI: GRAVITY

Principle Investigator: Frank Eisenhauer (MPE, Garching)

Builders: The Gravity consortium:

- Max-Planck-Institut für Exterterrestrische Physik (Garching),
- LESIA, Observatoire de Paris, Section de Meudon,
- Laboratoire d'Astrophysique, Observatoire de Grenoble,
- Max-Planck-Institut für Astronomie (Heidelberg),
- I. Physikalisches Institut, Universität zu Köln,
- SIM, Faculdade de Ciências da Universidade de Lisboa

Assistance via the European Southern Observatory

Difference between radio- and optical/infrared interferometry:

In the radio the signal transport and delay compensation is done via at intermediate frequencies via cable, tape and electronically.
In the optical/IR you cannot stably and loss free mix down to an intermediate frequency, hence, it is done at sky frequecies via light and mirrors.

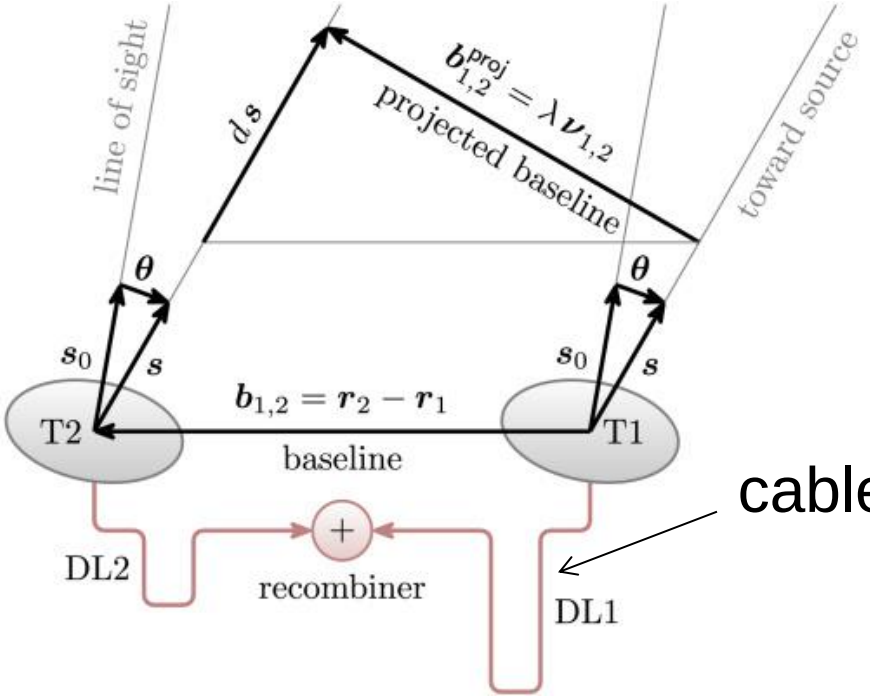

cables

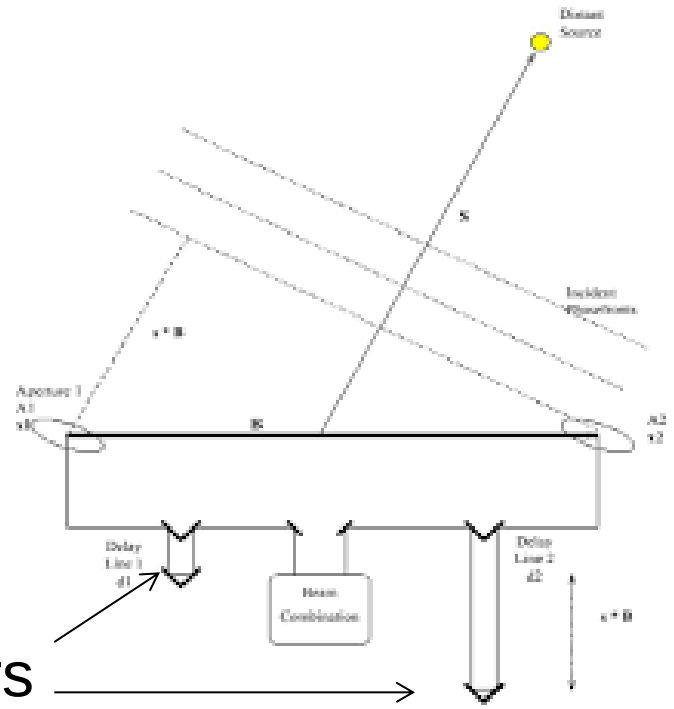

mirrors

VLTI: VLT Interferometry with GRAVITY

High angular resolution measurements via connecting individual telescope

VLTI: VLT Interferometry with GRAVITY

High angular resolution measurements via connecting individual telescope

VLTI: VLT Interferometry with GRAVITY

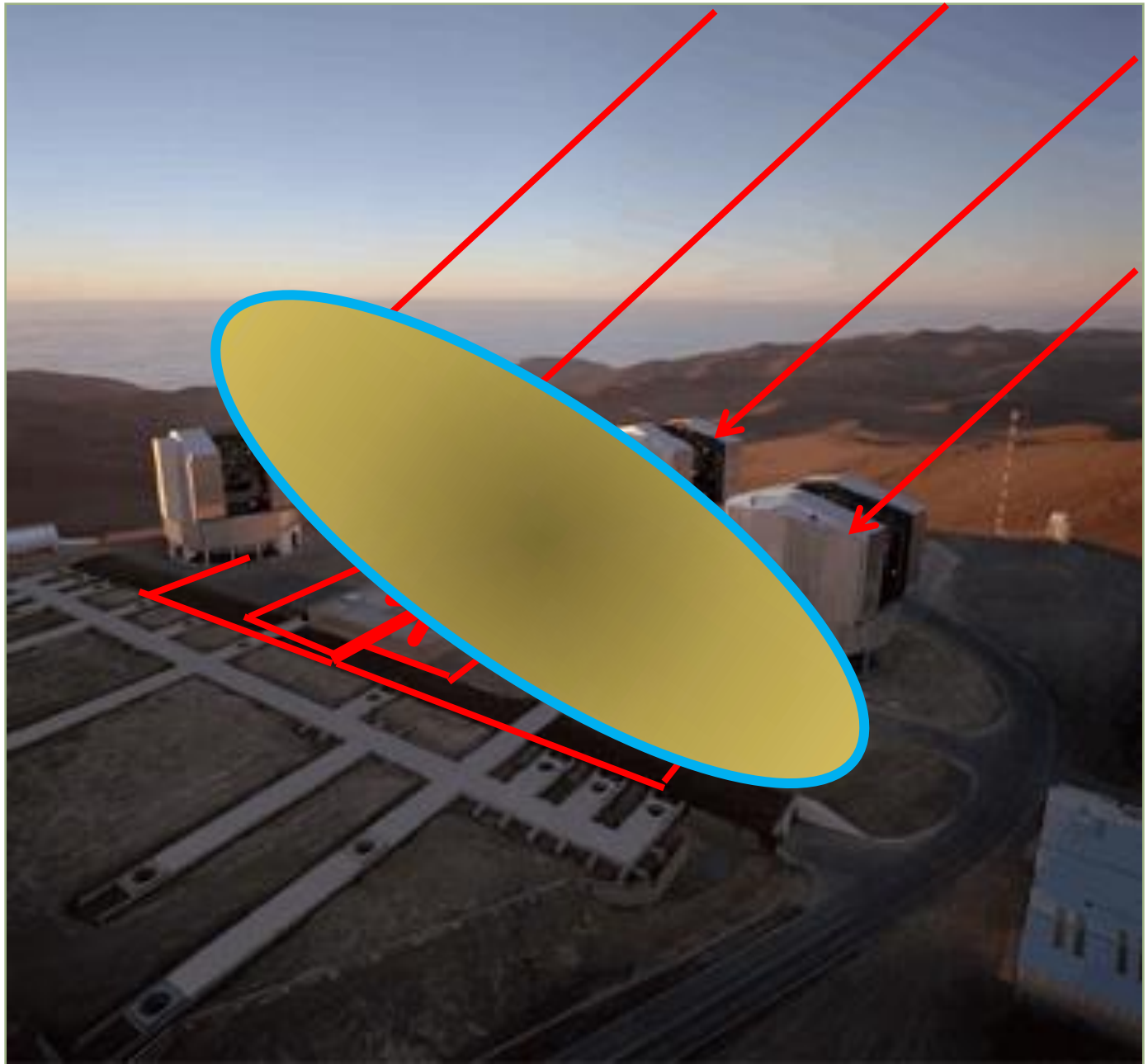

High angular resolution measurements via connecting individual telescope

This is how a telescope of much larger diameter is simulated

VLTI: VLT Interferometry with GRAVITY

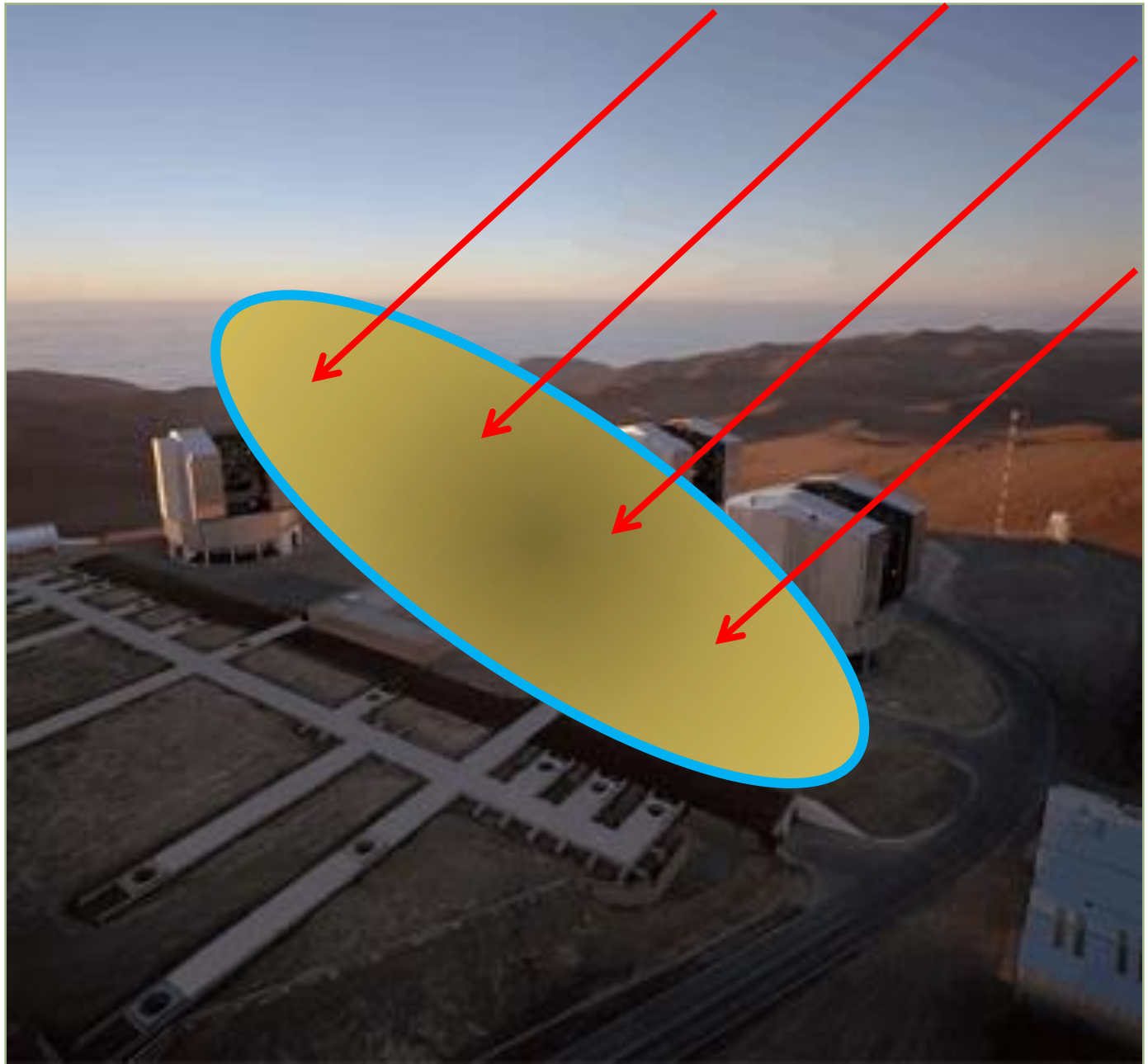

High angular resolution measurements via connecting individual telescope

This is how a telescope of much larger diameter is simulated

VLTI: GRAVITY

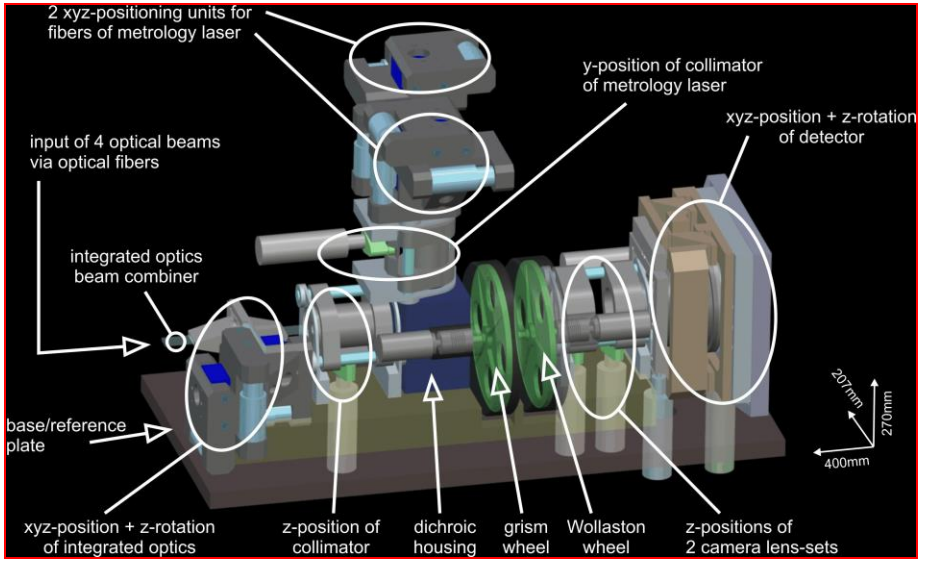

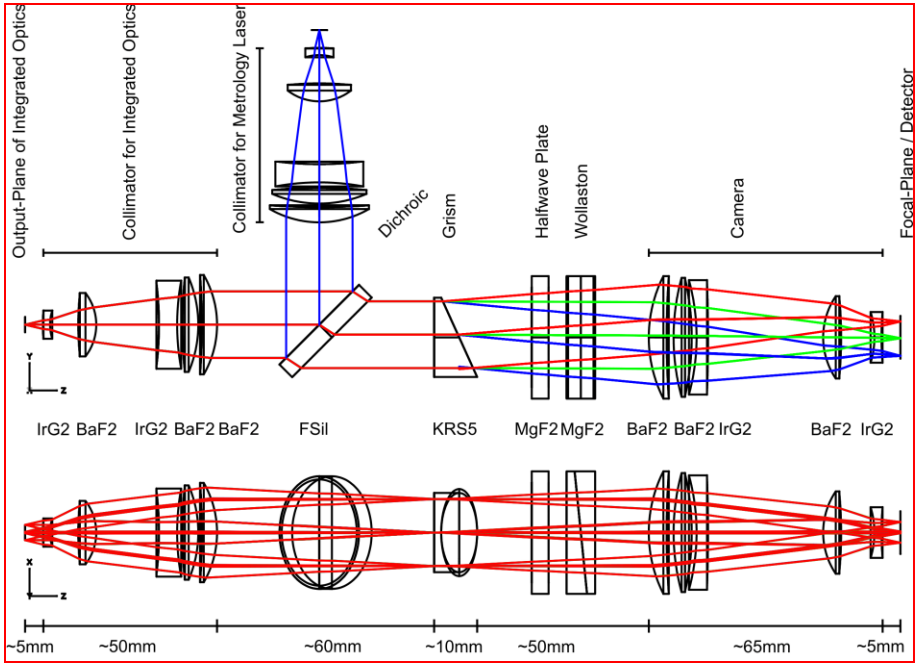

Cologne University provided the two beam combining spectrometers

Straubmeier, Eckart

ESO Beam combiner tunnels

The VLT Array on the Paranal Mountain

ESO PR Photo 14a/00 (24 May 2000) ©European Southern Observatory

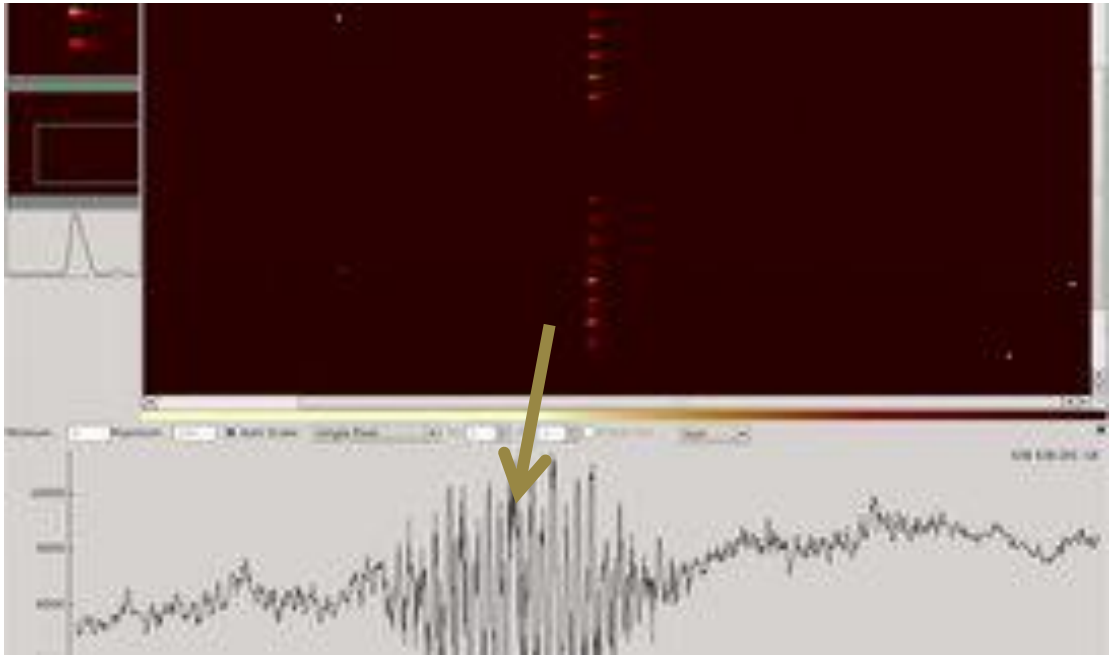

First light with the Cologne beam combination spectrometers (left) integrated into the beam combiner (below) of GRAVITY at the Paranal mountain in Chile

Schwarzschild Precession

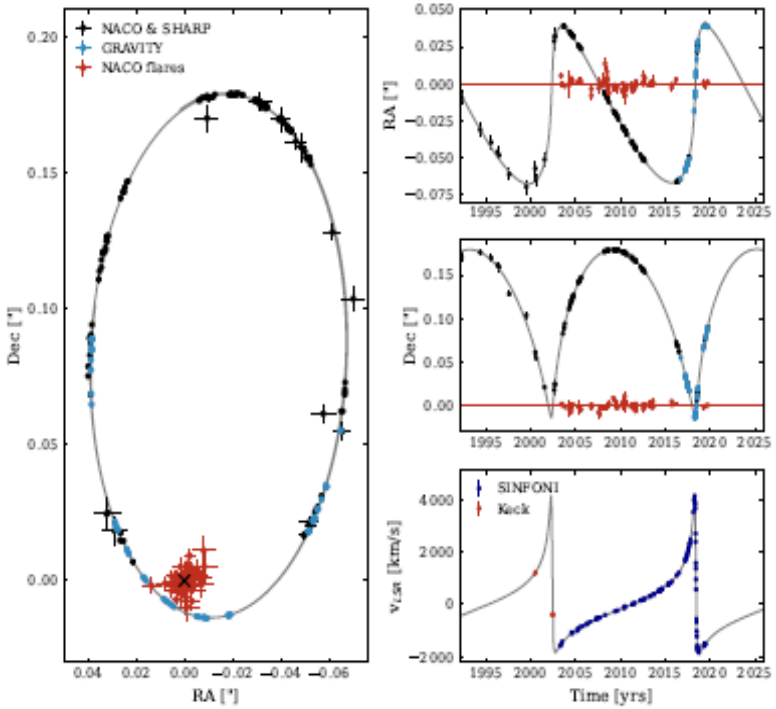

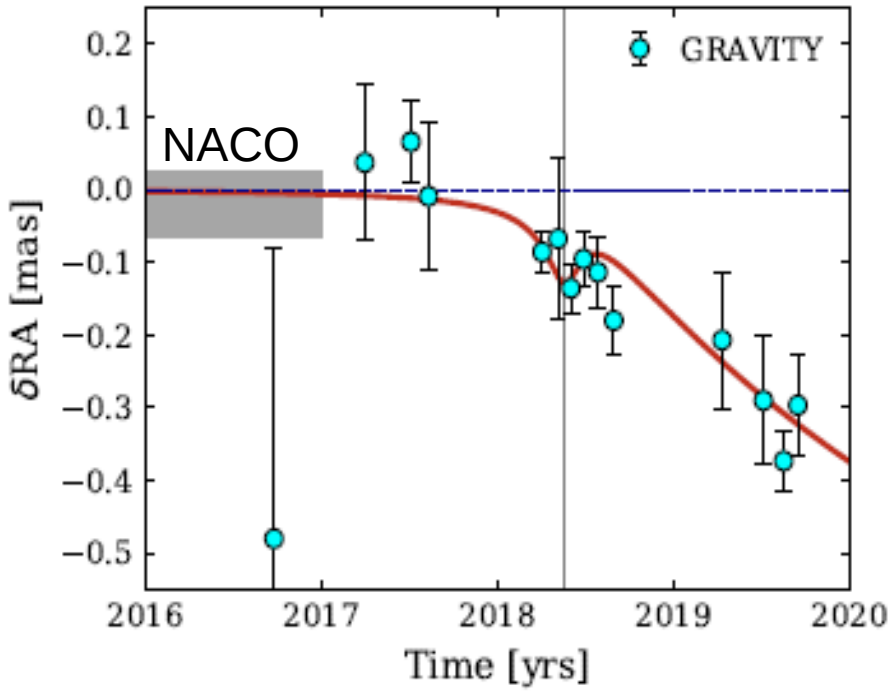

Detection of the Schwarzschild precession in the orbit of the star S2 near the Galactic centre massive black hole

Gravity Collaboration; 2020, A&A 636, L5

Gravitational Redshift

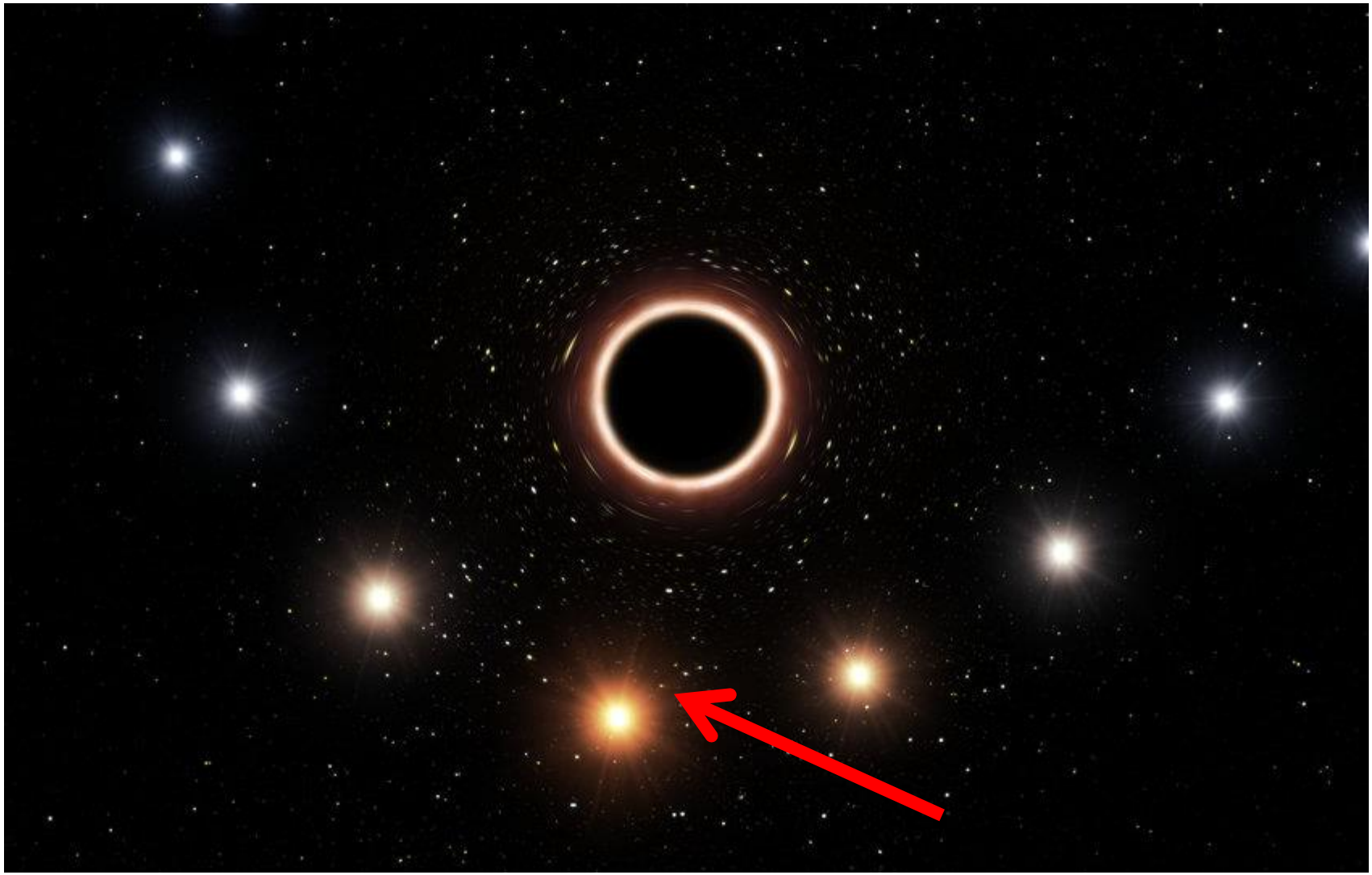

Observed redshift as a function of the 3 dimensional velocity β

$$z = \Delta\lambda / \lambda = B_0 + B_1\beta + B_2\beta^2 + O(\beta^3)$$

Relativistic Redshift

$$B_2 = B_{2,D} + B_{2,G} = \frac{1}{2} + \frac{1}{2}$$

$B_{2,G}$: gravitational redshift effect

$$z_G \equiv r_s / 4a + \frac{1}{2}\beta^2 = B_{0,G} + B_{2,G}\beta^2$$

$B_{2,D}$: special relativistic transverse Doppler effect

$$z_D \equiv (1+\beta\cos\vartheta)(1-\beta^2)^{-1/2} - 1$$

$$z_D \equiv z_{Newton} + z_{transverse} = \beta\cos\vartheta + \beta^2/2 = B_1\beta + B_{2,D}\beta^2$$

Zucker et al. 2006

Gravitational Redshift

B 2,G

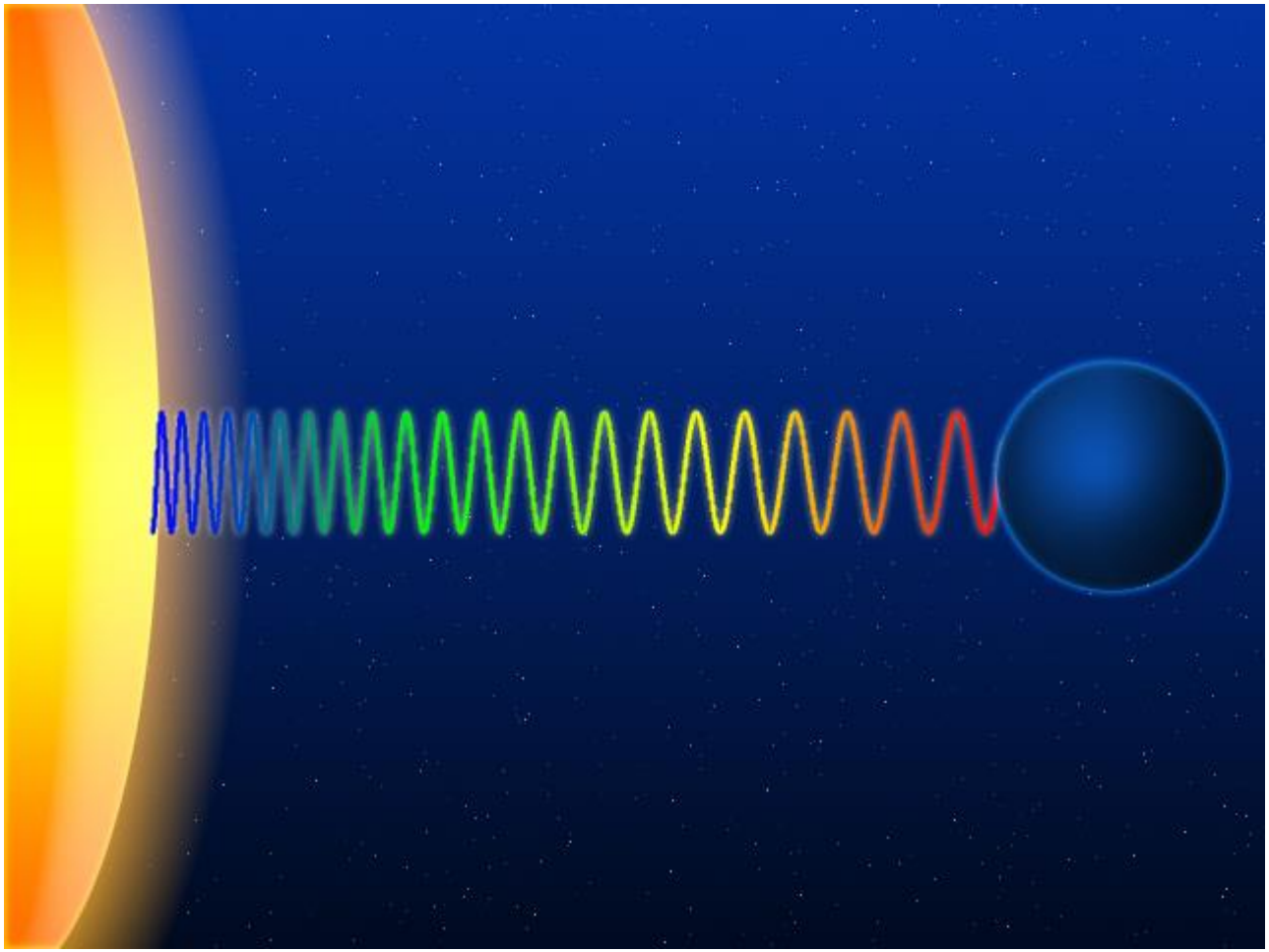

B 2,D plus – transversaler Dopplereffekt

$O(\beta^2)-$ effects should be observable with today's instrumentation:

$$(B_{2,D}+B_{2,G})\beta_P^2 \sim 10^{-3} > \frac{\delta\lambda}{\lambda} \sim 10^{-4}$$

$$\beta_P \sim \frac{v_{Peri}}{c}$$

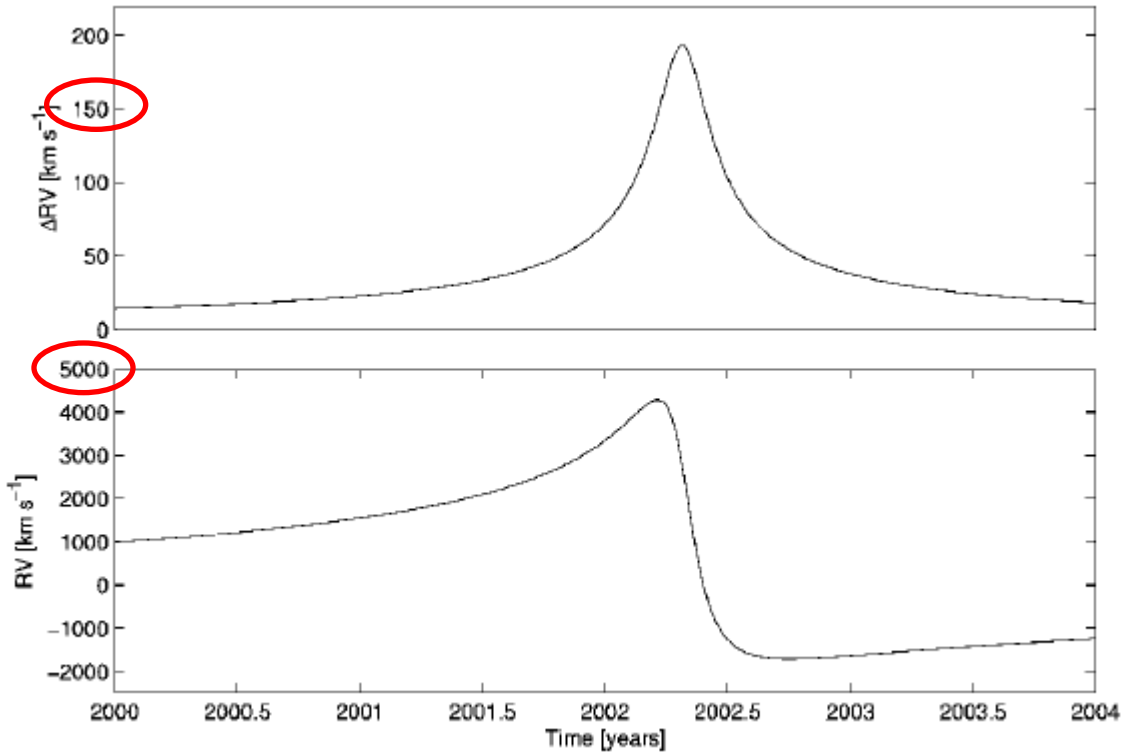

Contribution of the $O(\beta^2)-$ effects

full relativistic radial velocity of S2 near periaps

S2 e=0.88, r = 1500 rs

S14 e=0.94 r = 1400 rs

Zucker et al. 2006

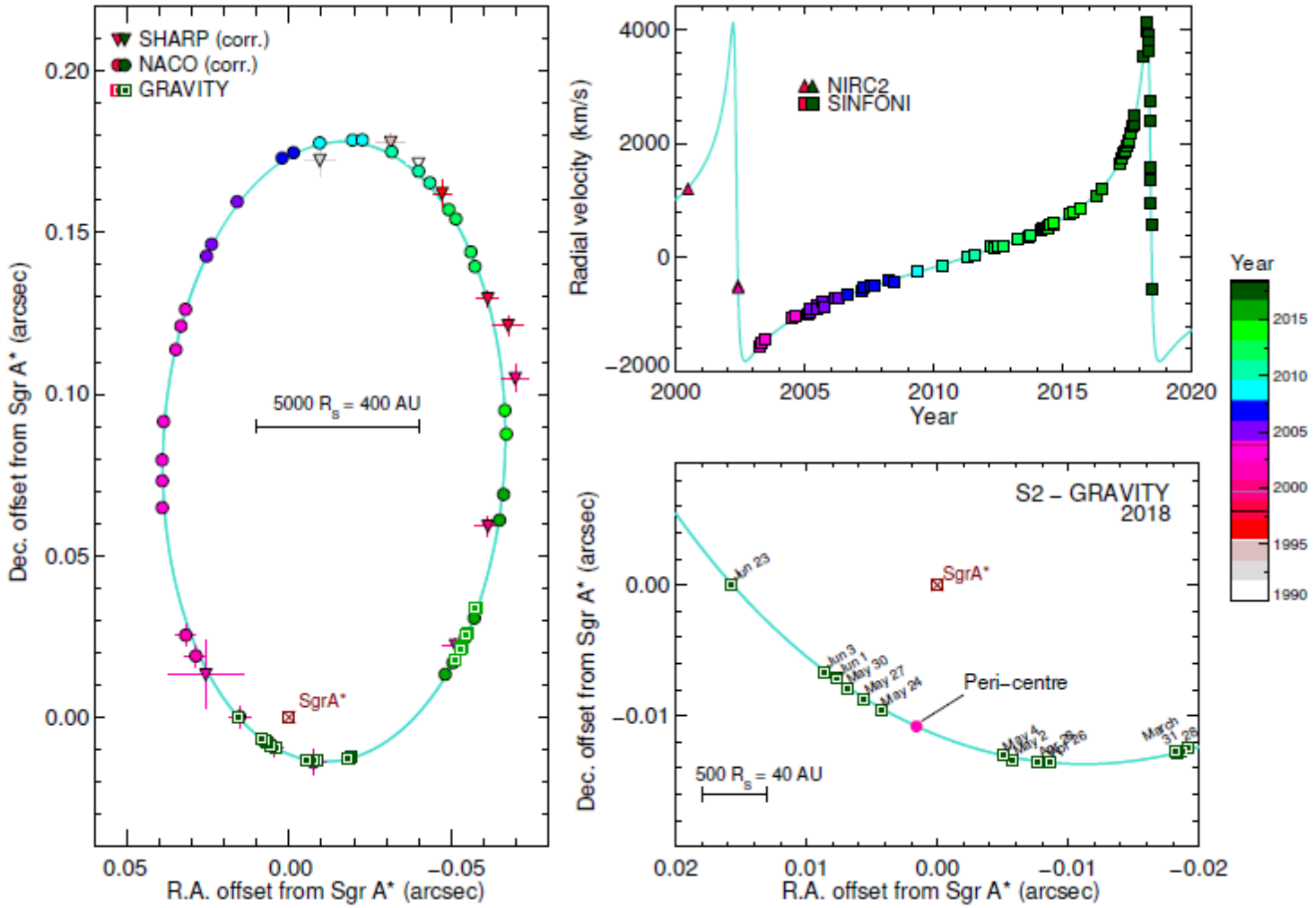

The S2 orbit from 1992 to 2018.

SHARP @ NTT – NACO & SINFONI @ VLT – GRAVITY @ VLTI

Observed Gravitational Redshift

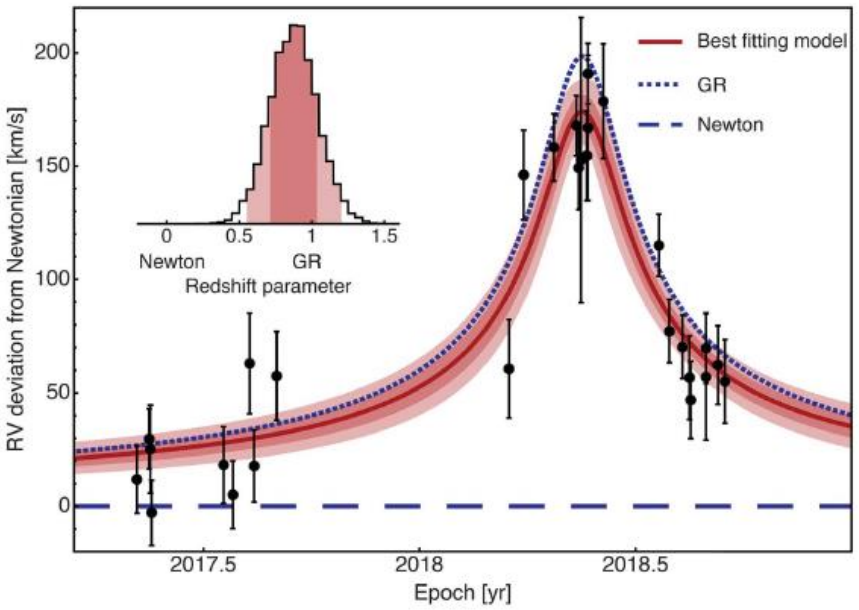

Do, Hees, Ghez et al. 2019, Sci 365, 664

Residual velocity for the best fitting Keplerian and relativistic orbit

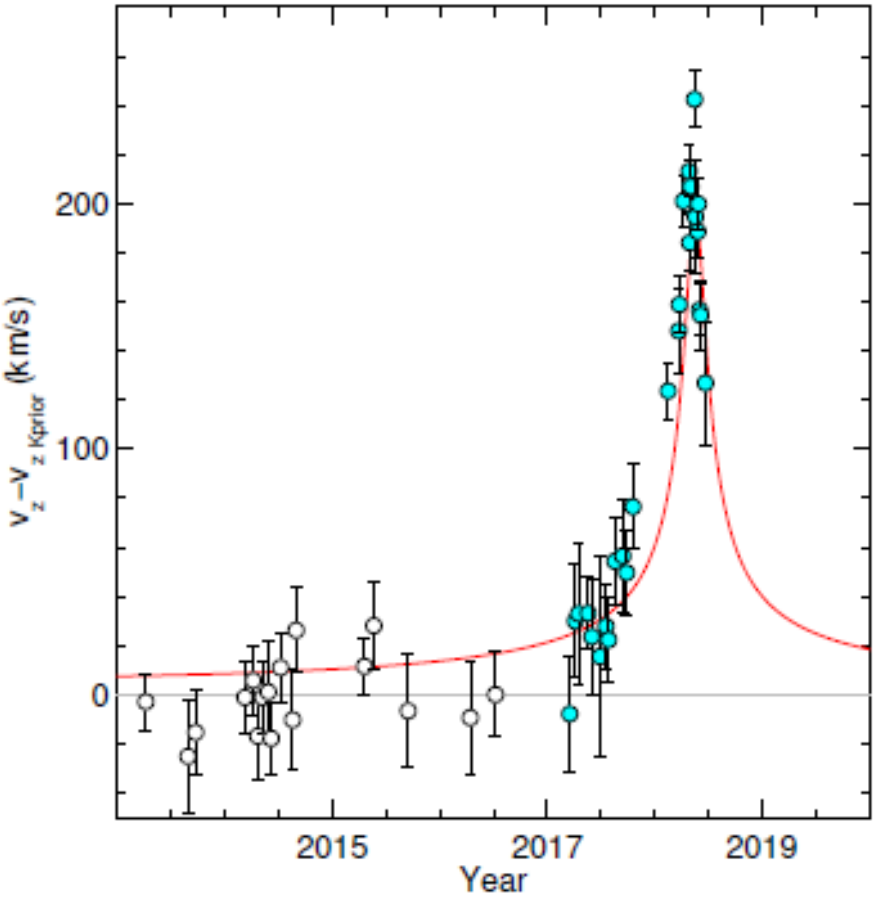

Gravity collaboration 2018, A&A 615, L15

Gravity collaboration 2018, A&A 615, L15

Best fit orbit parameters of S2 with and without Schwarzschild precession.

Parameter	Without Schwarzschild precession	With Schwarzschild precession	Unit
f	0.901 ± 0.090	0.945 ± 0.090	
$M_\bullet$	4.106 ± 0.034	4.100 ± 0.034	$10^6\, M_\odot$
R_0	8127 ± 31	8122 ± 31	pc
a	125.38 ± 0.18	125.40 ± 0.18	mas
e	0.88473 ± 0.00018	0.88466 ± 0.00018	
i	133.817 ± 0.093	133.818 ± 0.093	°
ω	66.12 ± 0.12	66.13 ± 0.12	°
Ω	227.82 ± 0.19	227.85 ± 0.19	°
P	16.0526	16.0518	yr
$t_{\rm peri}$	2018.37965 ± 0.00015	2018.37974 ± 0.00015	yr
	58257.667 ± 0.054	58257.698 ± 0.054	MJD

Flux density flares

Light and Shadow:

Using emitting plasma blobs
as probes for relativity
&
Shadow from the Black Hole ?

The X-ray / NIR / radio view

Credit:
ESO VLT
ISAAC composit
at 2 μm
Rainer Schödel
~3 arcmin
across
(22 light years)

First X-ray flare from SgrA*

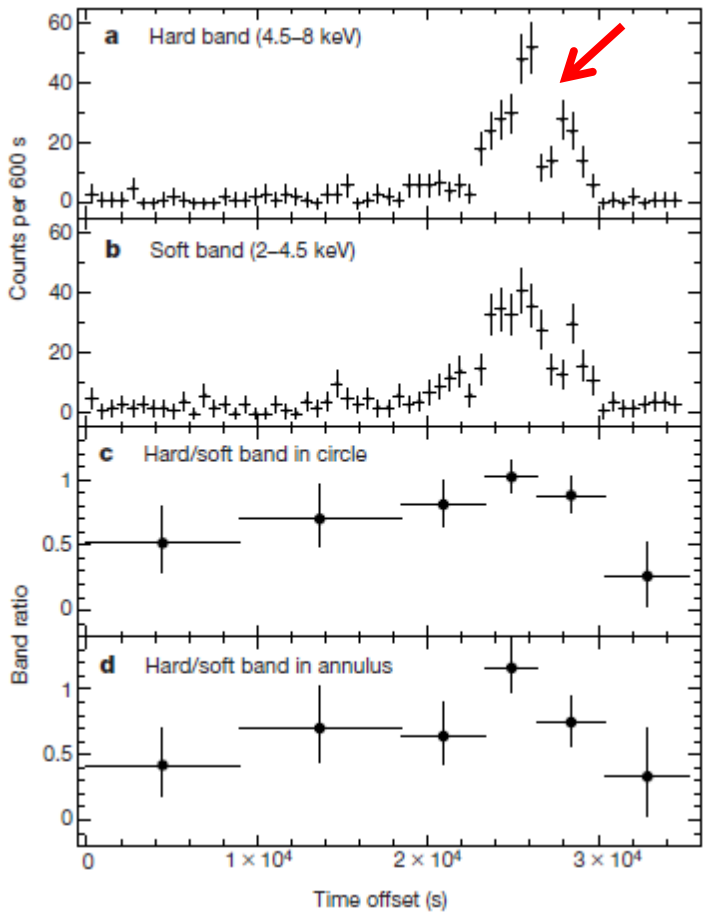

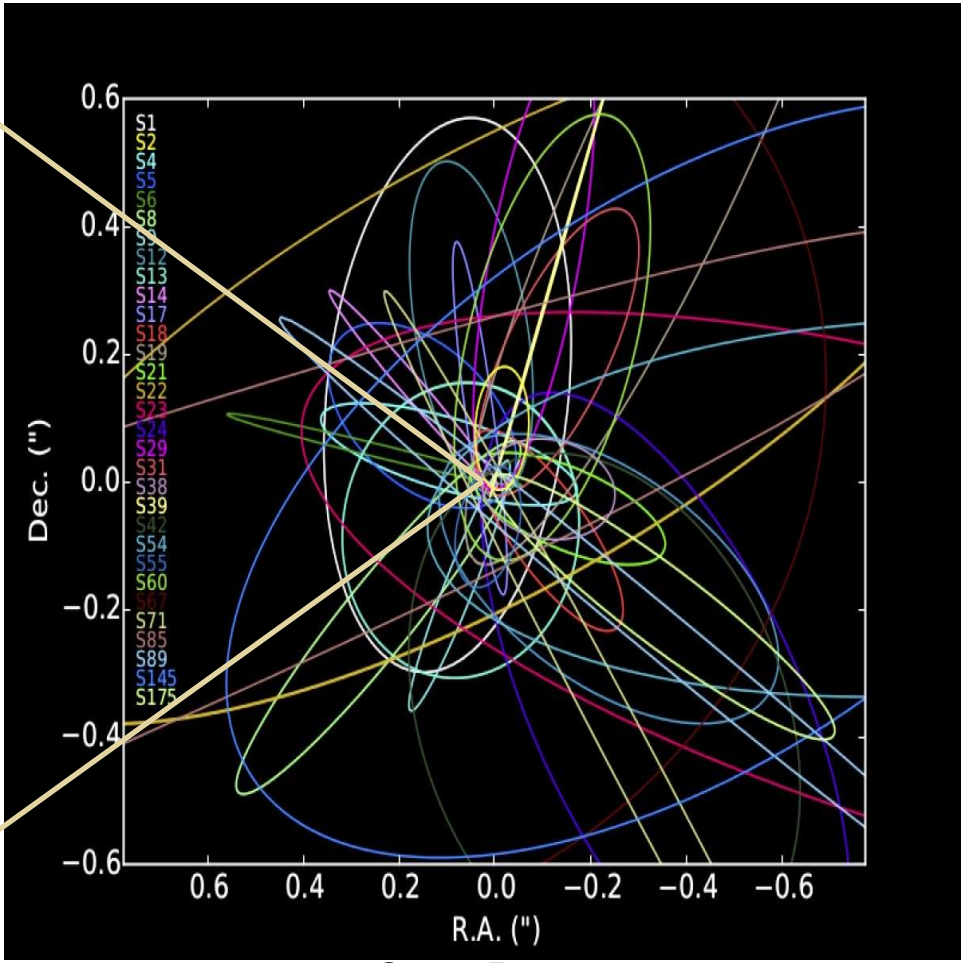

~6 mJy

Baganoff et al. 2001

~0.2 μJy

The compact radio/NIR/X-ray source at the center: Sagittarius A* (SgrA*)

First NIR flares from SgrA*

Genzel, R., Schödel, R.;Ott, T.;Eckart, A.;Alexander, T.;Lacombe, F.;Rouan, D.;Aschenbach, B.,
2003, Nature 425, 934

Near-infrared flares from accreting gas around the supermassive black hole at the Galactic Centre

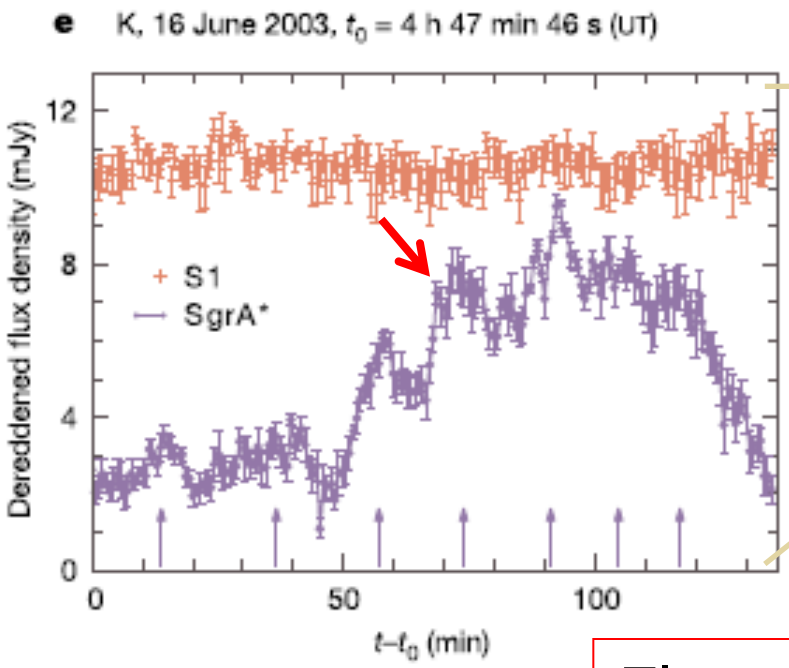

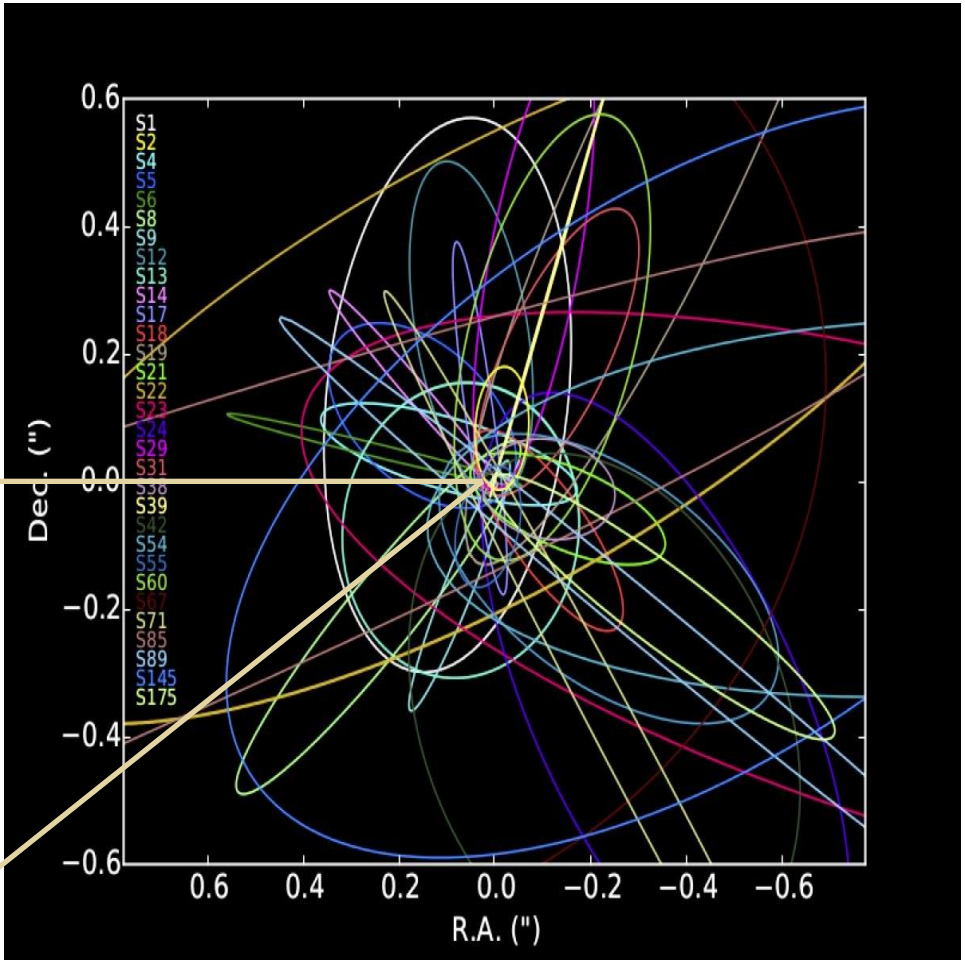

~6 mJy

Flares as positive flux density excursions from some ‘quiescent‘ state.

First NIR/X-ray detection of SgrA* Flares

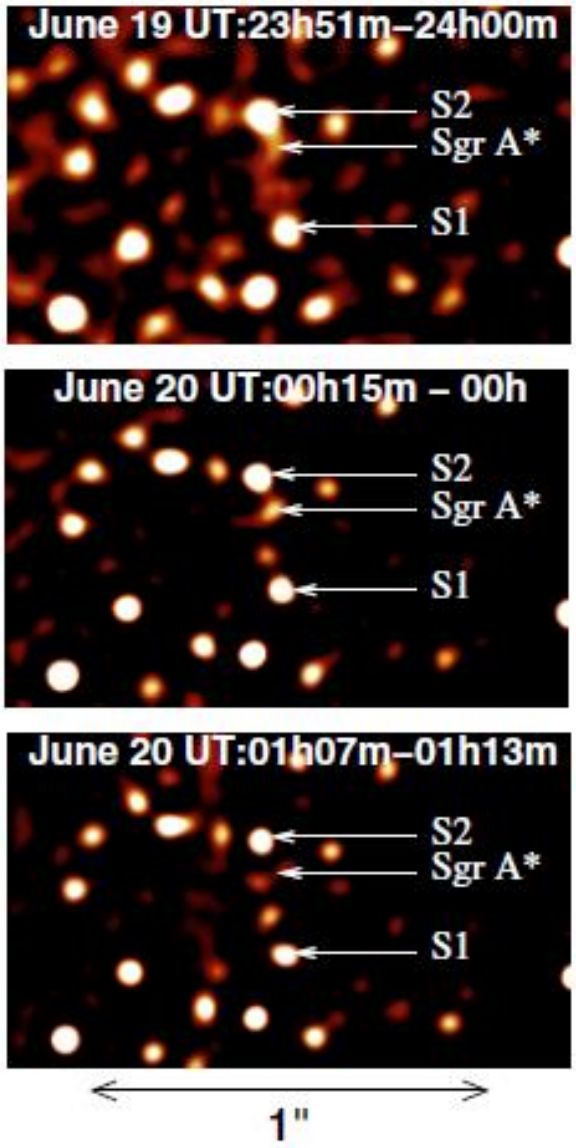

~0.04 μJy

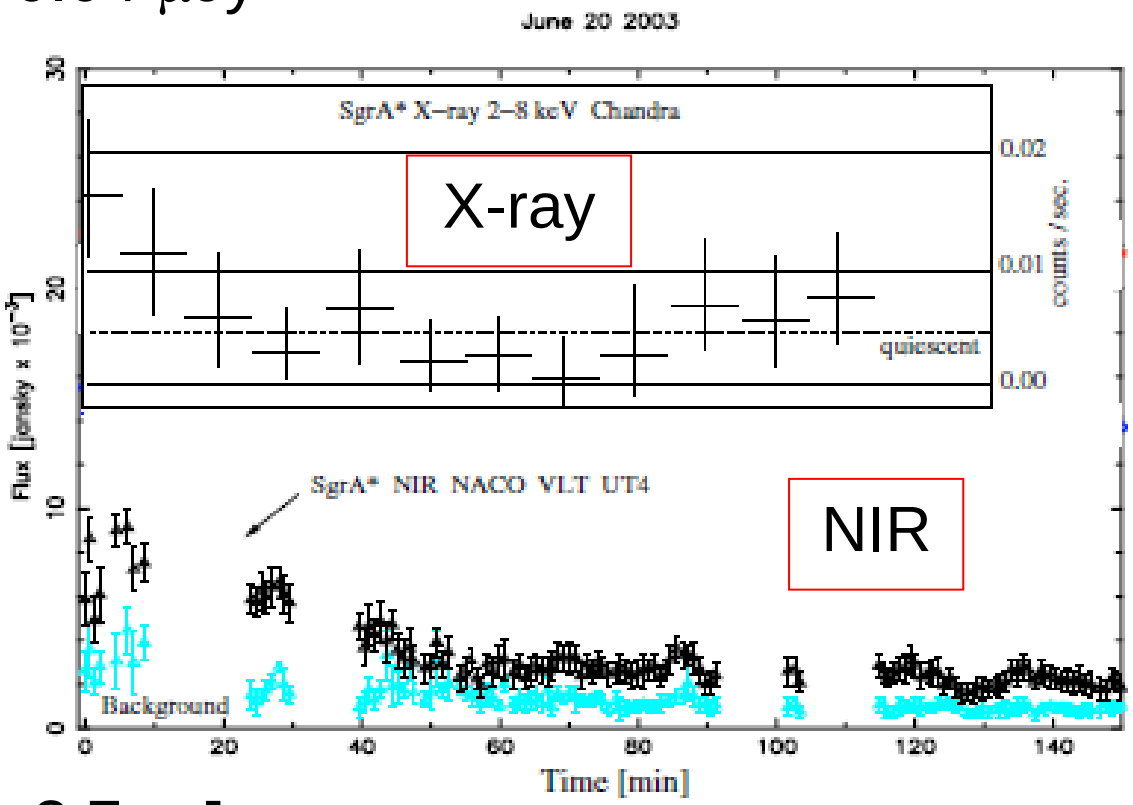

~3.7 mJy

Eckart, Baganoff, Morris, Bautz, Brandt, Garmire, Genzel, Ott, Ricker, Straubmeier, Viehmann, Schödel, Bower & Goldston, **2004**, A&A 427,1

Variability in the SYN-SSC case

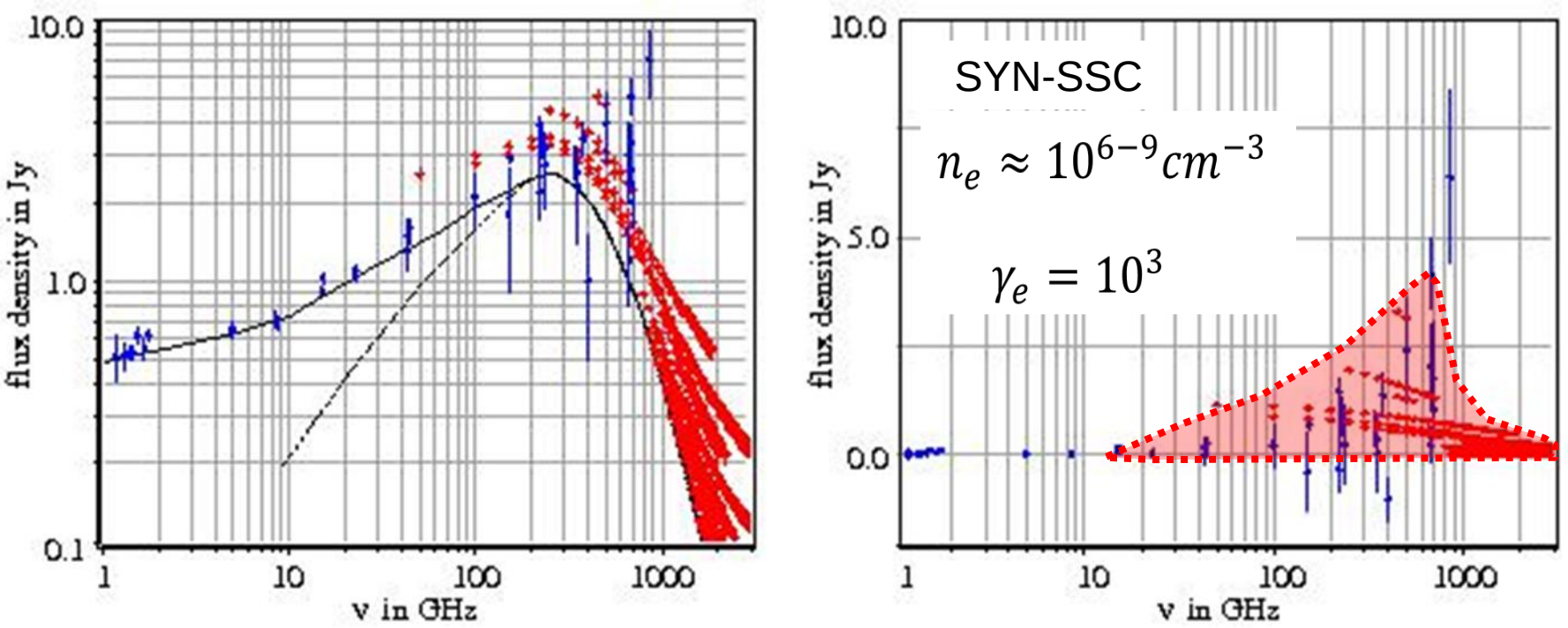

Millimeter to X-ray flares from Sagittarius A*;
2012, A&A 537, 52

Eckart, A.; García-Marín, M., Vogel, S. N.; Teuben, P.; Morris, M. R.; Baganoff, F.; Dexter, J.; Schödel, R.; Witzel, G.; Valencia-S., M.; Karas, V.; Kunneriath, D.; Straubmeier, C.; Moser, L.; Sabha, N.; Buchholz, R.; Zamaninasab, M.; Mužić, K.; Moultaka, J.; Zensus, J. A

Variability in the SYN-SSC case

2020, ApJ 898, 138

Synchrotron Self-Compton Scattering in Sgr A* Derived from NIR and X-Ray Flare Statistics

Subroweit, Matthias;Mossoux, Enmanuelle;Eckart, Andreas

2012, ApJS 203, 18

Source-intrinsic Near-infrared Properties of Sgr A*: Total Intensity Measurements

Witzel, G.;Eckart, A.;Bremer, M.;Zamaninasab, M.;et al.

Linking the radio/ sub-millimeter, Nearinfrared and X-ray variability in a Synchrotron Self-Compton model

Light and Shadow:

Using emitting plasma blobs
as probes for relativity

The X-ray view

Using orbiting hot spot models to explain NIR polarized flux from SgrA*

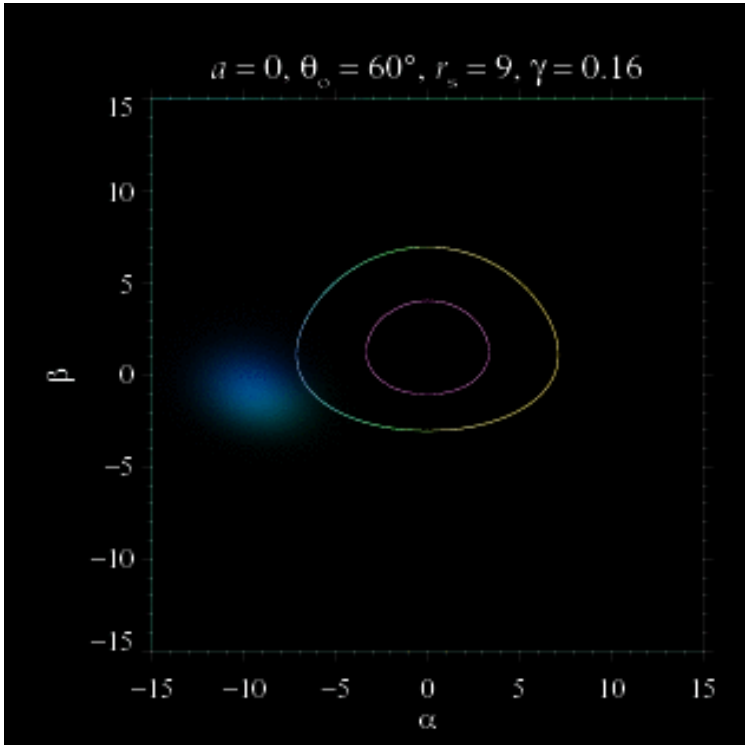

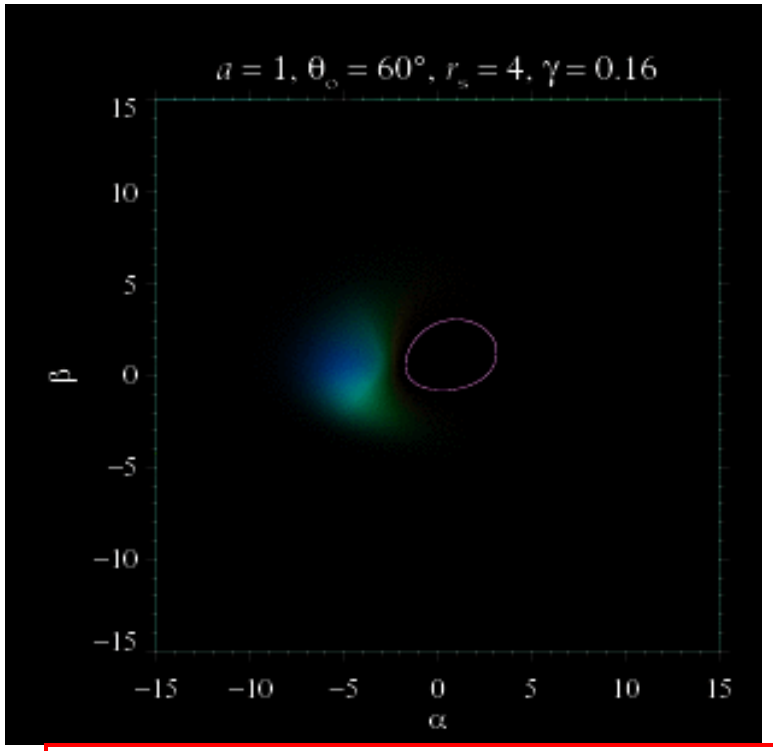

Dovciak, Karas & Yaqoob 2004, ApJS 153, 205
Dovciak et al. 2006

Meyer, Eckart, Schödel, Duschl, Muzic, Dovciak, Karas 2006a

The orbiting hot spot model approximates the situation in the midplane of the accretion stream

See also: Goldston, Quataert & Igumenshchev 2005, ApJ 621, 785
Broderick & Loeb 2005 astro-ph/0509237
Broderick & Loeb 2005 astro-ph/0506433

The Model

observer

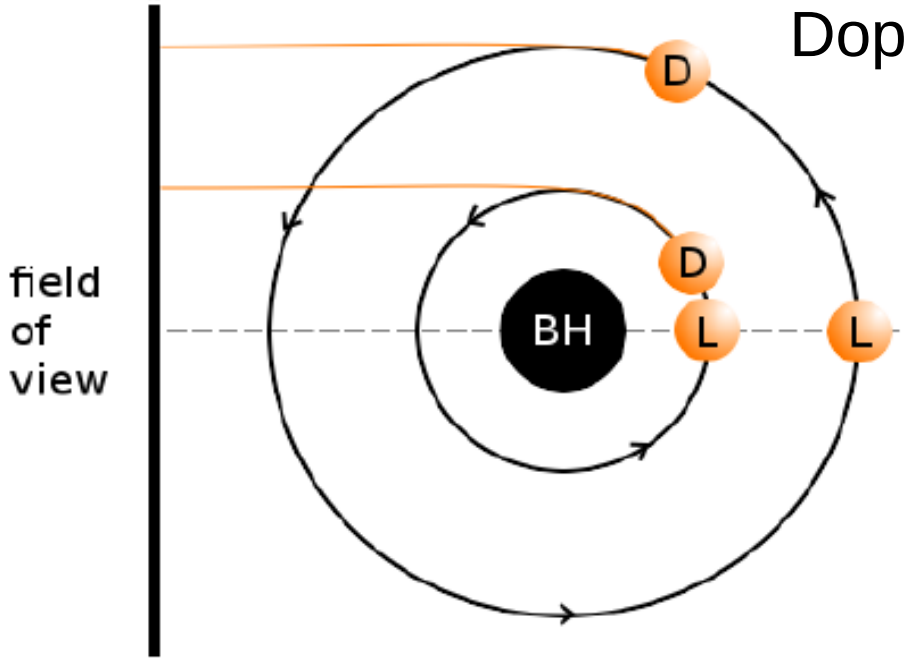

2017, MNRAS 472, 4422

Bright X-ray flares from Sgr A*

Karssen, G. D.;Bursa, M.;Eckart, A.;Valencia-S, M.;Dovčiak, M.;Karas, V.;Horák, J.

Fig. 1: Illustration of the origin of the double-peak structure in the total flux. The blobs marked with an 'L' are magnified by gravitational lensing, while they are behind the black hole from the observers point of view. That is, they are positioned on the focal line, as indicated by the dashed line. The blobs marked with a 'D' are Doppler-boosted, because they are moving 'directly towards' (in terms of geodesics) the observer, as indicated by the orange lines representing the geodesics from the source to the observer. The fraction of the orbit between these points varies with the radius of the orbit, owing to the stronger bending of the geodesics close to the black hole.

Karssen et al. 2017

Artificial Light Curves

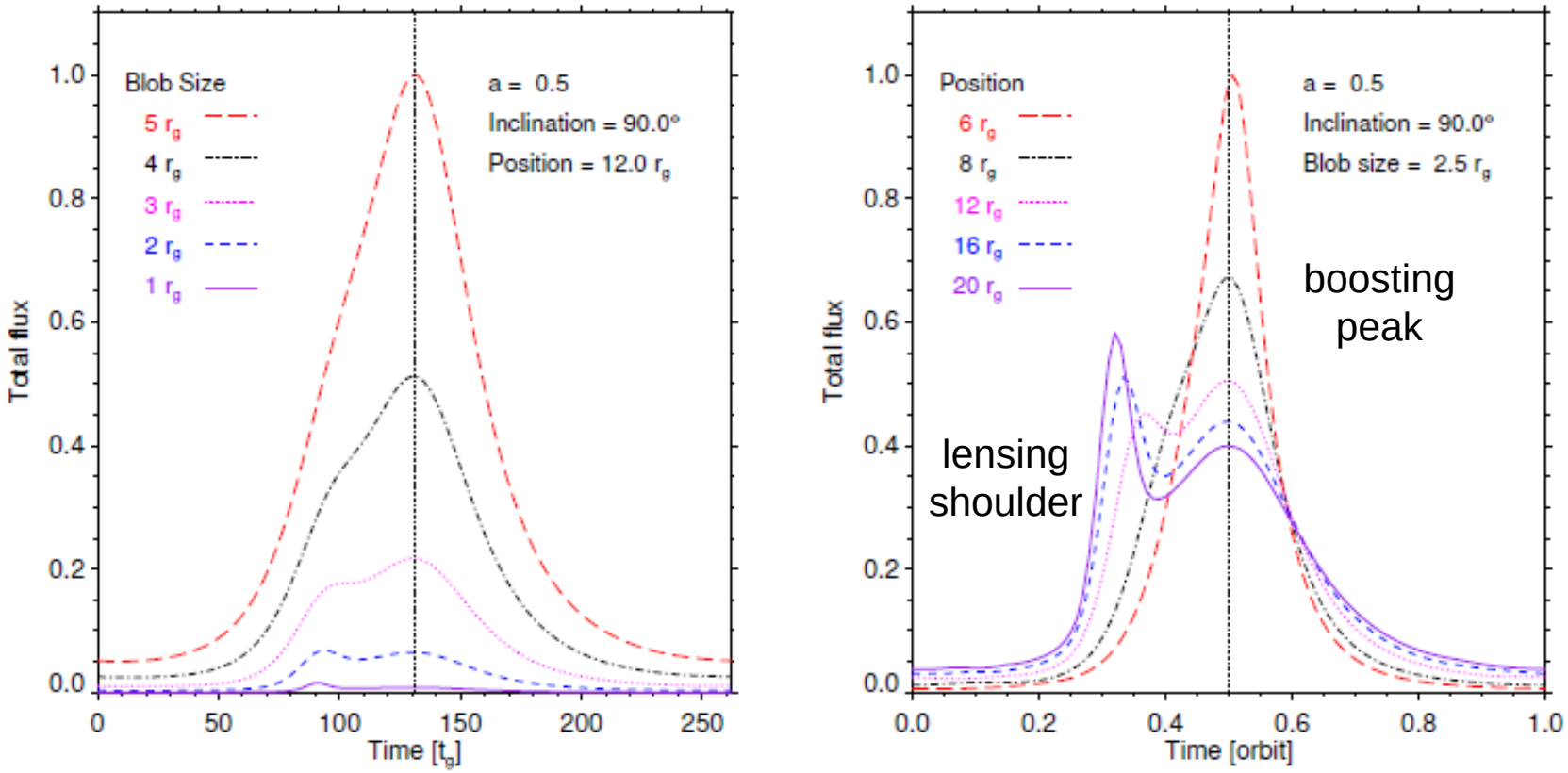

(a) Illustrates the influence of the blob's size on the shape of the light curve. The blobs of different sizes (5 r_g red long dashed, 4 r_g black dash-dotted, 3 r_g magenta dotted, 2 r_g blue short dashed and 1 r_g solid purple line) are orbiting at a radial position of 12 r_g around a black hole with spin 0.5, the viewing angle is 90 ° (edge on). The light curves are normalized to the maximum of the peak value of the light curve for the blob with the size 5 r_g and shifted such that the dopple peak is at the center.

(b) Illustrates the influence of the blob's position on the shape of the light curve. The blobs are orbiting at different positions (6 r_g red long dashed, 8 r_g black dash-dotted, 12 r_g magenta dotted, 16 r_g blue short dashed and 20 r_g solid purple line) and have a size of 2.5 r_g around a black hole with spin 0.5, the viewing angle is 90 ° (edge on). The light curves are normalized to the maximum of the peak value of the light curve for the blob with the size 5 r_g and shifted such that the dopple peak is at the center.

Karssen et al. 2017

Fitting Observed Light Curves

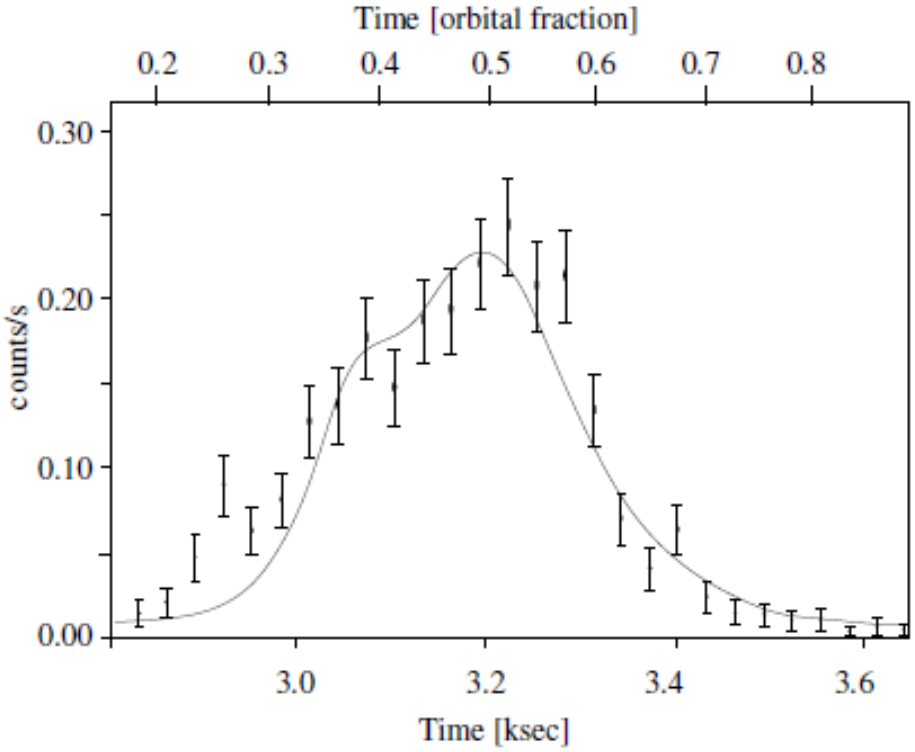

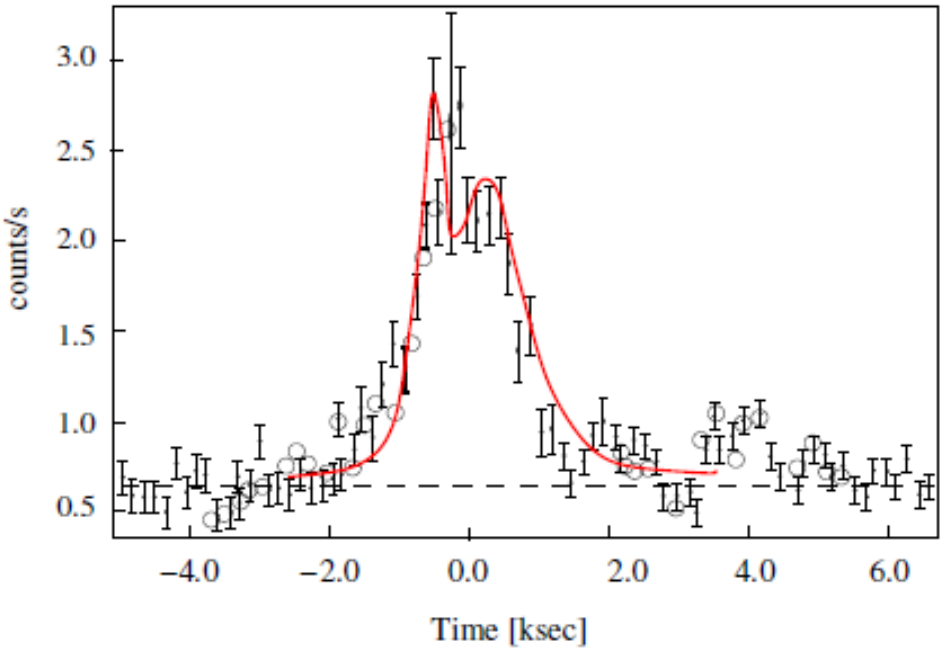

Figure 8: Left: Bright X-ray flare published by Nowak et al. (2012) shown with hotspot model fit by Karssen et al. (2017) for a spin of a=0.5, an inclination of 80^o, a spot radius of 18 r_s, a spot size of 5 r_s. **Right:** The bright flare reported by Ponti et al. (2017) compared to a hotspot model for a spin of a=0.5, an inclination of 90^o, a spot radius of 18 r_s, and a spot size of 2.5 r_s. In both cases the black hole mass implied by the X-ray flares is about $3.5\times10^6 M_\odot$ and compares well with the current value of $M_{BH} = (4.15 \pm 0.13 \pm 0.57) \times 10^6\ M_\odot$ derived form stellar dynamics (Parsa et al. 2017).

Karssen et al. 2017

Analysis of 4 bright X-ray flares

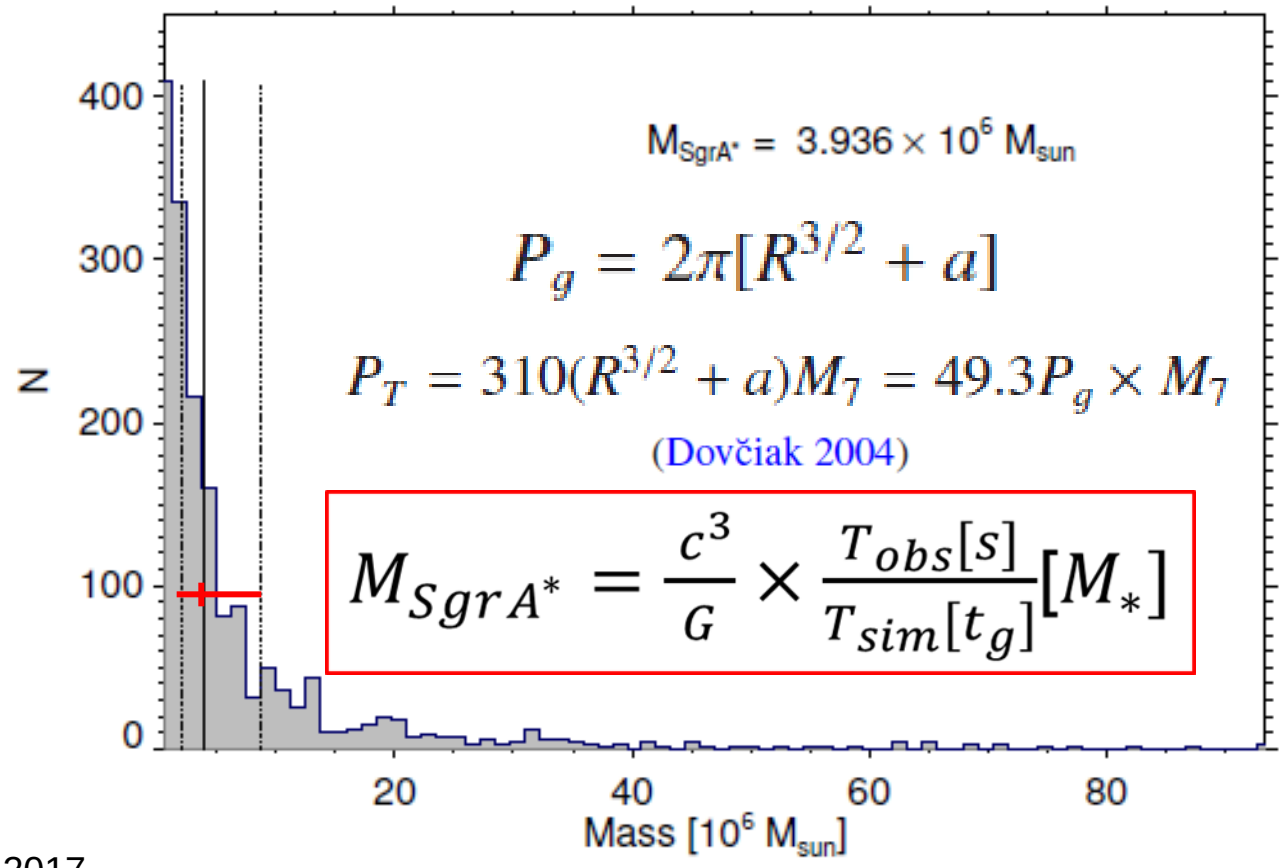

Karssen et al. 2017

We fit the flare shapes scale free. Introducing then the observed width of the flare in seconds introduces a black hole mass in solar masses.

Deriving the SgrA* Black Hole Mass

T_{obs} and T_{sim} are the durations of the observed and simulated light curves

$$M_{SgrA^*} = \frac{c^3}{G} \times \frac{T_{obs}[s]}{T_{sim}[t_g]} [M_\odot]$$

New inovative mothod to estimate the BH mass from light curves. Results for SgrA*:

Table 2. The median values of the mass model parameters M, i, R_0 and D_0 as well as the corresponding maximum amplification factor $\mathrm{Amp_{max}}$.

Flare	$M[10^6\,M_\odot]$	$i[^\circ]$	$R_0[r_g]$	$D_0[r_g]$	$\mathrm{Amp_{max}}$
Baganoff et al. (2001)	$4.86^{+6.80}_{-2.41}$	46.47	15.69	2.85	25
Porquet et al. (2003)	$3.45^{+4.07}_{-1.43}$	55.40	12.43	2.59	39
Porquet et al. (2008)	$3.13^{+3.81}_{-1.24}$	49.16	14.24	2.84	32
Nowak et al. (2012)	$3.54^{+1.02}_{-1.01}$	69.52	17.90	3.60	51
Median	3.49 ± 0.20				
All flare fit	$3.94^{+4.85}_{-1.86}$				
Mossoux et al. (2015) (Epic)	$3.18^{+5.56}_{-2.57}$	60.68	14.14	3.06	49

Karssen et al. 2017

Topic 4

Light and Shadow:

Using emitting plasma blobs
as probes for relativity

The NIR interferometric view

GRAVITY Collaboration, A&A,
2018arXiv181012641G

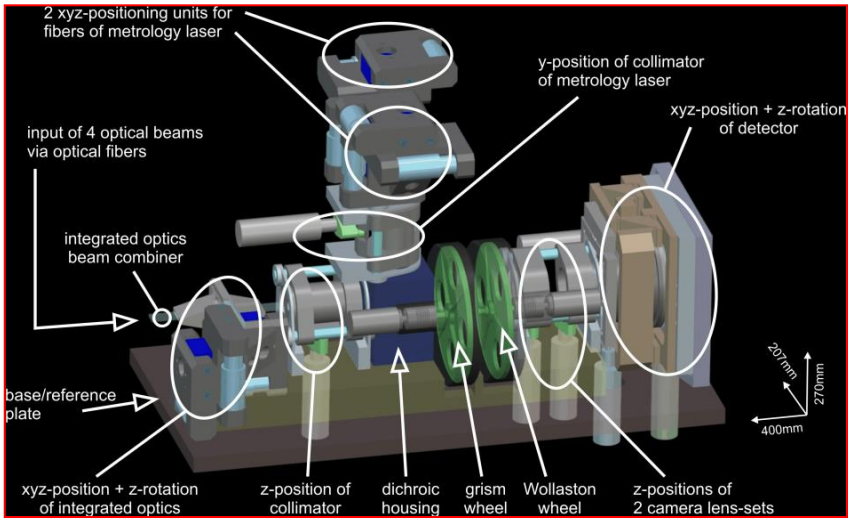

GRAVITY Collaboration: Detection of orbital motions near the last stable circular orbit of the massive black hole SgrA*

GRAVITY Collaboration*: R. Abuter[8], A. Amorim[6,14], M. Bauböck[1], J.P. Berger[5], H. Bonnet[8], W. Brandner[3], Y. Clénet[2], V. Coudé du Foresto[2], P.T. de Zeeuw[10,1], C. Deen[1], J. Dexter[1], G. Duvert[5], A. Eckart[4,13], F. Eisenhauer[1], N.M. Förster Schreiber[1], P. Garcia[7,9,14], F. Gao[1], E. Gendron[2], R. Genzel[1,11], S. Gillessen[1], P. Guajardo[9], M. Habibi[1], X. Haubois[9], Th. Henning[3], S. Hippler[3], M. Horrobin[4], A. Huber[3], A. Jiménez-Rosales[1], L. Jocou[5], P. Kervella[2], S. Lacour[2,1], V. Lapeyrère[2], B. Lazareff[5], J.-B. Le Bouquin[5], P. Léna[2], M. Lippa[1], T. Ott[1], J. Panduro[3], T. Paumard[2], K. Perraut[5], G. Perrin[2], O. Pfuhl[1], P.M. Plewa[1], S. Rabien[1], G. Rodríguez-Coira[2], G. Rousset[2], A. Sternberg[12], O. Straub[2], C. Straubmeier[4], E. Sturm[1], L.J. Tacconi[1], F. Vincent[2], S. von Fellenberg[1], I. Waisberg[1], F. Widmann[1], E. Wieprecht[1], E. Wiezorrek[1], J. Woillez[8], and S. Yazici[1,4]

2018, A&A 618, L10

Photo-Center motion for SgrA*

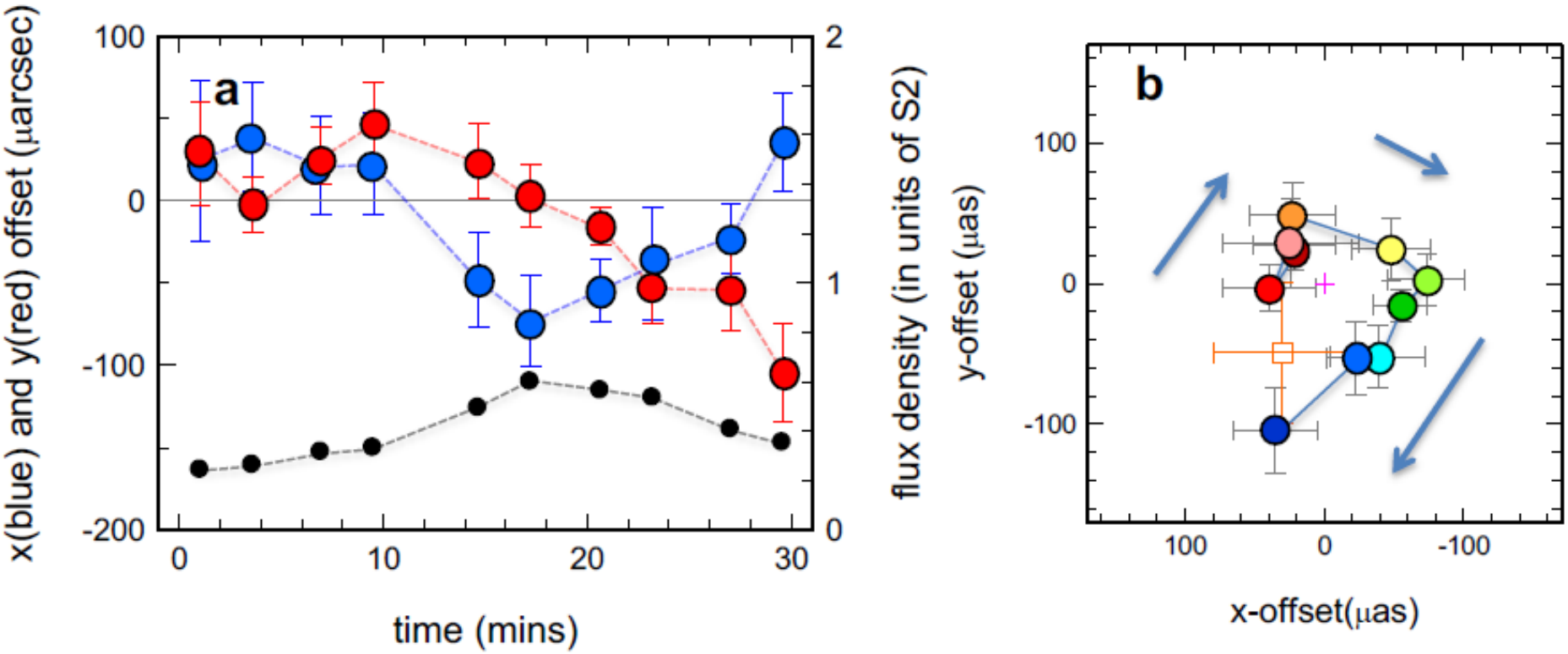

Centroid motion of one of the flare events:
Evidence for an orbiting hot spot

Gravity Collaboration, 2018, A&A 618, 125

Photo-Center motion for SgrA*

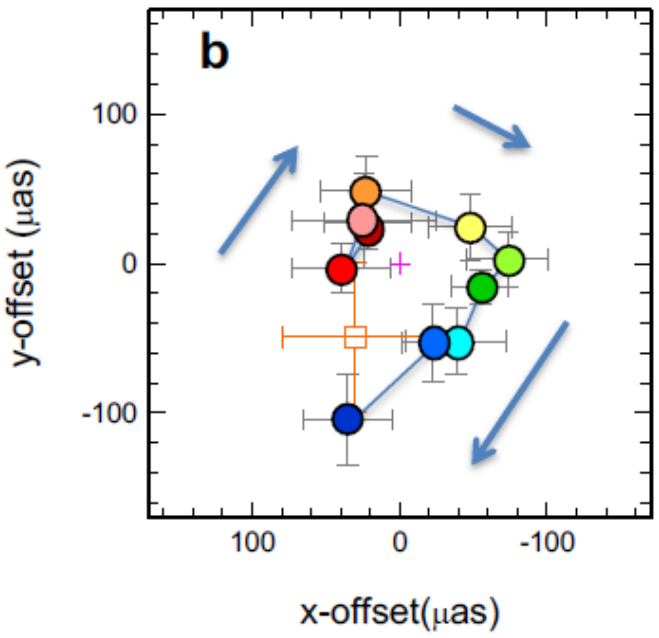

FIG. 10. Photocenter motion compared to a disk model. The example of a NIR photo-center motion as planned to be measured with the GRAVITY interferometer at the VLTI is taken from [256] and [257]. The simulation describes the apparent trajectory of flare events assuming material orbiting a non-rotation black hole at an inclination of 45° on the last stable orbit at a distance of 3 R_S from the center. Lensing (including multiple images), relativistic beaming and Doppler effect are included in the relative positioning of the resulting data points (red crosses) following the orbital track ([white line; further details in 256]). The image [162] is assumed to represent a mm-VLBI data disk model that shows luminous material for radii beyond the last stable orbit. The dashed and straight white arrows indicate the directions perpendicular and along the radio structure that we refer to in the text.

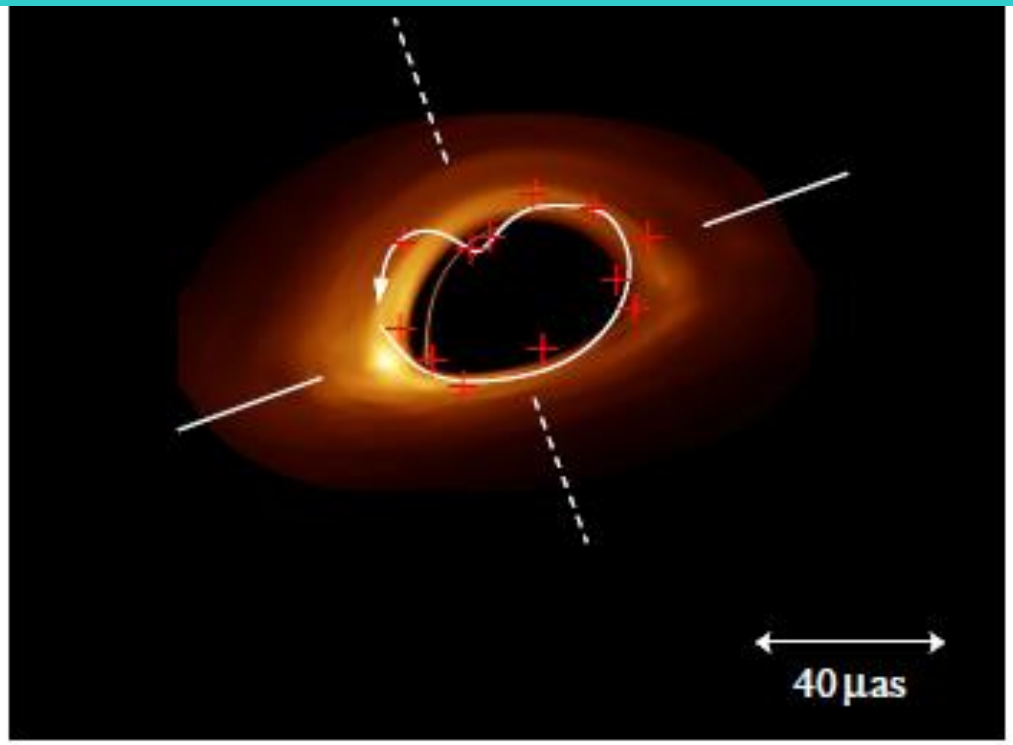

Eckart et al. FoPh 47, 553

The Milky Way‘s Supermassive Black Hole: “How good a case is it? A Challange fo Astrophysics and Philosophy of Science“ and references there in

Photo-Center motion for SgrA*

Radius/Period plot for the observed flare events

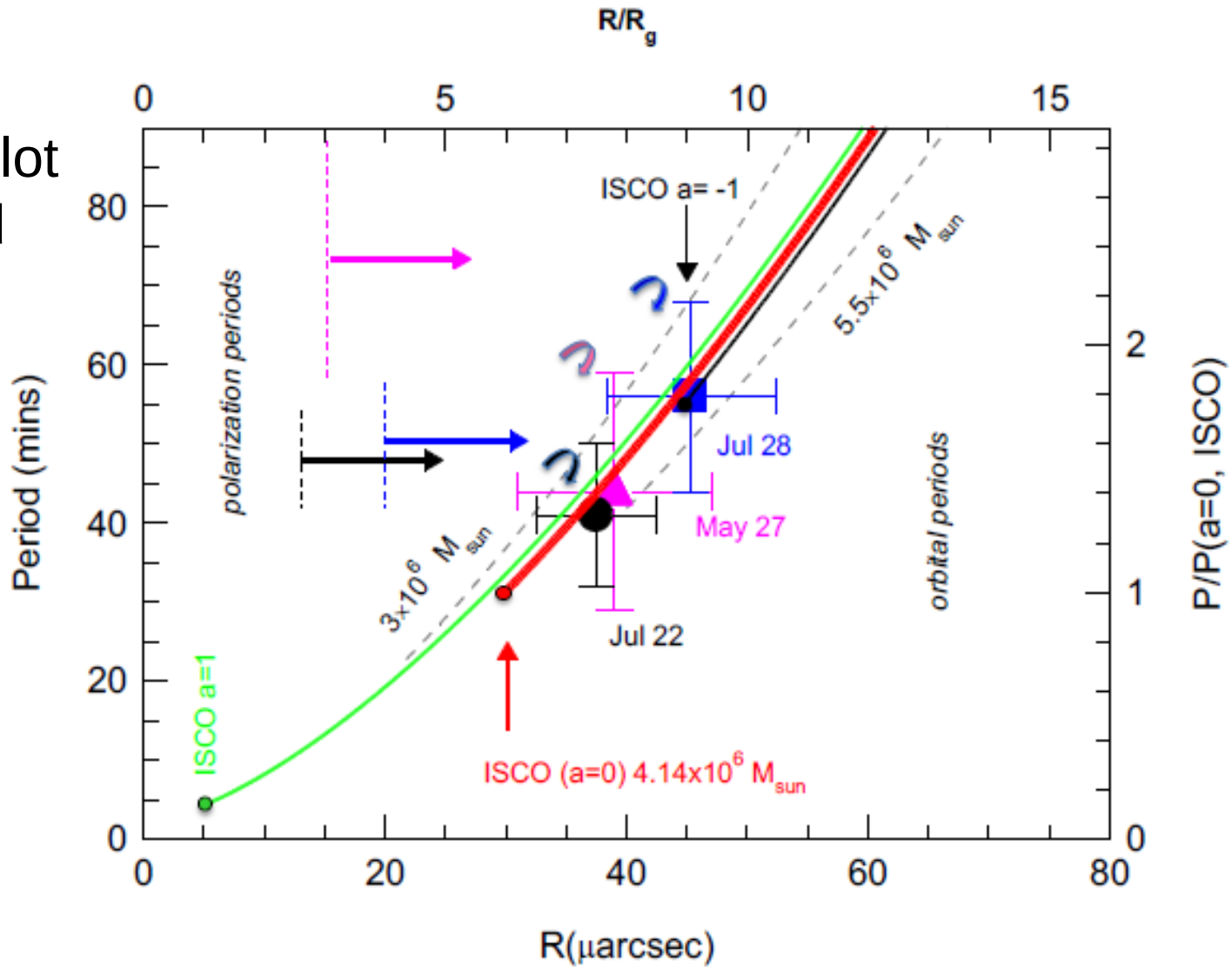

2018, A&A 618, 125

Electric Charge estimates for SgrA*

On the charge of the Galactic centre black hole

Michal Zajacek, Arman Tursunov,
Andreas Eckart, and Silke Britzen

The Galactic center supermassive black hole (SMBH), in sharp contrast with its complex environment, is characterized by three classical parameters ***mass, spin, and electric charge***. Its charge is poorly constrained. It is, however, usually assumed to be zero because of neutralization due to the presence of plasma.

Zajacek et al., 2018, MNRAS 480, 4408

Electric Charge estimates for SgrA*

In addition, we propose a novel observational test based on the presence of the **Bremsstrahlung surface brightness decrease**, which is more sensitive for smaller unshielded electric charges than the black-hole shadow size.

Based on this test, the current upper observational limit on the charge of Sgr A* is <3x10^8 C.

Zajacek et al., 2018, MNRAS 480, 4408

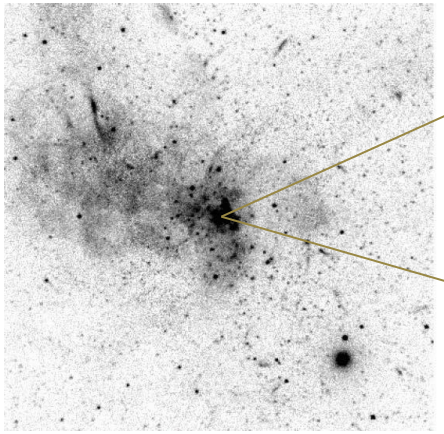

Mossoux & Eckart 2018

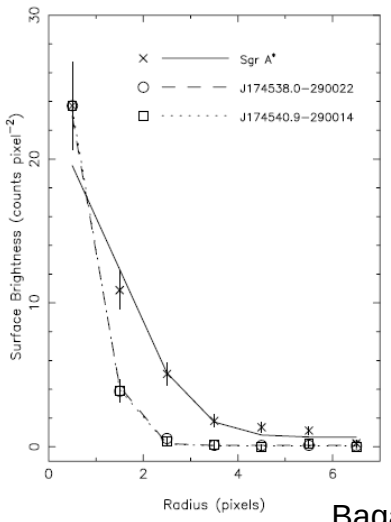

Baganoff et al. 2003

Electric Charge estimates for SgrA*

For relativistic orbital speeds the Lorentz force and the gravity may have comparable strengs.

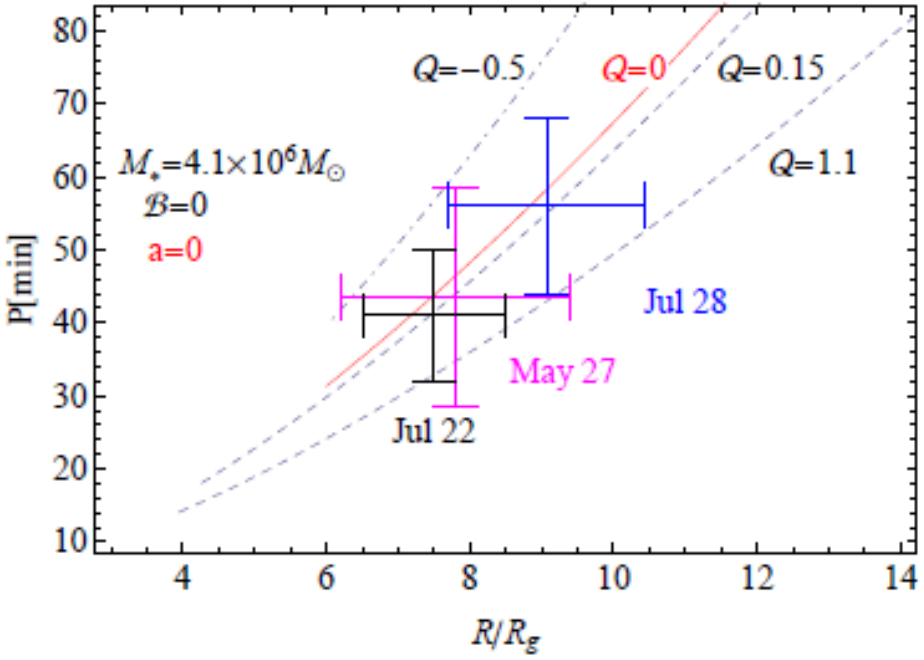

2020, ApJ 897, 99

Effect of Electromagnetic Interaction on Galactic Center Flare Components

Tursunov, Arman;Zajaček, Michal;Eckart, Andreas

Recently, near-infrared GRAVITY@ESO observations at 2.2 μm have announced the detection of three bright "flares" in the vicinity of the Galactic center supermassive black hole (SMBH) that exhibited orbital motion at a distance of about $6-11$ gravitational radii from an $\sim 4\times10^6\,M_\odot$ black hole. There are indications of the presence of a large-scale, organized component of the magnetic field at the Galactic center. Electromagnetic effects on the flare dynamics were previously not taken into account despite the relativistic motion of a plasma in magnetic field leading to the charge separation and nonnegligible net charge density in the plasma. Applying various approaches, we find the net charge number density of the flare components of the order of $10^{-3}-10^{-4}$ cm^{-3}, while the particles' total number density is of the order of 10^6-10^8 cm^{-3}. However, even such a tiny excess of charged particles in the quasi-neutral plasma can significantly affect the dynamics of flare components, which can then lead to the degeneracy in the measurements of spin of the SMBH. Analyzing the dynamics of recent flares in the case of the rapidly rotating black hole, we also constrain the inclination angle between the magnetic field and spin axis to $\alpha < 50°$, as for larger angles, the motion of the hot spot is strongly chaotic.

Topic 4

Light and Shadow:

Using emitting plasma blobs
as probes for relativity

The radio interferometric view

Johnson et al. 2018

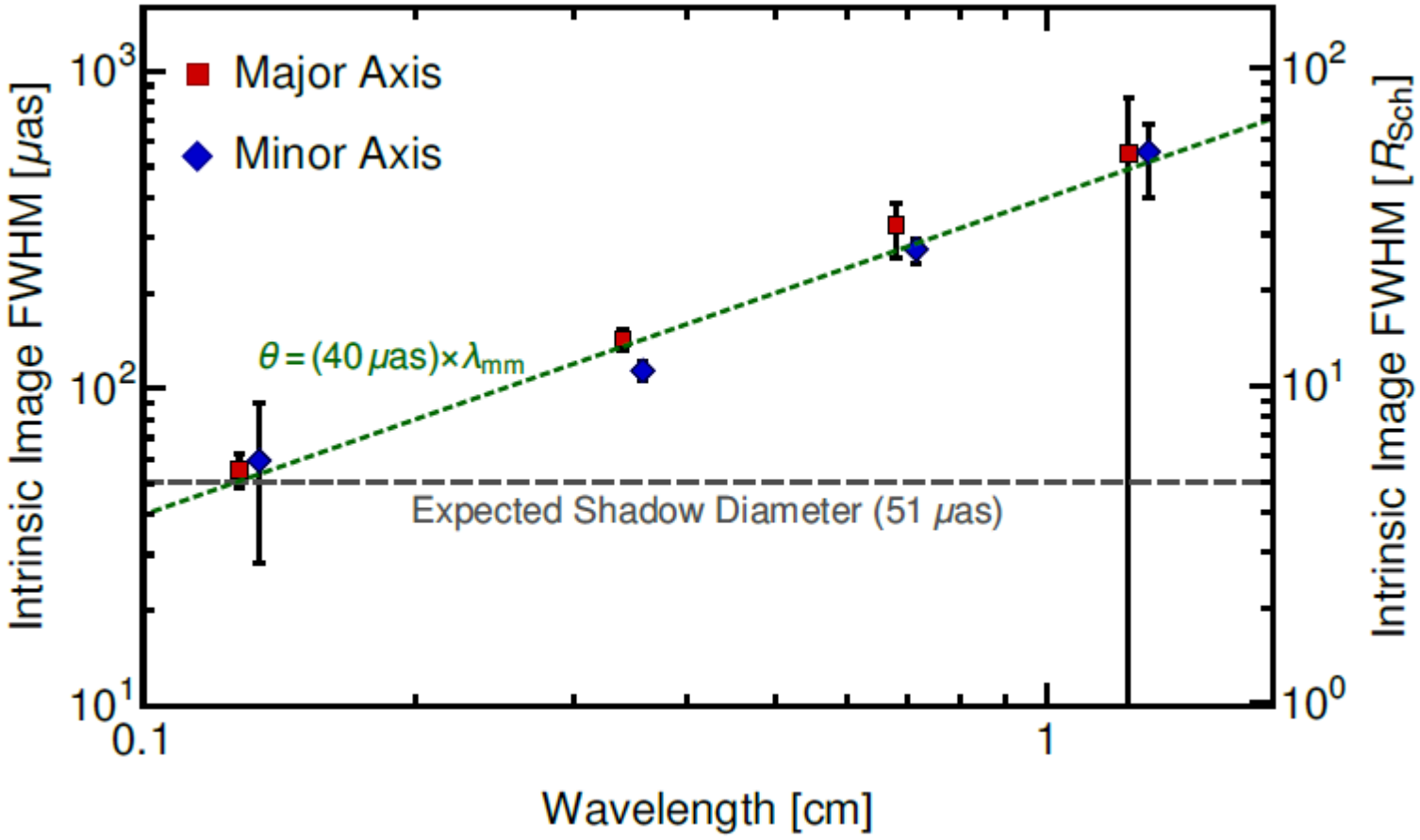

The major/minor axis markers are offset slightly in wavelength, for visual clarity. We also show the expected diameter of the black hole "shadow" and plot a simple isotropic source model with size directly proportional to wavelength. We do not find evidence for significant intrinsic anisotropy at any wavelength or for a steep scaling of intrinsic size with wavelength.

Expected Photo-Center motion for SgrA*

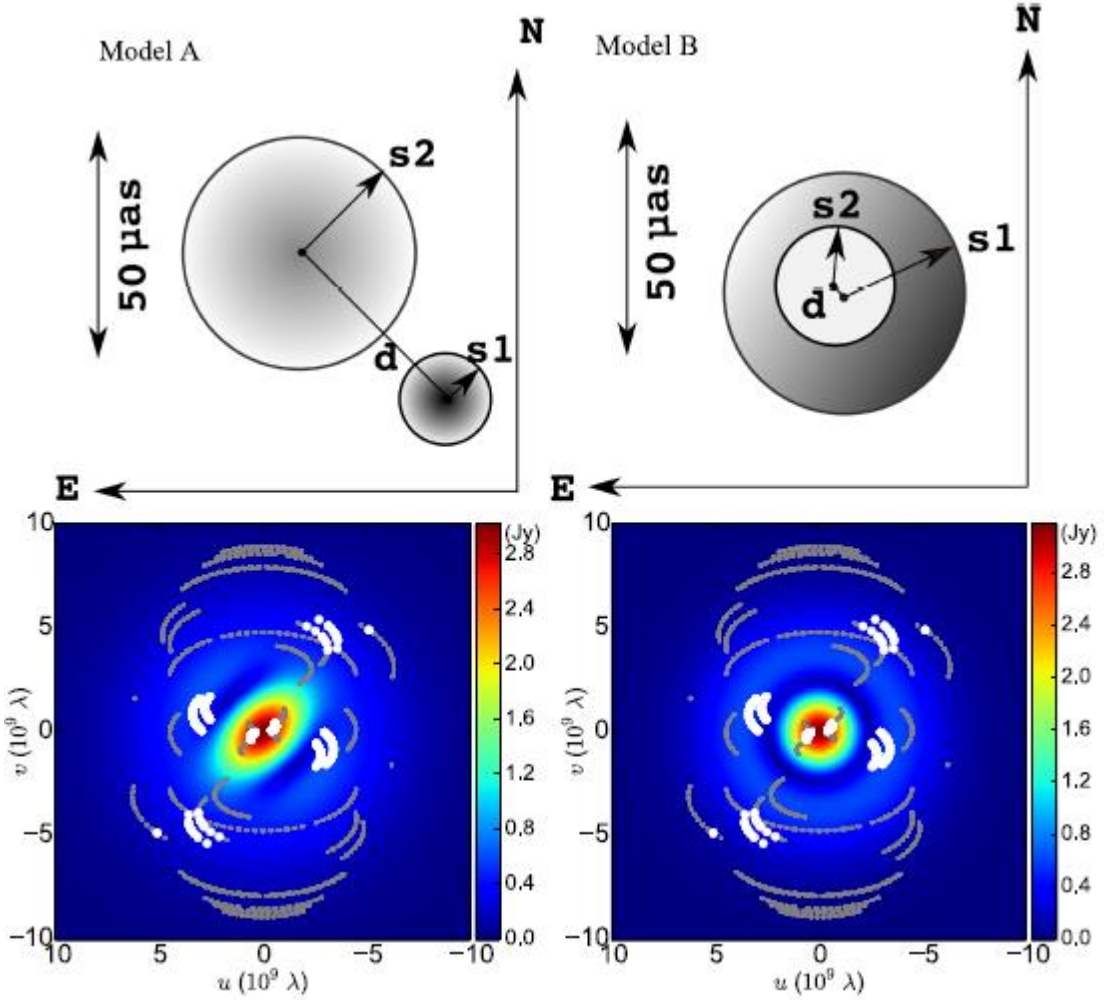

Ru-Sen Lu et al. (2018)

Monnier et al. 2006

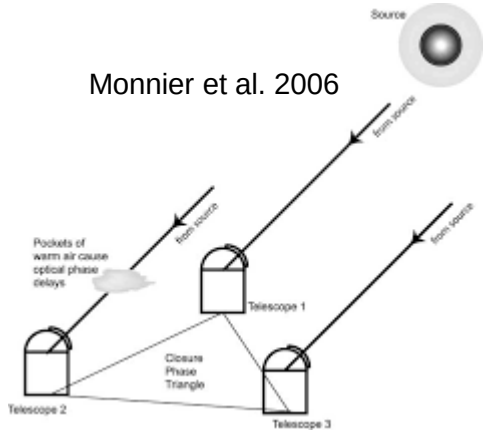

Non-zero closure phases clearly indicate an asymmetric source structure.

Question:
How does flare activity look like in this model?

Summary: Light and Shadow

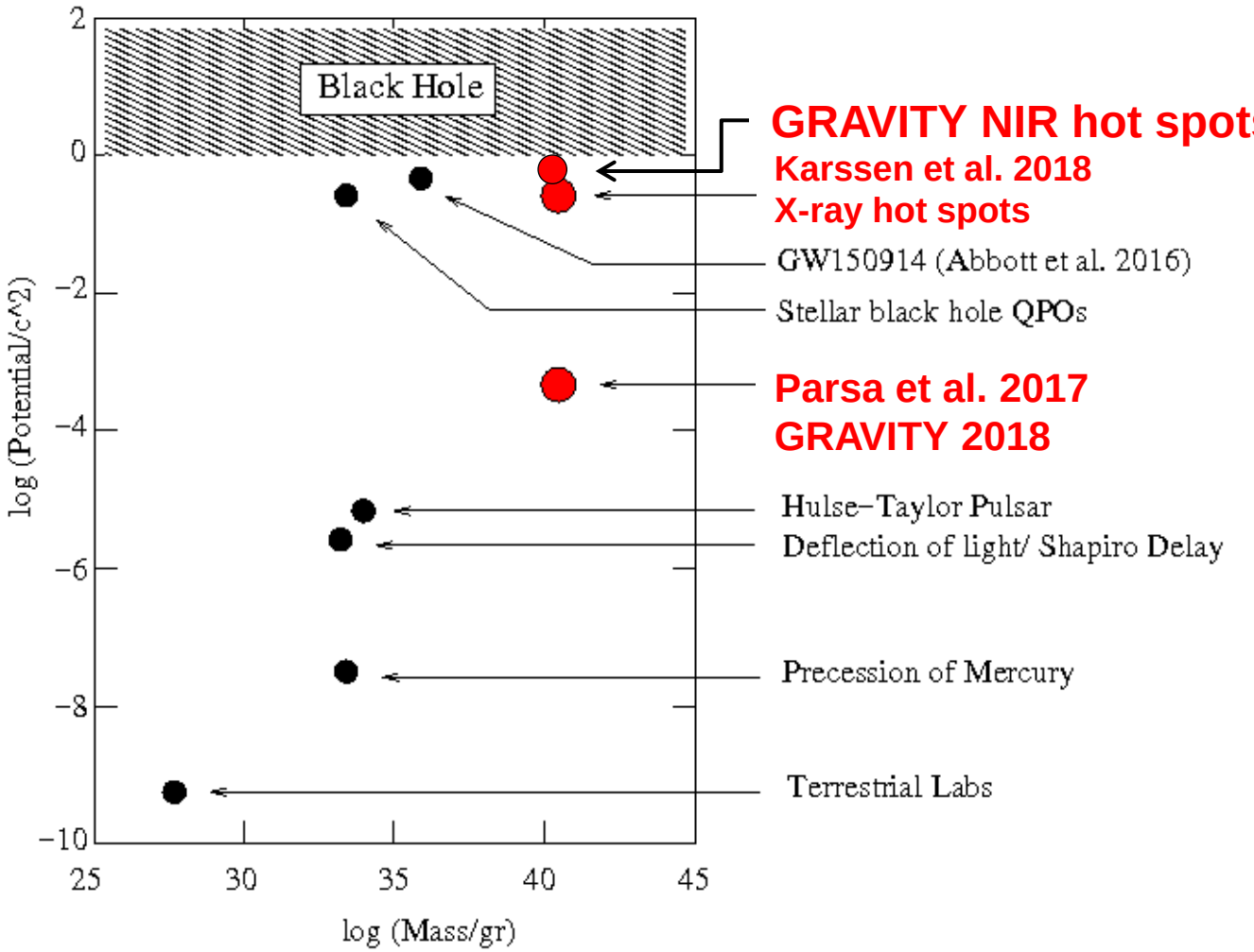

based on figure by
Psaltis 2004

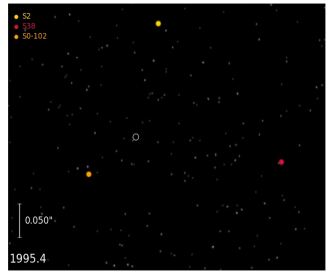

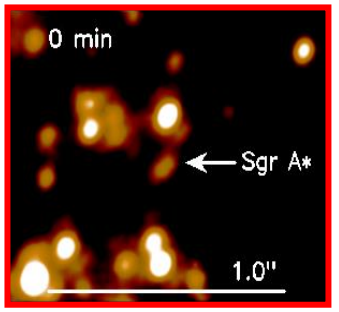

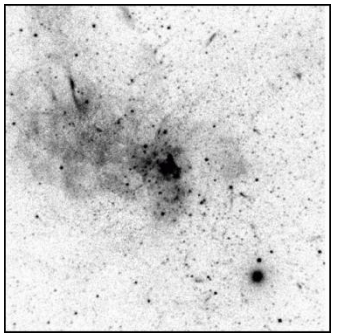

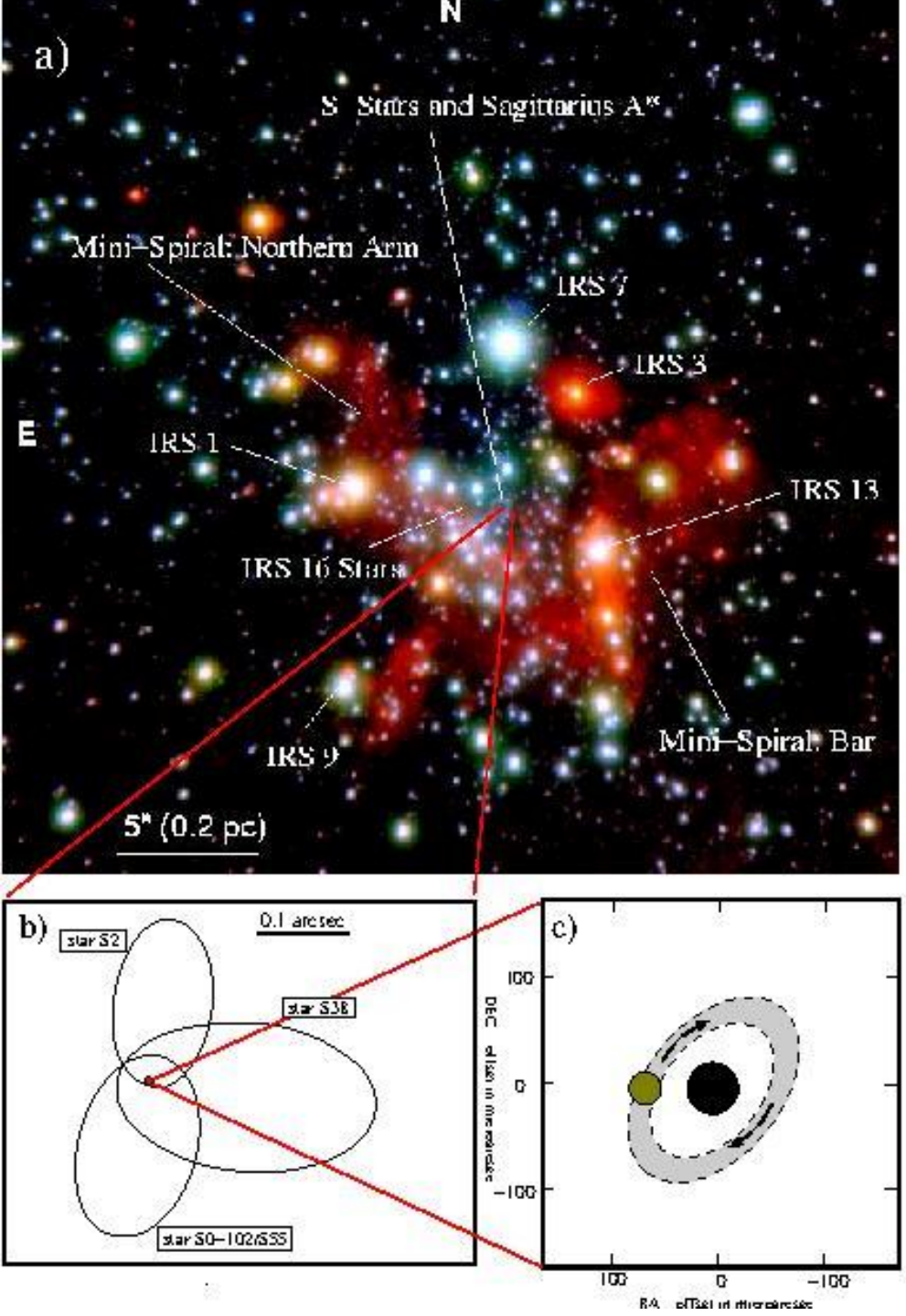

Summary

- Gas motion
- Stellar motion
- Proper motion
- Accelertions
- Test for relativity
- Moving gas close
- To the Black hole

The project is progressing in Cologne:

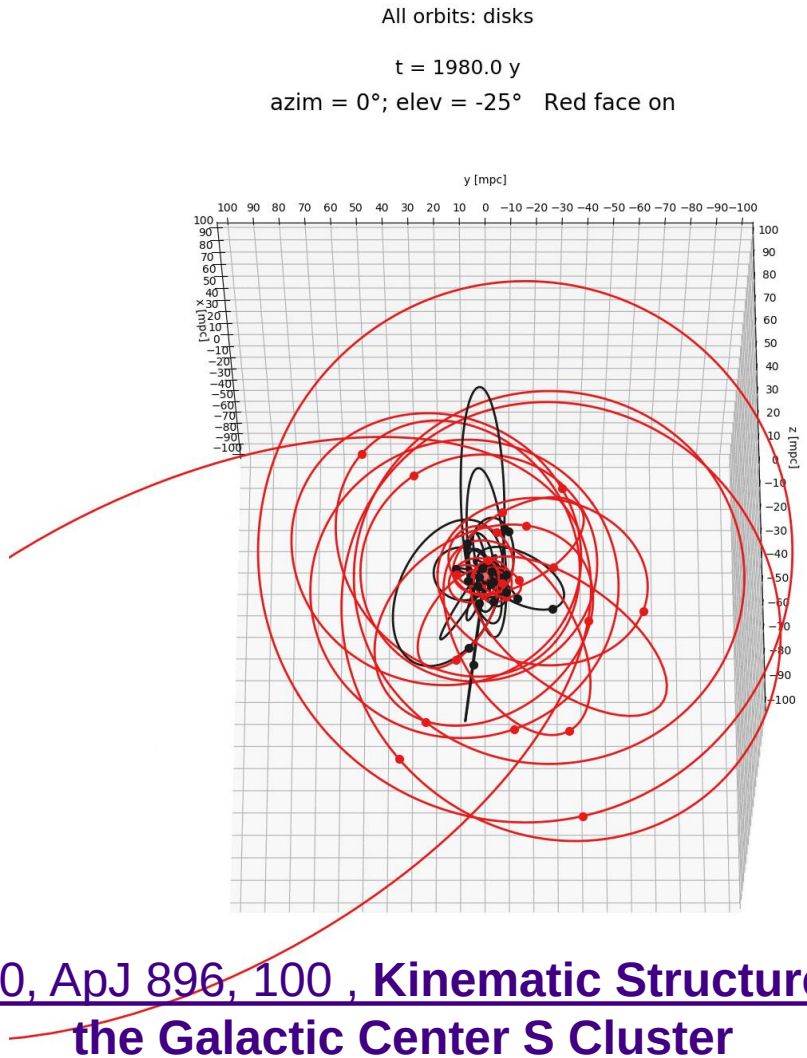

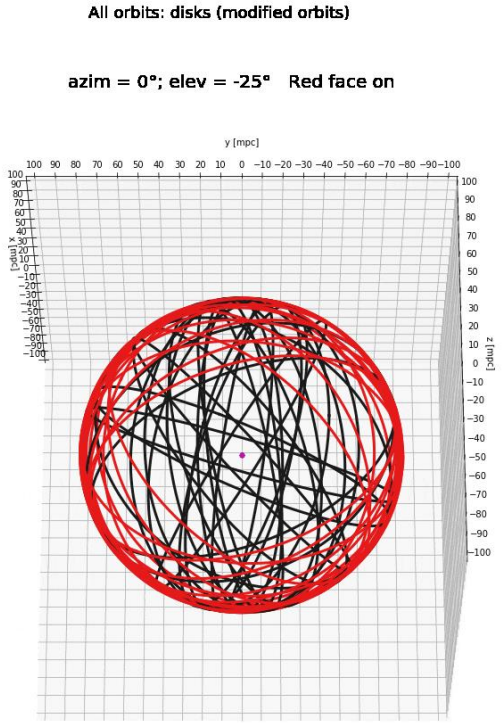

2020, ApJ 896, 100 , **Kinematic Structure of the Galactic Center S Cluster**

Ali, Basel; Paul, Daria; Eckart, Andreas; Parsa, Marzieh; Zajacek, Michal; Peißker, Florian; Subroweit, Matthias; Valencia-S., Monica; Thomkins, Lauritz; Witzel, Gunther

Kinematic structure of the S-cluster:
Two orthogonal thick disks
Ali et al. 2020

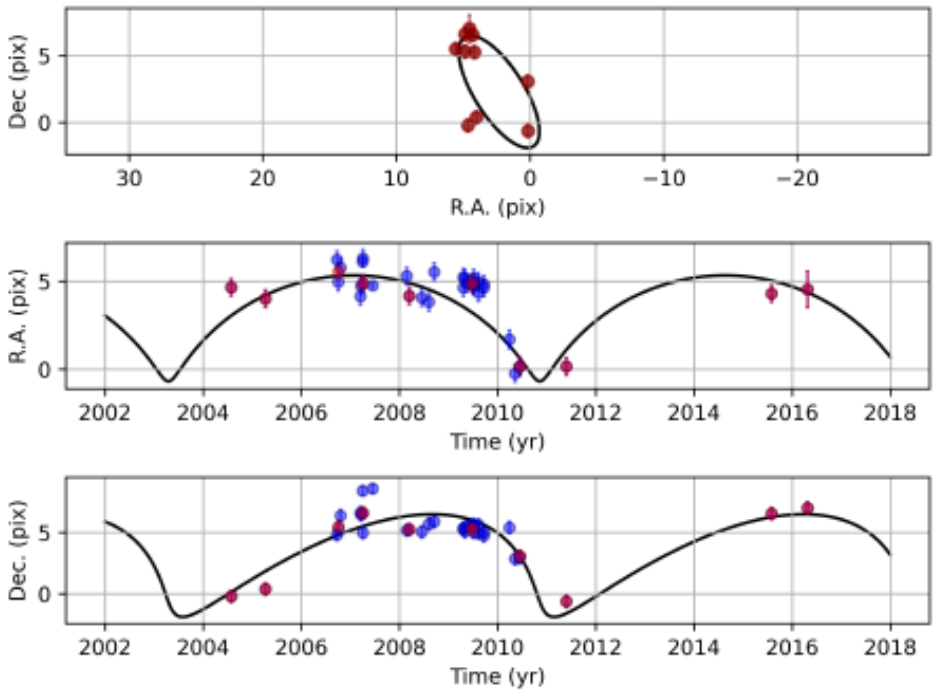

S4711

The star that gets closest to the Galactic Center

Ap(4711)=13 AU; ap(S2)=119 AU

S62 and S4711: Indications of a Population of Faint Fast-moving Stars inside the S2 Orbit—S4711 on a 7.6 yr Orbit around Sgr A*

Peißker, Florian; Eckart, Andreas; Zajaček, Michal; Ali, Basel; Parsa, Marzieh, 2020, ApJ 899, 50

Near- and Mid-infrared Observations in the Inner Tenth of a Parsec of the Galactic Center Detection of Proper Motion of a Filament Close to Sgr A*

Peißker, Florian; Eckart, Andreas; Sabha, Nadeen B.; Zajaček, Michal; Bhat, Harshitha, 2020, ApJ 897, 28

VLTI: GRAVITY

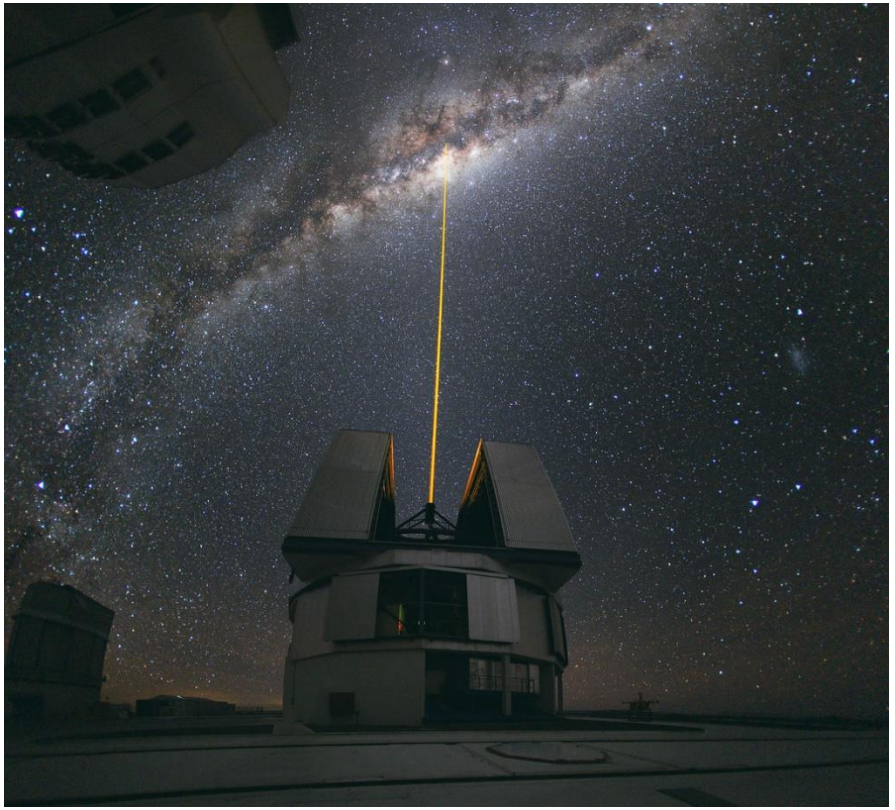

GRVITY + :
Cologne University: Supports high level wave front sensing for the VLT unity telescopes in interferometry mode using GRAVITY

Christian Straubmeier, Metthew Horrobin, Andreas Eckart

End